

**University of Alberta**

**Novel Polymer and Lipid-Based Nanocarriers for Gene Delivery**

by

**Ross Edward Billy Fitzsimmons**

A thesis submitted to the Faculty of Graduate Studies and Research in partial fulfillment of the requirements  
for the degree of

**Master of Science**

**In**

**Biomedical Sciences**

**Department of Biomedical Engineering**

©Ross Fitzsimmons

Spring 2012 Edmonton, Alberta

Permission is hereby granted to the University of Alberta Libraries to reproduce single copies of this thesis and to lend or sell such copies for private, scholarly or scientific research purposes only. Where the thesis is converted to, or otherwise made available in digital form, the University of Alberta will advise potential users of the thesis of these terms.

The author reserves all other publication and other rights in association with the copyright in the thesis and, except as herein before provided, neither the thesis nor any substantial portion thereof may be printed or otherwise reproduced in any material form whatsoever without the author's prior written permission.

## **ABSTRACT**

The following thesis describes the progress made in the field of viral gene therapy, and then addresses the need for non-viral alternatives. The latter is conducted by first reviewing the viral components critical for the success of gene delivery and incorporation of desired properties into non-viral carriers, followed by original studies assessing the gene delivery efficacy of novel non-viral carrier combinations. The first panel of non-viral carriers tested are termed AVPs (artificial viral particles), in reference to their structural similarity to enveloped viruses, and were fabricated in a composite manner using a variety of polymers and lipids in order to deliver plasmid DNA. The most effective carrier found in these studies was 25 kDa PEI (polyethylenimine), with none of the AVPs showing a clear superior effect to that of 25 kDa PEI. While a highly effective gene carrier, PEI is extremely cytotoxic and hence studies were performed in attempt to decrease its toxicity while maintaining its functionality. These studies were performed by conjugating the highly hydrophilic polymer, PEG (polyethylene glycol), to PEI and then assessing the polymers for cytotoxicity and DNA binding. This was followed by investigating the particle size, cell uptake, and gene delivery of polyplexes fabricated with plasmid DNA and the PEI-PEG conjugates. Ultimately, it was found that PEGylation generally decreased the transfection efficacy of PEI, but under ideal conditions of PEG substitution and polymer/DNA (w/w) ratio, this decrease in efficacy can be circumvented, providing a highly effective carrier formulation for transfection.

## **Acknowledgements**

I would like to thank my committee members Drs. Robert Burrell, Ravin Narain, Hasan Uludağ, and Larry Unsworth.

The stipend which allowed me to complete this thesis was provided by a Canadian Institutes of Health Research (CIHR) Frederick Banting and Charles Best Canada Master's Scholarship, and a CIHR-Skeletal Regenerative Medicine Team Trainee Award.

I would like to thank Dr. Vishwa Somayaji for performing the proton-NMR and Dr. Hasan Uludağ for conducting the TNBS assay in this thesis; Drs. Remant Bahadur and Hamidreza Aliabadi for providing lipid-conjugated PEI; Dr. Guilin Wang for his advice regarding conjugation chemistry; Charlie Hsu for his suggestions regarding DNA uptake studies; summer student Anuja Samuel for her helpful assistance with flow cytometry; and Dr. Ravin Narain and his lab for kindly allowing me to use their ZetaPlus.

I thank all the members of the Uludağ Lab for their kindness, assistance, and friendship: Meysam Abbassi, Hamidreza Aliabadi, Charlie Hsu, Vanessa Incani, Cezary Kucharski, Breanne Landry, Nesrine Mostafa, Laura Rose, and Guilin Wang.

Most of all, I wish to express my gratefulness to Dr. Hasan Uludağ for his innumerable assistances and kind guidance during my time in his lab. I am extremely thankful.

# **TABLE OF CONTENTS**

<b>Section</b>	<b>Title</b>	<b>Page No.</b>
1)	Scope	1
2)	Introduction	4
2.1)	Viral Gene Delivery	4
2.1.1)	Retrovirus	6
2.1.2)	Adenovirus	7
2.1.3)	Adeno-associated Virus	8
2.1.4)	Herpesvirus	9
2.2)	Gene Therapy Trials	10
2.3)	Mimicking Viruses in Non-Viral Gene Delivery Using Peptides	14
2.3.1)	Cellular Uptake and Vesicular Escape	16
2.3.2)	Nuclear Import	18
2.4)	Mimicking Viruses in Non-viral Gene Delivery Using Viral Structure	19
2.4.1)	Lipids and Sterol Moieties	21
2.4.2)	Protamine	23
2.4.3)	Poly-L-Lysine	24
2.4.4)	Polyethylenimine	25
2.5)	PEI PEGylation	27
3)	Materials and Methods	29

3.1)	Cell Culture	29
3.2)	Lipid Preparation	30
3.3)	AVP Production and Transfection	30
3.4)	Flow cytometry and Plate Reader Measurements	31
3.5)	PEI-PEG Synthesis and Characterization	32
3.6)	Polymer Toxicity Assay	32
3.7)	Assessing Polymer-DNA Binding Affinity	33
3.8)	Dynamic Light Scattering Measurements of PEI-PEG	34
3.9)	Labelled DNA Uptake Studies with PEI-PEG	34
3.10)	Transfection of HEK293 Cells with PEI-PEG	35
4)	Results and Discussion	36
4.1)	Efficacy of PRT-based AVP Formulations on Modification of HEK293 Cells	36
4.2)	Efficacy of PLL-based AVP Formulations on Modification of HEK293 Cells	40
4.3)	Efficacy of Unmodified PEI-based AVP Formulations on Modification of HEK293 Cells	42
4.4)	Efficacy of PEI-PA and PEI-based AVP Formulations on Modification of HEK293 Cells	44
4.5)	Efficacy of PEI-LA, PEI-PEG and PEI-based AVP Formulations on Modification of HEK293 Cells	47
4.6)	Efficacy of AVP Formulations on Modification of BMSCs	49

4.7)	General Discussion and Conclusions: AVPs	50
4.8)	Polymer Characterization	53
4.9)	Polymer Toxicity	57
4.10)	Polymer/DNA Binding	61
4.11)	Sizes of PEI-PEG Polyplexes	66
4.12)	Plasmid Uptake Properties of PEI-PEG	69
4.13)	Transfection Properties of PEI-PEG	72
4.14)	General Discussion and Conclusions: PEI-PEG Transfections	86
5)	References	91
6)	Appendix A: NMR Spectra	103

## **LIST OF TABLES**

		<b>Page No.</b>
Table 1	Conditions for which gene therapy trials have been approved.	13
Table 2	A survey of the composite materials in AVP formulations with the polycationic condensing agents protamine (PRT), poly-L-lysine (PLL), and polyethylenimine (PEI).	20
Table 3	<sup>1</sup> H-NMR Results.	55
Table 4	TNBS Assay Results.	55
Table 5	N/P Ratio Calculations.	64

## **LIST OF FIGURES**

		<b>Page No.</b>
Figure 1	Viral peptide-mediated trafficking of DNA nanocarriers.	15
Figure 2	HEK293T flow cytometry results of AVPs using protamine (PRT) as a DNA condensor.	39
Figure 3	HEK293T flow cytometry results of AVPs using poly-L-Lysine (PLL) as a DNA condensor.	41
Figure 4	HEK293T flow cytometry results of AVPs using polyethyleneimine (PEI) as a DNA condensor.	43
Figure 5	HEK293 flow cytometry results of AVPs using unmodified PEI and palmitic acid-modified PEI (PEI-PA) as DNA condensers.	46
Figure 6	HEK293T flow cytometry results of AVPs using PRT, PEI, PEI-PEG, and linoleic acid-modified PEI (PEI-LA) as DNA condensers.	48

Figure 7	BMSC (bone marrow stromal cell) transfection results of AVPs using PRT, PEI, PEI-PEG, and linoleic acid-modified PEI (PEI-LA) as DNA condensers.	49
Figure 8	Reaction scheme for the PEGylation of PEI.	54
Figure 9	<sup>1</sup> H-NMR spectra of polymer products.	54
Figure 10	TNBS assay and correlation to NMR data.	56
Figure 11	Assessment of polymer cytotoxicity.	59
Figure 12	Correlation between cytotoxicity and PEG composition.	60
Figure 13	Assessment of polymer binding to plasmid DNA.	63
Figure 14	Polymer binding by N/P ratio and correlation to PEG composition.	65
Figure 15	Polyplex size measurements.	68
Figure 16	Assessment of plasmid uptake.	71
Figure 17	Surface plot of plasmid uptake.	72
Figure 18	Transfection efficacy of PEI-PEG.	73
Figure 19	Mean fluorescence as a function of PEG composition.	80
Figure 20	Percent transfection as a function of PEG composition.	81
Figure 21	Transfection efficacy as a function of N/P ratio.	83
Figure 22	Surface plots of mean fluorescence and percent transfection.	85

## **LIST OF ABBREVIATIONS**

AAV	adeno-associated virus
Ad	adenovirus
AVP	artificial viral particle
BC50	50% binding concentration
bFGF	basic fibroblast growth factor
BMSCs	bone marrow stromal cells
CAR	coxsackie-adenovirus receptor
CE	cellulose ester
CHCl <sub>3</sub>	chloroform
CHEMS	cholesteryl hemisuccinate
Chol	cholesterol
Cy3	cyanine 3
D <sub>2</sub> O	deuterated water
DDAB	dimethyldioctadecyl-ammonium bromide
ddH <sub>2</sub> O	double distilled water
DLPE	1,2-dilauroyl-sn-glycero-3-phosphoethanolamine
DLS	dynamic light scattering
DMEM	Dulbecco's modified eagle medium
DMSO	dimethyl sulfoxide
DNA	deoxyribonucleic acid
DOPE	1,2-Dioleoyl- <i>sn</i> -glycero-3-phosphoethanolamine
DOPS	1,2-dioleoyl-sn-glycero-3-phospho-L-serine
DOTAP	1,2-Dioleoyloxy-3-trimethylammonium propane chloride
DPPE	1,2-Dipalmitoleoyl-sn-glycero-3-phosphoethanolamine
dsDNA	double stranded deoxyribonucleic acid

EMSA	electrophoretic mobility shift assay
EPC	egg phosphatidylcholine
EPOPC	1-palmitoyl-2-oleoyl-sn-glycero-3-ethylphosphocholine
FBS	fetal bovine serum
FGFR	fibroblast growth factor receptor
FRET	fluorescent resonance energy transfer
GFP	green fluorescent protein
HA	hemagglutinin
HBSS	Hank's Buffered Salt Solution
HEK293	human embryonic kidney 293 cells
HEPES	4-(2-hydroxyethyl)-1-piperazineethanesulfonic acid
HIV	human immunodeficiency virus
hrs	hours
HSV	herpes simplex virus
kDa	kilodaltons
LA	linoleic acid
LMW	low molecular weight
LTRs	long terminal repeats
mg	milligrams
min	minutes
mL	millilitres
mM	millimolar
mPEG	methoxy-PEG
MTT	3-(4,5-Dimethylthiazol-2-yl)-2,5-diphenyltetrazolium bromide
N <sub>2</sub>	nitrogen gas
NHS	N-hydroxysuccinimide

NMR	nuclear magnetic resonance
NPC	nuclear pore complex
ODN	oligodeoxynucleotide
PA	palmitic acid
PDGF	platelet-derived growth factor
pDNA	plasmid deoxyribonucleic acid
PEG	polyethylene glycol
PEI	polyethylenimine
PLL	poly-L-lysine
PNA	peptide nucleic acid
PRT	protamine
R8	octaarginine
RNA	ribonucleic acid
scFv	single-chain variable fragment
siRNA	small interfering ribonucleic acid
ssDNA	single stranded DNA
SV40	simian virus 40
TNBS	trinitrobenzene sulfonate
VSV	vesicular stomatitis virus
μg	micrograms
μL	microlitres

## 1) Scope

The focus of this thesis is the field of gene delivery and the development of non-viral alternatives to traditionally used viral vectors. This thesis provides a review of such viral vectors and the efforts being made to translate their capabilities to nanopharmaceutics (drug delivery systems in the 1-1000 nm range) for the purpose of improving controllability, scalability, and safety. The efforts described include the incorporation of specific viral sequences into nanocarriers as well as the mimicking of general viral structure.

This thesis also reports a number of my own studies utilizing AVPs (artificial viral particles), which mimic the structure of enveloped viruses, and consist of plasmid DNA, a polycation, and lipid(s). While collectively in the literature, a multitude of AVPs with a variety of polymers and lipids have been assessed, most individual studies are conducted with limited reagents and combinations making comparisons between various AVPs difficult. Hence, the aim of my transfection studies was to systematically test a panel of AVPs using a broad range of polymers, lipids and preparation ratios, in order to obtain a general overview of the effectiveness of a large variety of AVP formulations. While these studies examined commercially available polymers and lipids already utilized for AVP production in the literature (PEI, polyethylenimine; PLL, poly-L-lysine; PRT, protamine; DOTAP, 1,2-dioleoyl-3-trimethylammonium-propane chloride; DOPE, 1,2-Dioleoyl-*sn*-glycero-3-phosphoethanolamine; CHEMS, cholesteryl hemisuccinate), polymers made in-house were also utilized. These included 25 kDa PEI conjugated with 2 kDa PEG (polyethylene glycol); 2 kDa PEI conjugated with linoleic acid (LA); and finally 0.6, 1.2, and 2.0 PEI conjugated with palmitic acid (PA). These polymers permitted novel AVP formulations of cationic lipids combined with both highly hydrophilic and hydrophobic polycations. Studies using such a broad range of materials to make AVPs are unprecedented and serve as a useful means of comparison for the purpose of optimizing these nanoparticles.

These studies were performed with HEK293T cells and clinically important bone marrow stromal cells (BMSCs). BMSCs, containing a multipotent stem cell fraction, are a primary cell type with applications in bone regeneration and other types of mesenchymal tissue engineering. HEK293T cells permitted the detection of minute differences between each carrier's efficiency due to their high transfection efficiency, while transfection of BMSCs was performed to evaluate each carrier's effectiveness in modifying a cell type with low transfection efficiency and potential in cell-based gene therapies. While successful AVP formulations were found (containing either protamine or PEGylated polyethylenimine and DOTAP and DOPE as the coating lipids), ultimately the most effective carrier was the synthetic polycation PEI when used as the sole condensing agent.

While 25 kDa PEI was found to be most effective at gene delivery, its membrane-destabilizing properties cause high cytotoxicity. Hence, experiments were conducted with the aim of decreasing the toxicity of PEI while maintaining its high functionality. This thesis describes the covalent modification of PEI with polyethylene glycol (PEG) and subsequent studies assessing the functionality of a number of these PEGylated polymers. The effectiveness of PEI-PEG as a complexing agent was demonstrated to be highly dependent on the weight ratio of polymer/pDNA used. In fact, the results suggested that an optimal PEG substitution and weight ratio may even increase the effectiveness of PEI compared to unmodified polymer. PEI conjugates with increased PEG substitution demonstrated lower toxicity on a per total polymer weight basis, but failed to decrease toxicity on a per PEI backbone weight basis. Polymer/pDNA binding affinity was found to be unaffected by PEG substitution when the differing percentages of PEI backbone in each polymer was accounted for. Dynamic light scattering measurements indicated high PEG conjugation prevents an increase in polyplex size in the presence of serum, whereas polyplexes without PEG conjugation or with lower PEG substitution increased in size. However, due to the small changes in size, differences in particle size resulting from PEGylation are unlikely to

affect transfection efficiency. Particle uptake was found to have a complex relationship with increasing PEGylation, dependent on polymer/pDNA weight ratio. Interestingly, this increased uptake with increasing weight ratio was not accompanied with increased transgene expression and hence PEGylation may modulate the intracellular behaviour of PEI polyplexes. Determining the characteristics of PEGylated polyplexes which modulate the effectiveness of PEI will permit the intelligent design of novel PEI-PEG polymers that overcome the hurdles attributed to PEGylation.

Taken together, these studies involving AVPs and PEGylated PEI strive to advance the search for an effective and non-toxic nanocarrier for therapeutic nucleic acids. With the promise of gene therapy and the growing number of silencing techniques, it is of utmost importance to successfully engineer a nanodelivery system capable of actualizing nucleic acid-based therapeutics as a viable treatment option.

## **2) Introduction**

*A version of this chapter has been published.*

*Rose et al. 2011. Gene Therapy in Bone Regeneration: A Summary of Delivery Approaches for Effective Therapies. Intracellular Delivery: Fundamentals and Applications. pp. 813-846.*

With the ongoing maturation of modern molecular biology and the recent completion of the human genome project, the prospect of nucleic acid-based therapies is quickly entering into the forefront of viable treatment options for numerous pathologies. Diseases caused and/or affected by a single or small number of genes are the frontrunners for therapeutic development of this nature due to the relative ease of delivering smaller amounts of nucleic acid intracellularly. Such therapies may exploit both augmentation and elimination strategies by either gene therapy or siRNA/ODN (small interfering RNA/oligodeoxynucleotide) delivery in order to treat conditions resulting from both deficient gene products and those in excess, respectively.

While many therapeutic and pathologically relevant genes are known, the current challenge is essentially concerned with the intracellular delivery requisite for successful treatment. To this end, viral carriers have been extensively engineered for therapeutic purposes with mixed success. While generally effective in terms of delivery and expression, these carriers have numerous safety issues associated with them, namely oncogenic integration and immunological complications. While their direct use may prove unviable for most applications, they do serve as useful models for highly effective intracellular nucleic acid delivery.

### **2.1) Viral Gene Delivery**

Fostered by millions of years of evolution, viruses are the masters of intracellular delivery of nucleic acid. Their extraordinary efficiency permits effective gene delivery to a multitude of cell types while providing an effective model of gene delivery that can be emulated with non-viral

carriers. The general paradigm for engineering viruses into useful experimental reagents and therapeutics requires disabling their replication and pathogenicity while forcing them to express a desired genetic material. The usual method for this involves separating the viral genome into two (or more) DNA molecules (1). One molecule (the vector construct) carries the desired foreign sequences and any *cis*-acting viral elements necessary for transcription and packaging the foreign DNA into viral particles and the other (the packaging construct, which is either a plasmid or a genomically-inserted cassette of a packaging cell line) encodes viral structural proteins and any other proteins essential for the production of viral particles. Genes that are deemed nonessential or associated with pathogenicity are excised in order to maximize the space available for foreign sequences, as well as to prevent deleterious effects on infected cells in the event of unintended recombination between constructs (2). In this way, the engineered viral particles can not replicate post-infection due to the absence of the packaging construct and can not cause detrimental effects for viral replication, cell lysis, immunoreaction, and rampant infection.

Viral vectors often utilized include members of the retrovirus family (lentivirus, oncoretroviruses, spumaviruses), adenovirus, adeno-associated virus, and herpesvirus (1, 2). While retroviral vectors are particularly easy to engineer, more complicated vectors such as adenovirus pose more of a challenge. The retroviral genome can essentially be swapped out of its flanking LTRs (long terminal repeats) in exchange for foreign sequence to make the vector construct and retroviral particles can easily be manufactured in packaging cell lines (3). Viruses such as adenovirus, however, require elaborate recombination strategies and helper-dependent systems to produce functional particles free of pathogenic and replication-associated genes (4-6). The complex genetic engineering and optimization of viral gene combinations to create safe and functional constructs are two hurdles associated with viruses that non-viral gene delivery largely circumvents. That said, the necessary engineering of viral carriers is rewarded with exceptional transduction efficiencies due to their ability to efficiently navigate their genome past numerous cellu-

lar barriers. Cellular barriers for effective viral nucleic acid delivery include passage through cell membrane (either by direct fusion or vesicular escape) and trafficking through the cytoplasm and the nuclear envelope. As outlined below, each virus has acquired highly specialized features (due to evolution and human modifications) allowing them to overcome these barriers and successfully express a gene sequence.

### **2.1.1) Retrovirus**

Members of the family *Retroviridae* are enveloped viruses principally characterized by their ability to reverse transcribe their single stranded RNA genome into integrating DNA. Retroviral infection begins with nonspecific binding to the cell surface followed by specific attachment between the viral envelope glycoproteins (Env proteins) and their target receptors (7) (8). Following this binding, the membranes of both the cell and enveloped-virus fuse mediating the entry of the retroviral nucleocapsid into the cytoplasm (9). The tropism of retroviral vectors has been greatly expanded by exchanging the wild-type attachment-protein genes with those from related viruses (in the packaging cell line or packaging construct), a technique known as pseudotyping (10). Pseudotyping is most commonly performed with the Env glycoprotein of vesicular stomatitis virus (VSV-G), which bestows an extremely broad tropism (11). Following the release of the nucleocapsid into the cytoplasm, the viral RNA genome is reverse-transcribed into dsDNA (with the exception of Foamy Virus particles which can reverse-transcribe their genome and deliver a DNA genome) (3, 12). Prior to inserting into the host's genome, the preintegration complex can either be actively imported through the nuclear envelope by cellular proteins (in the case of lentiviruses, like HIV) or remain cytoplasmic until the nuclear membrane is disrupted during mitosis (13-15). With the exception of lentiviruses, this inability to pass through the nuclear envelope is a

major bottleneck to most retroviral vectors and hence generally limits their use to cells with high mitotic activity (16).

### **2.1.2) Adenovirus**

Members of the family *Adenoviridae* are non-enveloped viruses with icosahedral capsids which contain (generally) non-integrating linear dsDNA. Cellular internalization is initiated by most adenoviral serotypes through binding of their fibre knobs to the Coxsackie-adenovirus receptor (CAR) (17). Subsequent binding of their penton base proteins to alpha-V integrins predominantly results in clathrin-mediated endocytosis (18, 19). Expanding the tropism of non-enveloped viruses through pseudotyping is slightly more challenging than their enveloped counterparts due to the fact that foreign proteins engineered into the virus must be structurally compatible with the native capsid proteins and cannot simply be inserted into a lipid bilayer (20). That said, the tropism of individual adenoviral strains have been successfully expanded by replacing fibre proteins with homologous proteins from related serotypes, unrelated viruses and even with single-chain variable fragment (scFv) antibodies to confer specific targeting (21-23). Once endocytosed, it is generally accepted that the decrease in pH along the endocytic pathway induces a conformational change of the penton base proteins causing membrane disruption and permitting escape to the cytosol (24, 25). The virion is then transported to the nucleus in a dynein/dynactin-dependant manner where the dsDNA genome is actively imported through the nuclear pore complex (NPC) (26, 27). Nuclear uptake is an elaborate process whereby NPC docking is mediated by viral hexamer proteins followed by the entry of the genome and the DNA-condensing proteins mu and VII through the NPC (28, 29). The host proteins Nup214, histone H1, and hsc70 have also been implicated in adenovirus docking, capsid disintegration and DNA uptake (28, 27). This nuclear targeting is a considerable feat considering that the commonly used serotypes Ad2 and Ad5 have a ~36 Kb genome (virion size, 70-100 nm), which is much larger than most non-viral plasmid-

based systems in terms of DNA payload (30-32). Generally, the adenoviral genome then remains episomal in the nucleus (not integrating into the host genome) (33). The episomal preference of adenoviral vectors, and their ability to actively import into the nucleus, make them both safer and more efficient compared to most retroviral strains. That said, adenoviral vectors carry the disadvantages of occasional integration, transient transgene expression (as a consequence of non-integration), and immunological reactivity resulting from prior exposure (34). Some studies have focused on using less common serotypes, than the typically used Ad2 and Ad5, in order to decrease the possibility of an immune reaction (35).

### **2.1.3) Adeno-associated Virus.**

AAV belongs to the family *Parvoviridae*, and similar to adenovirus has a non-enveloped icosahedral capsid and a DNA genome, however its genome is single stranded and has a higher propensity to integrate (2). Unlike adenovirus, AAV carries the distinct advantage of not being associated with any pathogenic conditions and is generally considered to produce a less severe immune response (2, 36). Also unlike adenoviruses, AAV serotypes used in gene delivery studies bind to a diverse array of cellular receptors naturally resulting in a variety of preferential cell-types. For example, the commonly used serotype AAV2 utilizes heparan sulfate proteoglycan and the coreceptors FGFR1 and integrin  $\alpha_v\beta_5$  (37-39); AAV4 uses sialic acid, as does AAV5, though with a different carbohydrate linkage and an interaction with PDGF receptors (40, 41). The precise mechanism by which AAV escapes the endocytic pathway after clathrin-mediated endocytosis has not been fully elucidated. Endosomal acidification is required, but unlike adenovirus, the intact virion appears to enter the nucleus without the loss its capsid coat; this is debateable, however, and may be a serotype specific phenomenon (42, 43). The ability of the entire capsid to pass through the NPC is likely a result of its small size of ~26 nm, as molecules <40-60 kDa may passively diffuse through the NPC (44, 45). Following viral uncoating in the nucleus the ssDNA

load may be converted to dsDNA and then remain episomal like adenovirus, or integrate into the host's genome if the viral rep gene is present (46, 47). Much safer compared to retroviruses, AAV usually integrates at a highly specific location (AAVS1) in the human genome on chromosome 19, hence having a lower probability of oncogenic mutation (48). AAV does carry disadvantages, however, most notably its limited payload of ~5 kb and the necessity of infecting packaging cells with helper viruses (such as adenovirus or herpesvirus) due to its inability to replicate itself (49, 43).

#### **2.1.4) Herpesvirus.**

Members of the family *Herpesviridae* are enveloped viruses containing a non-integrating dsDNA genome. In stark contrast to AAV, Herpes simplex virus type I can hold over 30 Kb of foreign sequence (50). HSV infection is more complicated than the fore-mentioned vectors in that cellular entry requires many protein interactions. Cell binding is mediated by viral proteins gB and gC interacting with heparan sulfate, while gD binds to herpesvirus entry mediators HveA and HveC (51). Membrane fusion between the cell and the enveloped virion seems to require the presence of gB, gD, and gH/gL (52). The tropism of HSV may be expanded by genetically altering the glycoproteins gB, gD, and more successfully gC (53-56). Following active uptake into the nucleus, wild-type HSV may either follow a lytic cycle initiating transcription or (as in the case of engineered constructs) exist in a latent episomal state (57, 52). The transcriptional persistence of the foreign sequences largely depends on what specific class of vector was used: a recombinant HSV-1 vector or a HSV-derived amplicon vector. A rHSV-1 vector is replication deficient and can be produced in large quantities but its transgene expression is transient; additionally, it still contains large regions of the wild-type genome and carries the risk of expressing toxic and immunogenic proteins (1). HSV-derived amplicon vectors only carry essential *cis*-acting se-

quences along with a transgene that can be expressed long-term, but their production requires a replicating helper virus or the use of cosmids or artificial chromosomes expressing the essential structural proteins (58-60).

Ultimately, the appropriate choice of a viral vector for a clinical application is largely dependant on the nature of the condition being treated in terms of target cell-type, time-frame of protein expression, size of the transgene needed, and the degree of risk appropriate for the condition. Beyond their direct application, viral vectors of all types provide a useful model of nucleic acid delivery and their specific mechanisms may be exploited to create safer non-viral vectors.

## **2.2) Gene Therapy Trials**

These viral vectors, along with others, have been investigated in gene therapy trials for numerous diseases since 1989. The majority of these trials have utilized adenovirus (24.7% of total trials, n (# of specified trials) = 331) and retrovirus (22.8%, n = 305) with the other major contender being simply naked DNA (18%, n= 241) (61). Viral vectors utilized far less include both AAV (3.5%, n = 47) and HSV (3.2%, n = 43) also discussed previously (61). These vectors are being used to deliver genes to a wide range of pathological conditions.

The first implementation of human gene delivery was performed on five patients with metastatic melanoma by the insertion of the neomycin resistance gene with retrovirus into tumor-infiltrating lymphocytes, which were later reinfused (62). This was then followed by a study on two patients with the monogenic disorder SCID (severe combined immunodeficiency) characterized by a deficiency in the gene encoding ADA (adenosine deaminase) (63). Since these initial studies, the range of diseases undergoing clinical investigation using gene therapy has grown extensively. The vast majority of worldwide gene therapy clinical trials investigate cancer (66.5%, n = 871), cardiovascular disease (9.1%, n= 119), monogenic disorders (8.3%, n = 109), and infec-

tious disease (6.5%, n=85) (61), as well as neurological diseases (1.5%, n = 20) and ocular diseases (0.9%, n =12) to a far lesser extent. The specific conditions for which trials have been approved are listed in Table 1. The predominance of trials for both cancer and cardiovascular disease is explained by the high prevalence of these serious conditions and the large burden they place on the medical system. The relatively large proportion of trials devoted to monogenic disorders is explained by the obvious necessity of gene therapy for such conditions.

While gene therapy trials have largely focused on the use of viral vectors, issues regarding the safety of using viruses have been noted and presently act as a major barrier to the common clinical usage of gene therapy. One such issue is immunogenicity, which can not only result in the inactivation of a viral-based therapy, but in some cases, can result in serious side-effects for the patient if the inflammatory reaction is severe. Such an immune reaction was first noted in a trial in 1999, in which a patient with ornithine transcarbamylase (OTC) deficiency was treated with an Ad5 vector and had a systemic inflammatory response resulting in his death (64). This event had a major effect on the field of gene therapy with the FDA halting multiple trials as a result (65). It also placed new importance on the need for serotypes and viral vectors not commonly exposed to patients pre-treatment, and highlighted the potential risks associated with multi-administered doses of viral vector.

The second major safety issue of viral gene therapy regards the risk of insertional mutagenesis resulting in cancer. This was initially noted in one of the first conditions treated with gene therapy, SCID; however, in this particular case the disorder was caused by mutations in the gene encoding an interleukin receptor instead of the form previously mentioned resulting from ADA deficiency. While the trial was initially thought to be a success (66), several of the patients developed leukemia resulting from retroviral insertion in close proximity to the LMO2 (LIM domain only 2) proto-oncogene (67). Similarly, insertion near this genomic site was noted in a patient treated for Wiskott-Aldrich syndrome who also developed leukemia (68).

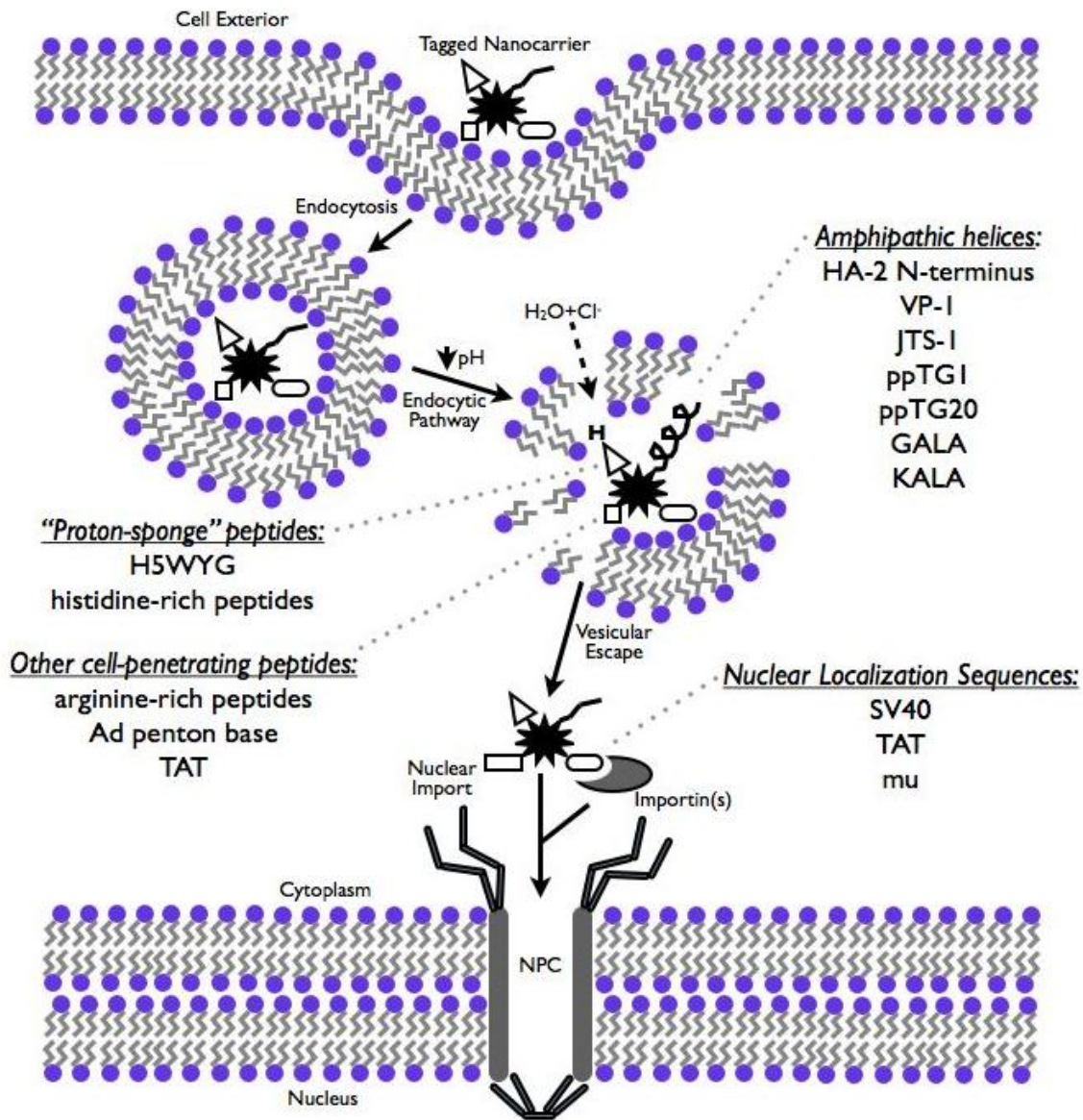
Given these dramatic risks, alternatives to viral vectors are now being investigated for non-viral gene therapy. The rationale being that nanocarriers carry less risk of inducing an immune response, as they have not been exposed to the patient prior to treatment, and can be made to evade the immune system with various modifications. Additionally, the risk of a plasmid integrating within the host genome, resulting in insertional mutagenesis, is considered far less compared to most viral vectors. The main challenge to this avenue of study is the development of nanocarriers with the same efficacy of viruses, which presently exceed that of synthetic carriers. For this reason, viral-based clinical trials are far more numerous than non-viral. In fact, only 7.6% of all clinical trials conducted between 1989 and 2007 were performed using lipofection (61). However, given the better safety profile of non-viral methods and ongoing research into improving the efficacy of nanocarriers, the prevalence of non-viral methods in clinical trials will undoubtedly increase. Not only will this permit safer options for conditions presently being investigated by viral methods but will allow gene therapy research into conditions considered insufficiently detrimental to warrant the risk of viral vectors.

Table 1. Conditions for which gene therapy trials have been approved. Adapted from the work of Edelstein *et al.*(61) .

<p><b>Monogenic disorders</b>            Cystic fibrosis            Severe combined immunodeficiency (SCID)            Alpha-1 antitrypsin deficiency            Haemophilia A and B            Hurler syndrome            Hunter syndrome            Huntington's chorea            Duchenne muscular dystrophy            Becker muscular dystrophy            Canavan disease            Chronic granulomatous disease (CGD)            Familial hypercholesterolaemia            Gaucher disease            Fanconi's anaemia            Purine nucleoside phosphorylase deficiency            Ornithine transcarbamylase deficiency            Leukocyte adherence deficiency            Gyrate atrophy            Fabry disease            Familial amyotrophic lateral sclerosis            Junctional epidermolysis bullosa            Wiskott-Aldrich syndrome            Lipoprotein lipase deficiency            Late infantile neuronal ceroid lipofuscinosis            RPE65 mutation (retinal disease)            Mucopolysaccharidosis</p> <p><b>Cardiovascular disease</b>            Peripheral vascular disease            Intermittent claudication            Critical limb ischaemia            Myocardial ischaemia            Coronary artery stenosis            Stable and unstable angina            Venous ulcers            Vascular complications of diabetes            Pulmonary hypertension            Heart failure</p> <p><b>Infectious disease</b>            HIV/AIDS            Tetanus            Epstein-Barr virus            Cytomegalovirus infection            Adenovirus infection            Japanese encephalitis            Hepatitis C            Hepatitis B            Influenza</p>	<p><b>Cancer</b>  <b>Gynaecological</b>            - breast, ovary, cervix  <b>Nervous system</b>            - glioblastoma, leptomeningeal carcinomatosis, glioma, astrocytoma, neuroblastoma  <b>Gastrointestinal</b>            - colon, colorectal, liver metastases, post-hepatitis liver cancer, pancreas  <b>Genitourinary</b>            - prostate, renal  <b>Skin</b>            - melanoma  <b>Head and neck</b>            - nasopharyngeal carcinoma  <b>Lung</b>            - adenocarcinoma, small cell, non small cell  <b>Mesothelioma</b>  <b>Haematological</b>            - leukaemia, lymphoma, multiple myeloma  <b>Sarcoma</b>  <b>Germ cell</b></p> <p><b>Neurological diseases</b>            Alzheimer's disease            Carpal tunnel syndrome            Cubital tunnel syndrome            Diabetic neuropathy            Epilepsy            Multiple sclerosis            Myasthenia gravis            Parkinson's disease            Peripheral neuropathy</p> <p><b>Ocular diseases</b>            Age-related macular degeneration            Diabetic macular edema            Glaucoma            Retinitis pigmentosa            Superficial corneal opacity</p> <p><b>Other diseases</b>            Inflammatory bowel disease            Rheumatoid arthritis            Chronic renal disease            Fractures            Erectile dysfunction            Anaemia of end stage renal disease            Parotid salivary hypofunction            Type I diabetes            Detrusor overactivity            Graft versus host disease</p>
---	---

### **2.3) Mimicking Viruses in Non-viral Gene Delivery Using Peptides**

Non-viral carriers share some general properties with viral particles (nano-scale size and a capacity to penetrate the plasma membrane) and they have been often engineered to emulate viral gene delivery in a specific manner. These systems mimic the specific molecular mechanisms to overcome each cellular barrier to nuclear delivery. This is generally accomplished through incorporating short viral peptides into the non-viral system permitting binding to and penetration through the plasma membrane, and targeting to and through the nuclear envelope (Fig. 1).



**Figure 1.** Viral peptide-mediated trafficking of DNA nanocarriers. The association of a nanocarrier with peptides derived from viral proteins can facilitate the navigation of DNA past cellular barriers to the nucleus. Peptides which facilitate endocytic escape include those that form membrane-destabilizing amphipathic helices upon acidification, proton-sponge peptides which disrupt endosomes by osmotic effects, and those that penetrate membranes by alternate (or unknown) means. Nuclear targeting can be accomplished by utilizing nuclear localization sequences that recruit importin proteins which guide the nanocarrier through the nuclear pore complex (NPC).

### 2.3.1) Cellular Uptake and Vesicular Escape

Nanocarrier internalization can potentially be mediated by a number of uptake mechanisms. These routes include clathrin-mediated endocytosis, caveolae-mediated endocytosis, macropinocytosis, and a variety of less well-defined mechanisms (69, 70). Clathrin-mediated endocytosis is characterized by the involvement of specific receptor-ligand interactions resulting in concentrated ligands within clathrin-coated pits which are internalized as coated vesicles by the action of dynamin. Caveolae-mediated endocytosis is also receptor mediated, but instead of entry regions being coated with clathrin, caveolae are enriched with caveolin, cholesterol, and sphingolipids. Uptake by macropinocytosis is non-specific (ie. not requiring receptors) and occurs in ruffled regions on the cell membrane using actin dynamics resulting in fluid phase endocytosis in which ligands are internalized relatively unconcentrated compared to the extracellular fluid. Following uptake by these mechanisms, vesicular escape is required to allow nuclear uptake and, depending on the endocytic mechanism, to prevent enzymatic degradation in lysosomes. A number of peptides have been utilized to disrupt vesicular membranes to facilitate this escape.

One commonly used motif is the pH-sensitive amphipathic helix, which has aspartic and/or glutamic residues concentrated on one side of the helix. At neutral pH, the peptide has no secondary structure, but as the pH decreases along the endocytic pathway and the acidic residues become protonated, alpha-helix formation results that can lead to protein multimerization and membrane destabilization (71). The fusogenic N-terminus of hemagglutinin HA-2 from influenza virus is one example and has been used in both poly-L-lysine and liposomal systems to successfully increase endosomal escape (72, 73). Endosomal escape has also been increased with the synthetic peptide H<sub>5</sub>WYG (GLFHAI AHFIHGGWHGLIHGWYG) which is a derivative of the HA-2 N-terminus (GLFGAIAGFIEGGWTGMIDGWYG) with 5 residues replaced with histidines (74). The proton sponge effect is thought to impart the endosomolytic property of H<sub>5</sub>WYG whereby the histidyl secondary amines become protonated at low pH causing endosomal rupture.

Another molecule employing membrane-destabilizing helix formation is the VP-1 protein from rhinovirus and the synthetic peptides JTS-1, ppTG1, ppTG20, GALA, and KALA which all mimic the same viral model of helix-mediated endosomal escape (75-79).

The arginine-rich TAT peptide from the lentivirus HIV has also been used to facilitate vesicular escape. This peptide has been utilized in both polymer and liposomal systems to increase transfection (80-82). A number of linear and branched arginine-rich synthetic peptides inspired by the TAT peptide have been developed that can also act as cell-penetrating peptides (83-85). While TAT and similar synthetic peptides have been used in a variety of non-viral systems, both their preferential endocytic route (likely a combination of direct fusion, clathrin-mediated endocytosis and macropinocytosis) and their mechanism of traversing membranes remain ill-defined (86, 87). It appears that their ability to bind to cell membrane plays a functional role as much as their role in endosomal escape.

Also notable of the viral peptides utilized by nanocarriers is the penton base protein of adenovirus serotype 5 (Ad5) (88). As mentioned before, this peptide permits binding to alpha-V integrins mediating cellular internalization and causes membrane destabilization at low pH permitting endocytic escape. While penton base complexes have been shown to follow multiple endocytic routes (as with native adenovirus), it is thought that the nanocarrier population that contributes to nuclear delivery follows a clathrin-mediated endocytic route (89). Also similar to native adenovirus, penton base proteins seem to be capable of utilizing microtubules and dynein to traffic to the perinuclear region, potentially making them useful for not only vesicular escape but for increasing nuclear uptake as well (89).

### **2.3.2) Nuclear import**

The viral peptides specifically involved in nuclear targeting have also benefited non-viral nanocarriers. While many carriers can successfully achieve cytoplasmic localization, nuclear targeting remains a major rate-limiting step. This is especially true in cells with low mitotic activity where nanocarriers are faced with the barrier of an intact nuclear envelope. Most viral vectors are far more effective at nuclear delivery and hence integrating their targeting peptides into non-viral systems has become a common approach to overcoming this bottleneck. Studies using nuclear import signals have overwhelmingly utilized the Large T-antigen NLS (nuclear localization sequence) of SV40 (Simian Virus 40). This monopartite NLS binds importin-alpha, which itself has a bipartite NLS that can bind to importin-beta resulting in the import of the entire complex through the nuclear pore (90). A number of approaches have been undertaken to facilitate nuclear DNA delivery using the SV40 NLS. Plasmid DNA has been modified with the peptide by simple electrostatic interactions, peptide nucleic acid (PNA) coupling, streptavidin-biotin systems, and covalent linking (91-94). The peptide can also be associated with polymer or lipid-based carriers instead of being linked to the DNA directly (95-97). While eclipsed by the use of SV40 NLS, other viral peptides can facilitate nuclear targeting of non-viral carriers as well. The HIV-derived TAT peptide, mentioned above for its membrane-destabilizing properties, can also serve as a nuclear-localizing agent when complexed with DNA (81). Similarly, the mu peptide from the core complex of adenovirus was initially used to condense DNA but was later found to have nuclear localizing properties when used in liposomal formulations (98-100).

The appropriate choice and further optimization of viral peptides for gene-delivery is largely dependent on the strengths and weaknesses of the carrier and the role they must fulfill in the non-viral system. The mechanisms by which viral peptides function are inherently very specific, yet they effectively demonstrate the general means by which less specific nanocarriers must also function.

#### **2.4) Mimicking Viruses in Non-viral Gene Delivery Using Viral Structure**

While specific viral sequences have been utilized for non-viral gene delivery, nanocarriers that mimic basic viral structure have also been an avenue of extensive study. Multiple groups have investigated the efficacy of such nanocarriers, which are structurally similar to enveloped viruses in that their nucleic acid payload is condensed with a polycationic polymer and then associated with lipids. This general structural feature is reminiscent of the molecular architecture of the retrovirus and herpesvirus families discussed earlier. For each of the three components (nucleic acid, polymer/peptide, lipid(s)) of these Artificial Viral Particles (AVPs), there is a variety of materials that may be utilized, and hence, there is a plethora of variations of which these nanocarriers can be composed (Table 2). Such diversity permits for the optimization of these particles for particular conditions and also allows for a large range applications.

**Table 2.** A survey of the composite materials in AVP formulations with the polycationic condensing agents protamine (PRT), poly-L-lysine (PLL), and polyethylenimine (PEI). Unspecified protamine type is indicated by question mark (?).

Polycation	Lipids/Sterols	Nucleic Acid	Additional Components	Cells/Tissue	Reference
Free-base PRT, PRT sulfate	DDAB	pDNA	-	COS-7, HeLa, NIH3T3, MDCK, BHK-21C13	(101)
PRT(?)	Cationic Chol, DC-Chol, DOTMA	pDNA	-	NIH3T3	(102)
PRT sulfate	DOTAP:Chol (1:0.9)	pDNA	asialofetuin	HepG2, <i>in vivo</i> mouse liver	(103)
PRT sulfate	DOTAP:Chol (1:1)	pDNA	-	Nude mouse tumor xenograft (MDA-MB-361, WSUHN-31)	(104)
PRT sulfate	Monostearin + 0-20% (wt) oleic acid	pDNA	-	HEK293, MCF-7	(105)
PRT sulfate	DOPE:Chol (1:1)	pDNA	PEI 800 (conjugated to Chol)	A549, MCF-7	(106)
PRT(?)	EPOPC:Chol (1:1), DOTAP:DOPE (1:1), DOTAP:Chol (1:1)	pDNA	HSA	COS-7	(107)
PRT sulfate	DOPE:CHEMS (9:2)	pDNA	Stearylated SV40 NLS, Stearylated R8	BMDC, NIH3T3, HeLa	(108)
PLL, PRT Sulfate, Stearylated R8	DOPE/CHEMS (9:2)	siRNA	Stearylated R8	HeLa	(85)
PLL, PRT Sulfate, Stearylated R8	DOPE/CHEMS (9:2)	siRNA-encoding pDNA	Stearylated R8	COS-7	(109)
PLL	EPC/Chol (7:3)	pDNA	Stearylated R8	NIH3T3	(110)
PLL	EPC/Chol, DOPE/Chol, DOPE/CHEMS	pDNA	Stearylated R8	NIH3T3, HeLa, A549, dorsal mouse skin	(111)
PLL, PRT Sulfate, Stearylated R8	DOPE/CHEMS (9:2)	ODN	Stearylated R8	NIH3T3	(112)
5 kDa PEI (Lupasol G100) + jetPEI	DOPS:DLPE:Chol: <i>N</i> -glutaryl-DOPE (3:3:3:1)	pDNA	-	HEK293, HepG2, Jurkat	(113)

**Table 2.** Continued.

<b>Polycation</b>	<b>Lipids/Sterols</b>	<b>Nucleic Acid</b>	<b>Additional Components</b>	<b>Cells/Tissue</b>	<b>Reference</b>
5 kDa PEI (Lupasol G100)	DOPS:DOPE:Chol (1:1:1)	siRNA	-	Hippocampal neurons	(114)
5 kDa PEI (Lupasol G100) + 25 kDa PEI	DOPS:DLPE:Chol: <i>N</i> -glutaryl-DPPE (3:3:3:1)	pDNA	RGD cyclic peptide	MeWo	(115)
5 kDa PEI (Lupasol G100) + 25 kDa PEI	DOPS:DLPE:Chol: <i>N</i> -glutaryl-DPPE (3:3:3:1)	pDNA	RGD cyclic peptide	HUVEC, Saos-2, DU-145, LoVo, A549, JEG-3	(116)

In terms of nucleic acids therapeutics used for clinical applications, both gene augmentation and gene silencing strategies have been attempted using plasmid DNA, plasmid DNA-expressing siRNA, and siRNA alone (113, 109, 114). Cationic polymers typically include protamine (PRT), poly-L-lysine (PLL), and polyethylenimine (PEI), to name a few.

#### **2.4.1) Lipids and Sterol Moieties.**

The lipid coating in AVP is also a variable component consisting of either a sole cationic lipid (such as 1,2-Dioleoyloxy-3-trimethylammonium propane chloride (DOTAP)), or a combination of lipids (such as DOTAP and 1,2-Dioleoyl-*sn*-glycero-3-phosphoethanolamine (DOPE)), or alternatively a combination of lipids and sterols (such as DOPE and cholesteryl hemisuccinate (CHEMS)). Each of the lipids and sterols used in AVP production have unique properties. Some of the most commonly used lipids/sterols, and the ones I selected for my own studies, include DOTAP, DOPE, and CHEMS. The cationic lipid DOTAP is an effective transfection reagent when used alone and is suggested to facilitate escape from endosomal compartments by its ability to destabilize membranes (117). As with other cationic lipids, DOTAP is frequently combined with sterol moieties or neutral *helper lipids*, such as cholesterol or DOPE, respectively. Such bi-

component formulations have been demonstrated to increase lipoplex stability in the presence of competing cations (such as serum), and to increase the efficiency of delivery after cellular uptake by increasing endosomal escape (118, 119).

This increase in effectiveness with the addition of the fusogenic lipid DOPE, in particular, has been largely attributed to a conformational shift in the structure of the lipoplex from a lamellar structure towards a more hexagonal-phase structure (a  $H_{II}$  phase) (120, 121). This characteristic of DOPE originates from its molecular structure being an inverted cone shape, meaning it has a small head group relative to its hydrophobic tails. This “conical” shape of the lipid is thought to encourage lipid exchange between the membranes of the endocytic vesicle and the lipoplex, resultant causing fusion leading to endosomal escape (122). This shape prevents DOPE being able to form liposomes on its own and hence it must be combined with other lipids or sterols with larger head groups.

Besides DOTAP, DOPE has also been combined with the sterol moiety CHEMS (and other acidic amphiphiles such as diacylsuccinylglycerols) to form pH-sensitive lysosomes and AVPs (123, 124, 85). It is thought that as the lipoplex moves along the lysosomal pathway and is exposed to an increasingly acidic environment, the amphiphile (such as CHEMS) undergoes protonation which results in local dehydration. This then removes the steric hindrance supplied by proximal water molecules between the endocytic vesicle and the lipoplex, leading to increased lipid exchange and eventual membrane fusion (125). Hence, it is understandable that the ratio of fusogenic lipid (most commonly DOPE) to amphiphile is of critical importance; a balance between sensitivity to low pH and sufficient structural stability at physiological temperature must be found. In terms of DOPE:CHEMS, in particular, it has been noted that a ratio of 9:1 imparts instability starting at pH 6, while liposomes with a higher CHEMS content (5:5, 6:4, 8:2) only become unstable once a pH of 5 has been reached (126). Considering this finding, and the exten-

sive work of the Harashima group with AVPs consisting of a ratio of 9:2, I opted for using the same low ratio of 9:2 for my own AVP studies.

#### **2.4.2) Protamine**

The polycationic polymers utilized for AVPs may be of natural or synthetic origin. Protamine, for instance, is a naturally occurring peptide serving as a DNA condenser in sperm and is commercially isolated from the smelt of various fish species, such as salmon and trout. Protamine is a short peptide (50-110 amino acids) and is extremely rich in positively charged amino acids—particularly arginine—and has been known to be an effective antidote to heparin for decades (127-129). Its excellent safety profile and already common usage make it an excellent candidate as a DNA/RNA complexing agent in gene/siRNA-based therapies. Beyond protamine's confirmed ability to condense nucleic acids due to its arginine residues, it also has nuclear-localizing ability (130, 131). Conceivably, this is due to its positive residues mimicking the cellular nuclear localization sequence (NLS) of nuclear-destined proteins, which are also typically rich in basic amino acids. In fact, it has been suggested that four such NLS regions are present within a single protamine 32-mer (132). This is an extremely useful feature of the peptide, considering that passing the nuclear envelope is a major bottleneck of plasmid delivery. The one major detriment of protamine, however, is its lack of endosomolytic activity, which may place its payload at risk of lysosomal degradation. For this reason, protamine is a good candidate for being combined with lipids in AVPs; the efficient complexation and nuclear targeting ability of protamine is well-complemented by the membrane-disrupting abilities of various lipids. Experimentally, this combination has proven effective in multiple AVPs. Protamine has been shown to increase the effectiveness of liposomal formulations composed of DDAB, cationized cholesterol, DOTAP/Chol, monostearin/oleic acid, DOPE/PEI 800-Chol, and EPOPC (1-palmitoyl-2-oleoyl-sn-glycero-3-ethylphosphocholine)/ Chol (101-107).

Further elaborate nanocarriers utilizing protamine have been developed by the Harashima group, which they have termed MENDs (multifunctional envelope-type nano devices) (133). Not only do these MENDs contain a protamine/nucleic acid core and a outer lipid coating, but also arginine-rich peptides (octaarginine, R8) anchored into the lipid layer with a stearic acid-based tail. This added arginine corona was a progression from the group's previous findings that stearylated R8 is more effective at gene delivery compared to R8 alone (without liposomes) (134). These octaarginine peptides have been attributed to increasing the effectiveness of AVPs through the prevention of lysosomal degradation by increasing particle uptake by macropinocytosis (110). This action of octaarginine on AVPs may conceivably be attributed to the peptide mimicking the activity of the arginine-rich TAT protein found in HIV, which also partially utilizes macropinocytotic uptake, as discussed earlier.

### **2.4.3) Poly-L-Lysine**

Poly-L-lysine (PLL) is another amino acid-based polycation used in AVP production. Unlike protamine, PLL is not of natural origin (prepared under synthetic conditions); however, its constituent lysine residues are still linked by amide bonds. This is advantageous in that it permits the hydrolytic breakdown typical of other peptides in the presence of appropriate enzymes, and hence, is cleared through degradation more readily compared to other synthetic polycations, such as PEI. Commonly used as plate-coating reagent to bind to non-adherent cells, this polymer is also an effective transfection reagent for pDNA and siRNA when used as the sole carrier (135, 136). Part of the success of this polymer is its demonstrated nuclear-targeting ability (131), but it is unfortunately devoid of endosomolytic activity. For this reason, combining PLL with various lipids into AVPs could conceivably be an effective formulation; that is, combining PLL with membrane-destabilizing lipids may provide complementation of abilities. PLL has been combined with a number of liposomal formulations such as DOPE/CHEMS, EPC (egg phosphatidyl-

choline)/Chol, and DOPE/Chol (85-111). In practice, however, AVPs using PLL as a condensing agent for pDNA and ODN (oligodeoxynucleotide) are significantly less effective compared to those using protamine (109, 112). Two possible explanations have been suggested which serve as useful guidelines for designing AVPs. One being that in protamine-condensed cores, the nucleic acid is less tightly bound (due to a fraction of non-charged amino acids), compared to those condensed with PLL and hence nucleic acids can become unbound more easily within the cell. This is supported by EMSA (electrophoretic mobility shift assay) data in which protamine-condensed pDNA is more easily dissociated with poly-aspartic acid than PLL-condensed pDNA, and that nuclear-injected protamine-complexed DNA transcribes more effectively than PLL-complexed DNA (109, 131). The second explanation (pertaining solely to pDNA) is that protamine-condensed DNA experiences increased nuclear uptake compared to PLL-condensed DNA (131). Both characteristics of easy dissociation and increased nuclear uptake should then be important considerations in designing AVPs and, by extension, all non-viral carriers.

#### **2.4.4) Polyethylenimine (PEI)**

Also used in AVP formulations is 25 kDa PEI—a highly effective synthetic polycation when used as the sole condensing agent. PEI was one of the first polycations found to act as a successful transfection reagent (137). This synthetic polymer still remains a leading candidate as a non-viral vector for intracellular nucleic acid delivery. Its capacity to complex nucleic acid is attributed to formation of ionic interactions with the negatively charged phosphate backbone of nucleic acid with its high density of charged amines. Upon condensation the positively charged polyplexes have been shown to bind and enter cells by various uptake processes depending on both cell-type and particle size (138-141). Following uptake, the gradual decrease in pH by proton pumps along the endocytic pathway is thought to cause a proton sponge effect by which increased protonation of PEI causes an influx of chloride ions and an inward osmotic gradient

hence rupturing the vesicular membrane and releasing entrapped polyplexes (142, 143). The ability of PEI to both condense and deliver nucleic acid intracellularly has led to extensive investigation into the effectiveness of various forms of the polymer in terms of varying molecular weights, and degrees of branching (144, 145).

However, despite optimization for the effectiveness of PEI by modifying the architecture of the polycation, the main detriment of PEI—its toxicity—must also be addressed. The cytotoxic effect of PEI has been attributed to both necrotic and apoptotic mechanisms resulting from membrane damage and can be reduced by decreasing branching and polymer weight (146-148). Unfortunately, however, the means to decrease toxicity often come at the considerable expense of decreasing transfection efficiency as well. One solution to this includes the incorporation of biodegradable linkages in PEI-based polymers to facilitate their breakdown to less toxic lower molecular weight PEI (149-151). This modification, however, conceivably has no effect on the toxicity of the polymer when in its intact high molecular weight state. This inconvenience of high toxicity at high molecular weight may explain its previous incorporation into AVPs.

While no explicit reasoning is given in the literature, regarding the combining of high molecular weight PEI with lipids, a logical rationale may be to decrease the amount of PEI necessary for effective transfection by supplementing lipids into the complexing mixture. The end goal is to decrease the toxicity of the formulation while maintaining effective plasmid/siRNA delivery. This is a pertinent objective considering the high toxicity of PEI, so reducing the amount of high molecular weight PEI necessary for successful transfection would conceivably be a reasonable objective of designing AVPs composed of 25 kDa PEI. This has been attempted for both modifying melanoma and endothelial cells using liposomes composed of DOPS/DLPE/Chol/N-glutaryl-DPPE(1,2-dioleoyl-sn-glycero-3-phospho-L-serine/1,2-dilauroyl-sn-glycero-3-phosphoethanolamine/Cholesterol/N-glutaryl-1,2-Dipalmitoleoyl-sn-glycero-3-

phosphoethanolamine) (115, 116). In both cases, combining high molecular weight PEI (25 kDa) with liposomes was ineffective.

The rationale for combining low molecular weight (LMW) PEI ( $\leq 5$  kDa) with lipids is perhaps more obvious (though also not explicitly stated in reports) in that its poor transfection ability may be improved by lipid association. The lipid formulations combined with LMW PEI include DOPS/DOPE/Chol, as well as the same lipids used for 25 kDa PEI (DOPS/DLPE/Chol/N-glutaryl-DPPE), and similarly DOPS/DLPE/Chol/N-glutaryl-DOPE (113-116). Unlike using 25 kDa PEI, these AVPs were demonstrated to be effective carriers; however, due to the lack of appropriate lipid-only controls, it can not be stated whether LMW PEI actually increased the effectiveness of the liposomes.

## **2.5) PEI PEGylation**

Besides combining PEI with lipids into AVPs to decrease its working concentration, an alternative solution is to directly decrease the toxicity of high molecular weight PEI by introducing polyethylene glycol (PEG) into the polymer. After such a modification, the conjugate may be used without lipid supplementation. The highly hydrophilic nature of PEG produces a hydration shell around its conjugated partner molecule, hence reducing intermolecular interactions and resultantly decreases toxicity. PEI synthesis with bifunctionalized PEG to form alternating block copolymers has been performed with a variety of linking chemistries (152-154). Similarly, simply grafting PEG to PEI has also been performed using a variety of PEG molecular weights and degrees of substitution (155-159). In all studies where toxicity is assessed covalent modification of PEI with PEG appears to reduce toxicity of the polymer, but its specific effect regarding nucleic acid delivery is poorly defined.

In terms of transfection efficacy (or gene silencing in case of siRNA), some studies have suggested incorporation of PEG into PEI-based polymers has either little effect or possibly a beneficial effect depending on the molecular weight of the PEG chains and the ratio of polymer to nucleic acid (154-156). While others demonstrate that PEGylation decreases the effectiveness of PEI (159-161). Indeed, this inhibitory effect may depend on the payload molecule itself (plasmid DNA or siRNA) and whether nuclear delivery is required or not. Additionally, regardless of whether a beneficial or inhibitory effect is noted for the various types of PEI-mediated delivery, both the ratio of polymer to nucleic acid and the degree of PEG substitution appear critical factors for the phenomena seen. In fact, these two variables may be responsible for both increasing and decreasing the effectiveness of PEGylated PEI in a multivariable relationship (158, 162). For this reason, my studies have focused on these two variables and their relationship to the physical properties and transfection efficiencies of PEI-PEG polyplexes.

### **3) Materials and Methods**

Polyethyleneimine (of all molecular weights), 24 kDa poly-L-lysine, protamine sulfate, cholesteryl hemisuccinate, HEPES, TNBS, MTT, DMSO, formaldehyde, and chloroform were purchased from Sigma Aldrich (St Louis, MO, USA). mPEG-NHS (Succinimidyl carboxy methyl ester) was purchased from Creative PEG Works (Winston-Salem, NC, USA). Dialysis tubing was from Spectrum Labs (Rancho Dominguez, CA, USA). DOTAP chloride and DOPE were purchased from Lipoid (Ludwigshafen, Germany). gWIZ-blank and gWIZ-GFP were produced by Aldevron (Fargo, ND, USA). SYBR Green I, DMEM (high and low glucose), Pen/Strep, and 0.05% trypsin/EDTA were purchased from Invitrogen (Carlsbad, CA, USA). Cy3 labelling kit was made by Mirus Bio (WI, USA). Patient BMSC samples were generously provided by Dr. Adetola Adesida (University of Alberta, Dept. of Surgery). Lipid modified PEI was generously synthesized by members of the Uludag Lab using published procedures (163-164): palmitic acid modified PEI (substituted at 0.3, 2.0 and 3.0 lipids/PEI for 0.6 kDa, 1.2 kDa and 2.0 kDa PEI, respectively) was synthesized by Dr. K.C. Remant Bahadur, and linoleic acid modified PEI (substituted at 2.14 lipids/PEI) was synthesized by Dr. Hamidreza Aliabadi and Dr. Vanessa Incani. 25 kDa PEI modified with 2 kDa PEG was synthesized by myself (substitutions summarized in following sections).

#### **3.1) Cell culture**

HEK293 cells were cultured in low glucose DMEM + 10% FBS (v/v) + 100 U/mL Penicillin + 100 g/L streptomycin; BMSCs were cultured in high glucose DMEM + 10% FBS (v/v) + 100 U/mL Penicillin + 100 g/L streptomycin + 5 ng/mL bFGF. BMSCs were extracted from bone marrow aspirate using an established procedure, in which isolated marrow was treated with 0.05% trypsin and passed through a cell strainer (165). Extraction was generously performed by Dr. Adetola Adesida. Routine passaging was performed at 90% confluence for both cell types,

whereby adhered cells were washed 2x with 1x HBSS followed by detachment with 0.05% trypsin and introduced into fresh media, splitting at an appropriate ratio (HEK293: ~1/6; BMSCs: ~1/3). HEK293 cells were used for transfection before 20 passages; BMSCs were used for transfection at passage three. Cells were seeded 24 hrs prior to transfection at 125,000 cells/well for 24-well plates, and 60,000 cells/well for 48-well plates.

### **3.2) Lipid Preparation**

AVPs were produced by a lipid film hydration method followed by mixing with polycation:pDNA complexes similar to an established procedure (124). The desired lipids were dissolved in  $\text{CHCl}_3$  and combined in round bottom flasks to produce 0.7 mM solutions at the appropriate molar ratios of lipid for each liposomal formulation (DOTAP alone, 1 DOTAP: 1 DOPE, or 9 DOPE: 2 CHEMS). The  $\text{CHCl}_3$  was then evaporated using either a rotary evaporator, or  $\text{N}_2$  gas (depending on the volume of the liposome preparation) to produce a thin lipid film, followed by drying under vacuum for 20 min. An appropriate volume of HEPES buffer (10 mM, pH 7.4) was then added to the films, and after a 10 min hydration the films were sonicated in a bath-type sonicator for 2 min to create 0.5  $\mu\text{g}/\mu\text{L}$  liposomal formulations.

### **3.3) AVP Production and Transfection**

Polycation:pDNA complexes were also formed in a HEPES buffer by combining gWIZ-GFP pDNA (and in the BMSC experiment, gWIZ-blank as well) with either PRT, PLL, PEI, PEI-PA, PEI-LA, or PEI-PEG at the desired N/P (nitrogen/phosphorus) or weight ratio and complexing for 15 min following vortexing ( $[\text{DNA}]_{\text{final}} = 0.12 \mu\text{g}/\mu\text{L}$ ). Multiple experiments were performed with various ratios of each polymer, collectively the ratios of these experiments include the following: PRT sulfate was complexed at N/P ratios 2, 3, 6, and 9; PLL (24 kDa) was complexed at N/P ratios 1.5, 3, and 6; PEI (25 kDa) was complexed at N/P ratios 9, 12, 15, and w/w

(polymer/DNA) ratios 3, 5 and 10; LMW PEI (0.6, 1.2, 2.0 kDa) with and without palmitic acid conjugation was complexed at a w/w ratio of 10; LMW PEI (2.0 kDa) with and without linoleic acid conjugation was complexed at a w/w ratio of 3; and PEI-PEG was complexed at a w/w of 3 as well.

The liposomal formulations were then thoroughly mixed in with the polycation/DNA complexes by repeated pipetting ( $[DNA]_{\text{final}} = 0.035 \mu\text{g}/\mu\text{L}$ ;  $[\text{lipid}]_{\text{final}} = 0.35 \mu\text{g}/\mu\text{L}$ ) and complexed for a further 15min after which the complexes were added to HEK293T cells or BMSCs (0.8  $\mu\text{g}$  DNA/well of 24-well plate). Cell media was replaced after 3 hrs (0.5 mL) and the cells were prepared for flow cytometry 48 hrs post-transfection.

### **3.4) Flow Cytometry and Plate Reader Measurements**

Cells were washed 2x with HBSS, followed by 0.05% trypsin-EDTA addition, and fixed with 3.7% formaldehyde/HBSS. HEK293T cells were analyzed by a Beckman Coulter Cell Lab Quanta flow cytometer, while each BMSC suspension was analyzed in a black 96-well plate by a Fluoroskan Ascent plate reader. Plate reader results of BMSCs were analyzed using SigmaPlot 11 by t-tests comparing gWIZ-GFP transfected cells to gWIZ-blank controls. Flow cytometry collected several parameters for each treatment group: mean fluorescence reg(1) which reports the mean fluorescence of an entire cell population, mean fluorescence reg(FL1+) which reports the mean fluorescence of only the positive cells in a population, and percent gated which reports the percentage of positive cells. Flow cytometry results of AVP transfections (Fig. 2-6) were analyzed by one way ANOVA, followed by all pairwise Tukey post hoc tests using SigmaPlot 11. Post hoc power analysis was also performed using SigmaPlot 11, using the common convention of a four-to-one weighting of  $\beta$ -risk to  $\alpha$ -risk (with an adequate power value being 0.8).

### **3.5) PEI-PEG Synthesis and Characterization**

PEG grafting was accomplished by conjugating NHS-functionalized PEG to the amines of PEI (Figure 8). PEI-PEG polymers were synthesized by combining 4 mg/mL branched 25 kDa PEI dissolved in phosphate buffer (0.1 M pH 7.2) with an equal volume of 75% DMSO containing 2 kDa mPEG-NHS (Succinimidyl carboxy methyl ester) at various concentrations (0.5, 2.5, 7.5 mM). After reacting for 4 hrs at room temperature, conjugates were extensively dialyzed against ddH<sub>2</sub>O with CE 12-14,000 MWCO tubing for 24 hrs and then lyophilized. Polymers were analyzed by <sup>1</sup>H-NMR in D<sub>2</sub>O and the degree of PEG substitution determined by comparing the peaks of CH<sub>2</sub>CH<sub>2</sub>O (~3.6 ppm) to CH<sub>2</sub>CH<sub>2</sub>N (~2.5-3.1 ppm). Differences in primary amines between each polymer were also detected via a colorimetric chemical assay in which 20 μL of aqueous polymer (at concentrations 6.25, 12.5, 25, 50, and 100 μg/mL) was combined in a 96-well plate with 180 μL TNBS solution (0.34 mM TNBS in 50 mM borate buffer, pH 9.0). Following a 0.5 hr incubation at 37 °C, absorbance of each sample was assessed at 405 nm with a microplate reader (ELX 800, Bio-Tek Instruments). The slope (*m*) of each polymer ( $\Delta$  absorbance/ $\Delta$  total polymer concentration) was compared to the slope of unmodified PEI in order to determine the detectable percent modification of primary amines using the equation  $100\% \times \{[m(\text{unmodified PEI}) - m(\text{polymer of interest})] \div [m(\text{unmodified PEI})]\}$ .

### **3.6) Polymer Toxicity Assay**

HEK293 cells were seeded in 24-well plates (125,000 cells/well) with 0.5 mL media (low glucose DMEM + 1% Pen/Strep + 10% FBS). Polymers were added 24 hrs later at concentrations of 2, 5, 10, 15 μg/mL. This was performed in two different manners; in one study the amount of polymer added was determined using the total polymer weight, and in the other only

the weight of the PEI backbone was accounted for in order to correct for the contribution of the PEG to the total polymer weight. After 24 hr 100  $\mu$ L of 5 mg/mL MTT was added to each well and incubated for 2 hrs, after which media was replaced with 0.5 mL DMSO. 100  $\mu$ L of each sample was transferred to a 96-well plate and the absorbance analyzed at 570 nm with a microplate reader (ELX 800, Bio-Tek Instruments). Relative cell viability (%) was determined by normalizing to the absorbance of untreated cells.

### **3.7) Assessing Polymer-DNA Binding Affinity**

Polymer:pDNA complexes were formed with polymer/DNA weight ratios ranging from 0-8. Two distinct studies were performed using polymer concentrations based on total polymer weight and solely the PEI component. 2  $\mu$ L of 0.025  $\mu$ g/ $\mu$ L gWIZ-GFP was vortexed with 118  $\mu$ L polymer of various concentrations (in 150 mM NaCl). After 30 min, 200  $\mu$ L of 1x SYBR GreenI was added and gently vortexed. 200  $\mu$ L of complexes were transferred to a 96-well plate and analyzed ( $\lambda_{\text{ex}} = 527$  nm,  $\lambda_{\text{em}} = 480$  nm) by a Fluoroskan Ascent microplate reader. Polyplexes were assessed for % complexation by comparing the fluorescence ( $F$ ) of samples to the reference which contained DNA but no polymer, and the background which contained neither:  $100\% \times \{[F(\text{DNA only}) - F(\text{polymer/DNA weight ratio})] \div [F(\text{DNA only}) - F(\text{background})]\}$ . Three parameter sigmoidal curves for each polymer were determined with SigmaPlot11 and  $BC_{50}$  values (polymer/DNA ratio with 50% binding) determined from each regression. Two independent quintuplicate experiments were performed for each experimental group.

### **3.8) Dynamic Light Scattering Measurements of PEI-PEG**

Polyplexes were formed by combining polymers (resuspended in 150 mM NaCl to 2 mg/mL) with either 4 µg gWIZ (control) or gWIZ-GFP plasmid DNA made up to a total volume of 100 µL with 150 mM NaCl, and immediately vortexing. Polymer/pDNA weight ratios were 2, 5, and 10 (determined with and without PEG weight correction). Following a 30 min incubation after vortexing, complexes were added to 0.6 mL media with 10% serum. DLS was performed immediately after adding to media and 1 hr later. Measurements were conducted with a Brookhaven ZetaPlus. Five consecutive measurements (20 sec) were made for each sample (25 °C, 660 nm,  $\text{real} = 1.333$   $\text{imag.} = 0$ ). Two independent samples were prepared per experimental group.

### **3.9) Labelled DNA Uptake Studies with PEI-PEG**

gWIZ-blank was labelled using a Mirus Cy3 *Label IT* kit and the extent of labelling determined using a GE NanoVue by analyzing the  $A_{260}$  and  $A_{550}$  values. The reacted plasmid was found to have ~ 24 labels/plasmid and was diluted with unlabelled plasmid such that there was an average of 5 labels/plasmid and the final gWIZ-blank concentration was 0.4 mg/mL. HEK293 cells were seeded the day prior to transfection in 48-well plates (65,000 cells/well) and were transfected with 0.5 µg DNA/well. Complexes were formed as for DLS measurements and added to the cells 30 min after vortexing. After 5 hrs incubation, media was replaced, and 24 hrs post-transfection cells were prepared for flow cytometry (as for AVP transfection) and analyzed for Cy3 fluorescence (FL2 channel).

### **3.10) Transfection of HEK293 Cells with PEI-PEG**

Complexes with gWIZ-GFP were formed as for DLS measurements and added to the cells seeded in 24-well plates 30 min after vortexing (1  $\mu$ g DNA/well). After 5 hrs incubation, media was replaced. 48 hours post-transfection, cells were processed for flow cytometry (as in the AVP study) and analyzed for GFP fluorescence (FL1 channel).

## **4) Results and Discussion**

Results of each experiment will be discussed individually; flow cytometry results are displayed in Figures 2-6, and the significant differences between lipid alone and the AVPs (dashed lines), as well as the differences between polymer alone and the AVPs (asterisks) are presented. Where appropriate, differences between unmodified and covalently modified polymers are highlighted as well (solid lines). Successful AVP formulations are defined as those that demonstrate a statistically significant increase in effectiveness compared to both their constituent polymer and lipid alone, in terms of mean fluorescence and percent gated cells, as determined by flow cytometry.

### **4.1) Efficacy of PRT-based AVP Formulations on Modification of HEK293 Cells**

In terms of increasing the mean fluorescence of the total cell population past the fluorescence of the lipids only control, no protamine-lipid combination in the first study was successful (Fig. 2a). However, when the mean fluorescence (Reg(1)) was compared between protamine only controls (at all ratios) and protamine combined with DOTAP and DOTAP/DOPE (but not CHEMS/DOPE) significant differences were noted (ranging from  $p < 0.05$  to  $p < 0.001$ ), indicating the ability of the lipid formulations to increase the effectiveness of PRT-DNA complexes. A similar increase was seen for the mean fluorescence of the positive cells (Reg(FL1+)) with the addition of lipids to various PRT ratios, for DOTAP/DOPE ( $p < 0.001$ ) and DOTAP alone (ranging from  $p < 0.01$  to  $p < 0.001$ ) (Fig. 2b). In terms of protamine affecting the mean fluorescence (Reg(FL1+)) of the various lipid formations, only one significant difference was noted: protamine obliterated the fluorescence of CHEM/DOPE at all N/P ratios. When comparing the percentages of fluorescent cells of each formulation (Fig. 2c), DOTAP combined with PRT at a N/P ratio of 2 was significantly increased compared to PRT alone ( $p < 0.001$ ) and the lipid alone ( $p < 0.01$ ); this is indicative of a successful AVP formation, and is one of the few found in my studies.

Collectively, this data suggests that the binding of DNA is a critical factor in formation of effective AVPs. The finding that liposomes with cationic lipids (DOTAP, and DOTAP/DOPE) increased the effectiveness of protamine/DNA complexes, while protamine/DNA complexes decreased the effectiveness of CHEMS/DOPE liposomes may be indicative of competitive DNA binding, instead of the desired synergy between components. At the neutral pH used for complexation, DOTAP containing liposomes are positively charged while CHEMS/DOPE liposomes are likely negatively charged at the pH used for complex formation, based on the measured pKa of CHEMS/POPC (1-palmitoyl-2-oleoyl-sn-glycero-3-phosphocholine) liposomes being ~5.8 (166). Hence, liposomes containing DOTAP can effectively form complexes with DNA when protamine is present by either sequestering the plasmid from PRT, or alternatively, by synergistically complexing with PRT as appears to be the case for at least one of the successful AVP formulations found. CHEMS/DOPE liposomes, however, appeared to have an additional challenge forming functional complexes in the presence of protamine. Even though they are negatively charged, CHEMS/DOPE appeared to be able to form particles with at least at a low degree of functionality (as demonstrated by their mean fluorescence Reg(FL1+) being higher than no treatment), likely formed by random incorporation of DNA into their lipid core during mixing. However, in the presence of a competing cation, such as PRT, the already limited ability of CHEM/DOPE to complex DNA was completely inhibited.

In addition to ineffective complexation, a carrier composed of both anionic and cationic components may have ineffective dissociation as well. Such carriers could have decreased stability due to reduced DNA-cation binding by steric and ionic inhibition by the anionic component leading to premature unpacking and ineffective gene delivery. Alternatively, if there is an excess of cations present to complex the DNA (combined with neutralizing anions), such polyplexes may have excess stability due to the large number of salt bridges and also result in decreased gene delivery. Hence, it appears that the specific pairing of lipids and polymers is of extreme im-

portance, and depending on the binding capacity and ionic interactions of both components, the pairing can either result in inhibitory or synergistic effects.

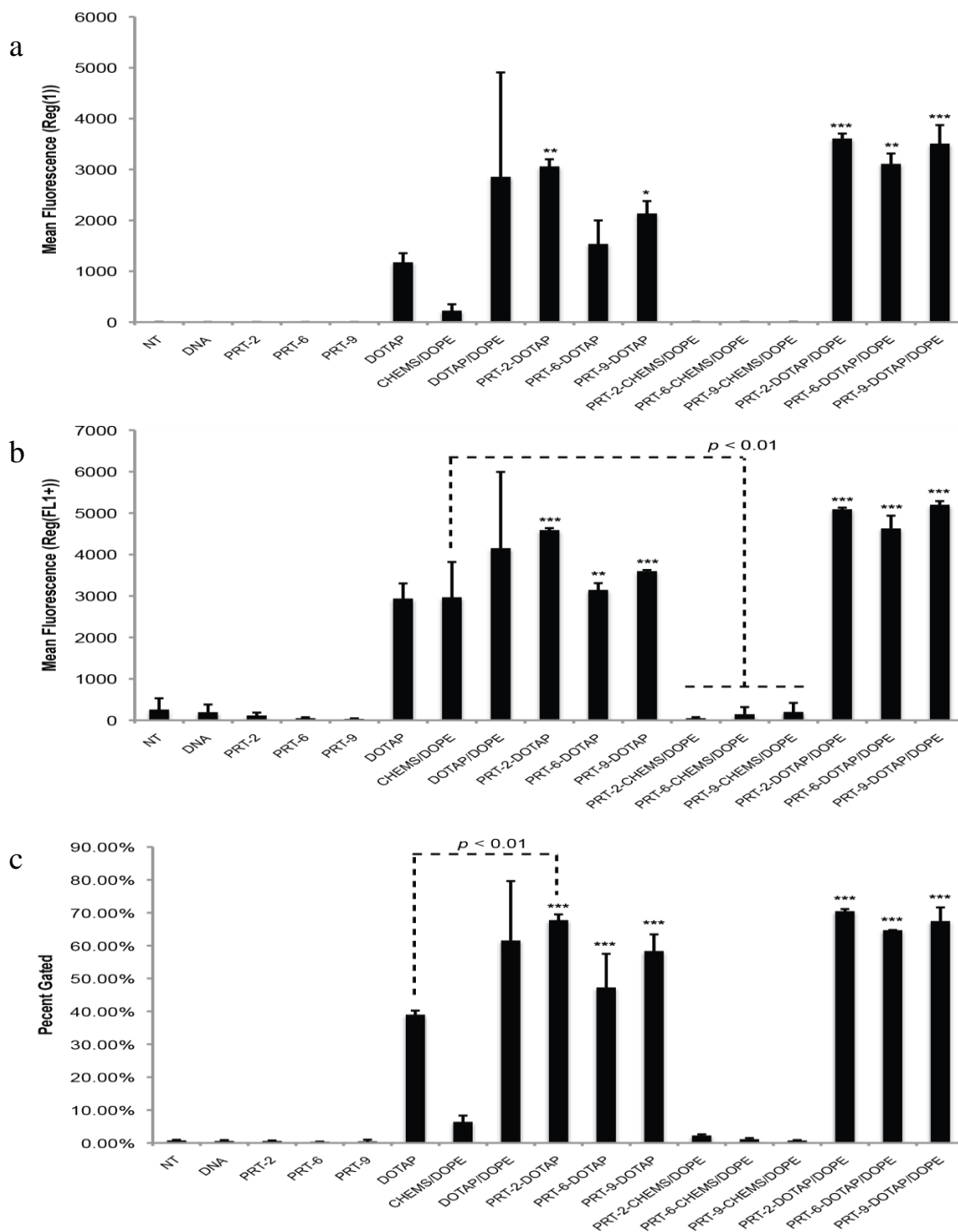


**Figure 2.** HEK293T flow cytometry results of AVPs using protamine (PRT) as a DNA condensor (performed in duplicate). Numbers indicate N/P ratio used for polymer/DNA complexation. Dashed line indicates significant differences between AVP formulations and lipids-only control. Asterisks indicate significant differences between AVP formulations and polymer-only control. \* =  $p < 0.05$  \*\* =  $p < 0.01$  \*\*\* =  $p < 0.001$

#### **4.2) Efficacy of PLL-based AVP Formulations on Modification of HEK293 Cells**

Due to the deficit of successful PRT-based AVPs, PLL was next tested as the condensing agent in order to assess if a polycation with a higher density of positive charges would produce more effective AVPs. The general mean fluorescence (Reg(1) and Reg(FL1+)) pattern seen with PLL was similar to that of PRT (Fig. 3a, 3b). CHEMS/DOPE experienced the same striking decrease in fluorescence with the introduction of PLL at all weight ratios ( $p < 0.01$ ), as seen with PRT. Unlike PRT, DOTAP/DOPE also exhibited a decrease in fluorescence (Reg(1)), which is significant at a w/w ratio of 1.5 ( $p < 0.05$ ). This was also seen with a significant decrease in percent gated (Fig. 3c) at the same ratio and at a ratio of 6 ( $p < 0.05$ ); DOTAP also experienced this decrease in percent gated at a ratio of 6 ( $p < 0.05$ ). Ultimately, unlike the PRT experiment, no successful AVP formulations were found using PLL, as no combination was higher (significantly or otherwise) than the constituent lipids or PLL alone.

As with the PRT-based experiment, these data appear to predominately highlight the importance of DNA binding. The presence of a polycation again appears to completely inhibit the already poor efficacy of CHEMS/DOPE as would be expected. Unlike the addition of PRT, though, the introduction of PLL resulted in a decrease for both DOTAP and DOTAP/DOPE in some cases. This may be a result of PLL having a stronger affinity to pDNA due to its higher density of positive charges, or may be a consequence of increased length compared to PRT disrupting the process of complexation. Regardless, these data suggested that using a polycation with a higher density of positive charges than PRT does not produce more effective AVPs.

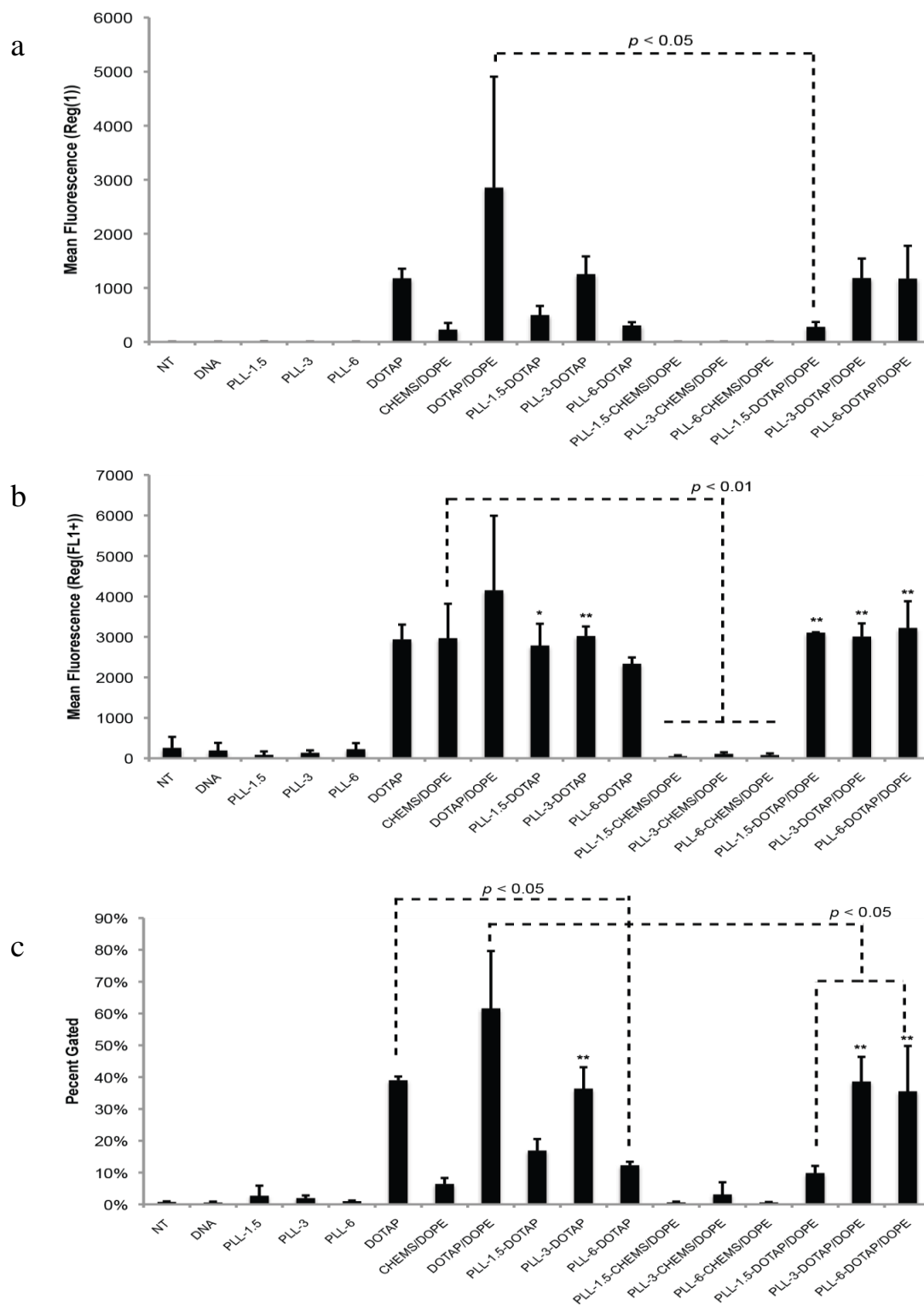


**Figure 3.** HEK293T flow cytometry results of AVPs using poly-L-Lysine (PLL) as a DNA condenser (n = 2). Numbers indicate N/P ratio. Dashed line indicates significant differences between AVP formulations and lipids-only control. Asterisks indicate significant differences between AVP formulations and polymer-only control. \* = p < 0.05 \*\* = p < 0.01 \*\*\* = p < 0.001

#### **4.3) Efficacy of Unmodified PEI-based AVP Formulations on Modification of HEK293 Cells**

Following the PLL-based AVP study, AVPs using PEI as the condensing polycation were assessed. This study was performed to confirm the observation that high molecular weight polymers with high charge density decrease the effectiveness of the lipids they are paired with, or if this was a phenomenon only observed using PLL as the polycation component. In the initial AVP experiment using 25 kDa PEI, ANOVA detected no significant difference amongst the groups in terms of mean fluorescence of the whole population ( $p = 0.173$ ) or the positive cells ( $p = 0.082$ ) (Fig. 4a, 4b). Analysis indicated that the power of these two data sets (0.232 and 0.397) was below the desired value of 0.8 and hence caution should be taken in assuming there is no significant differences. Percent gated (Fig. 4c) of this experiment did have sufficient power, however, and indicated that DOTAP/DOPE was less effective with PEI added at ratios 9 and 15 ( $p < 0.05$ ).

This decrease in percent gated cells of DOTAP/DOPE treated cells when polymer is added was similar to the results seen using PLL. Hence, this study further established the common phenomena in which the combination of a high molecular weight polymer with high charge density inhibits the ability of the cationic lipids in an AVP formulation, as this is only seen with PEI and PLL, and not PRT. It is also interesting to note that PEI did not appear to completely inhibit the effectiveness of CHEMS/DOPE in this study, which is surprising considering PLL, and even PRT, decrease its efficacy. Of course, this may simply be the result of insufficient power, but it may also suggest that the capacity of PEI to sequester DNA from CHEMS/DOPE is so acute that it can form highly functional complexes, hiding the complete inhibition of CHEMS/DOPE efficacy.

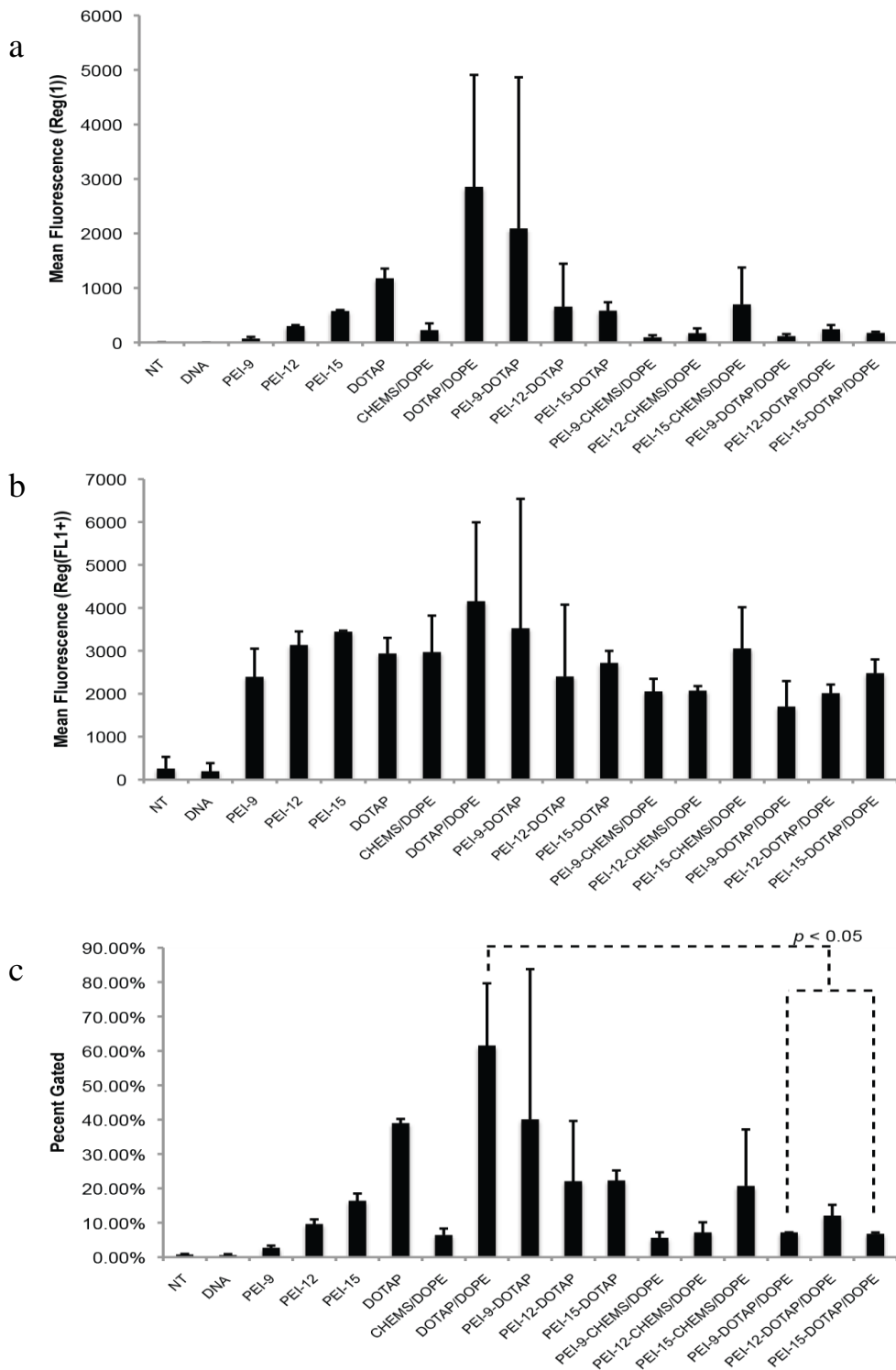


**Figure 4.** HEK293T flow cytometry results of AVPs using polyethyleneimine (PEI) as a DNA condensor (n = 2). Numbers indicate N/P ratio. Dashed line indicates significant differences between AVP formulations and lipids-only control. Asterisks indicate significant differences between AVP formulations and polymer-only control. \* =  $p < 0.05$  \*\* =  $p < 0.01$  \*\*\* =  $p < 0.001$

#### **4.4) Efficacy of PEI-PA and PEI-based AVP Formulations on Modification of HEK293 Cells**

Seeing that high molecular weight polymers with high charge density may decrease the ability of cationic lipids, several experiments were performed analyzing the effectiveness of AVP formulations composed of various types of low molecular weight PEI with and without palmitic acid conjugation. Since DOTAP/DOPE was the most successful lipid formulation in previous experiments, it was the only formulation continued to be tested. In addition, considering that the previous experiment described in Figure 4 had insufficient power, the number of replicates was increased in this study to allow more accurate comparisons.

In the first experiment of this nature, I utilized 0.6, 1.2, and 2.0 kDa PEI with and without palmitic acid conjugation (Fig.5). Without DOTAP/DOPE, palmitic acid modification was found to increase the effectiveness of low molecular weight PEI. A significant increase was noted for 2.0 kDa PEI when modified with palmitic acid, in terms of mean fluorescence ( $p < 0.05$ ) and percent gated cells ( $p < 0.001$ ); a significant increase in percent gated cells was also found for 1.2 kDa PEI ( $p < 0.001$ ). This increase due to palmitic acid conjugation was expected as this phenomenon has been demonstrated previously (163). While DOTAP/DOPE was able to increase the effectiveness of a number of modified and unmodified LMW polymers (asterisks in Fig. 5b, 5c), no combination yielded higher effectiveness than DOTAP/DOPE alone. In fact, compared to DOTAP/DOPE alone, the introduction of PEI decreased the mean fluorescence Reg(1) ( $p \leq 0.001$ ), mean fluorescence Reg (FL1+) ( $p < 0.05$ ), and in most cases the percent gated as well ( $p < 0.05$ ). It is interesting to note that when a higher weight ratio of 25 kDa PEI is used (5 and 10), compared to previous experiments, PEI is inhibited by the lipids ( $p < 0.001$  for every parameter), instead of the lipids being inhibited by PEI. Both appear to be detrimental to the other, instead of the synergistic intracellular delivery desired. There are two possible reasons for this. Firstly, the formed AVPs may be simply less effective than PEI polyplexes alone; it may be that the shielding provided by the lipid layer inhibits the proton sponge effect of PEI causing entrapment in the

endosomal pathway. Secondly, both polymeric and lipid reagents may compete for DNA binding, resulting in decreased and/or malformed complexes. Either way, using 25 kDa PEI as the sole transfection reagent appears the optimal choice in terms of the percentage of cells modified and the extent of their modification (fluorescence).

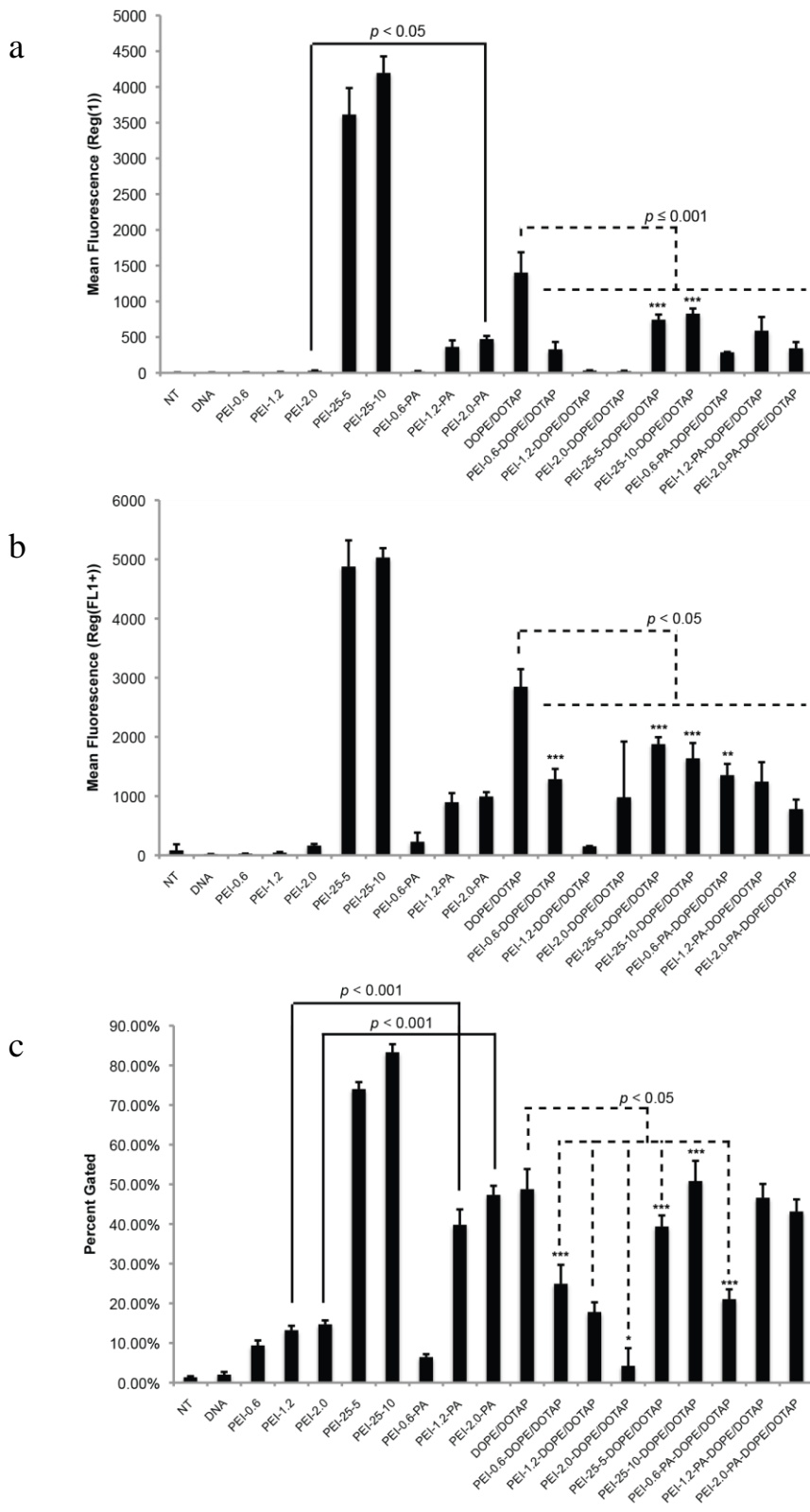


**Figure 5.** HEK293 transfection with AVPs using PEI and palmitic acid-modified PEI (PEI-PA) as DNA condensers (n = 3). Number indicates MW (kDa) of polymer; all use polymer/DNA (w/w) = 10 (25 kDa also used at w/w = 5). Dashed line indicates differences between AVPs and lipids-only control. Solid lines indicate differences between unmodified and modified polymer. Asterisks indicate significant differences between AVPs and polymer-only control. \* =  $p < 0.05$  \*\* =  $p < 0.01$  \*\*\* =  $p < 0.001$

#### **4.5) Efficacy of PEI-LA, PEI-PEG and PEI-based AVP Formulations on Modification of HEK293 Cells**

The final experiment examined PRT and two modified polymers along with their unmodified counterparts; one of which was 25 kDa PEI modified with 2 kDa PEG and 2 kDa PEI modified with linoleic acid (Fig. 6). This was conducted to further explore the possibility of PEI with decreased weight and charge being able to produce effective AVPs. Without DOTAP/DOPE, PEGylation decreased the effectiveness of PEI as seen with the mean fluorescence (Reg(1)) ( $p < 0.001$ ), mean fluorescence (Reg(FL1+)) ( $p < 0.001$ ), and percent gated cells ( $p < 0.001$ ). On the other hand, modification with linoleic acid increased the effectiveness of 2 kDa PEI as seen with each of the three parameters (all  $p < 0.001$ ). This increase due to linoleic acid conjugation has been noted previously, and has been attributed to increased nuclear association (163, 167). As with PEI-PA in the previous experiment, combining 2 kDa PEI and PEI-LA with DOTAP/DOPE did not create an AVP formulation with an effectiveness higher than that of the lipid or polymers alone. Also similar, was DOTAP/DOPE inhibiting the effectiveness of 25 kDa PEI for every parameter ( $p < 0.001$ ). Even PRT—included for comparison—was not particularly successful; while PRT was able to increase the mean fluorescence (Reg(FL1+)) past the level of both PRT ( $p < 0.001$ ) and DOTAP/DOPE ( $p < 0.01$ ), it was incapable of accomplishing the same for the mean fluorescence (Reg(1)) and percent gated. A successful AVP formulation was found in this experiment: PEGylated PEI with DOTAP/DOPE. The values of the combination exceeded that of the mean fluorescence (Reg(1)) of the polymer ( $p < 0.001$ ) and lipid alone ( $p < 0.001$ ), and that of the percent gated of the polymer ( $p < 0.001$ ) and lipid alone ( $p < 0.001$ ). Overall, the results of this study suggested that lipid-modification of PEI was not beneficial for AVPs, however modification with hydrophilic PEG could improve the efficacy of AVPs.

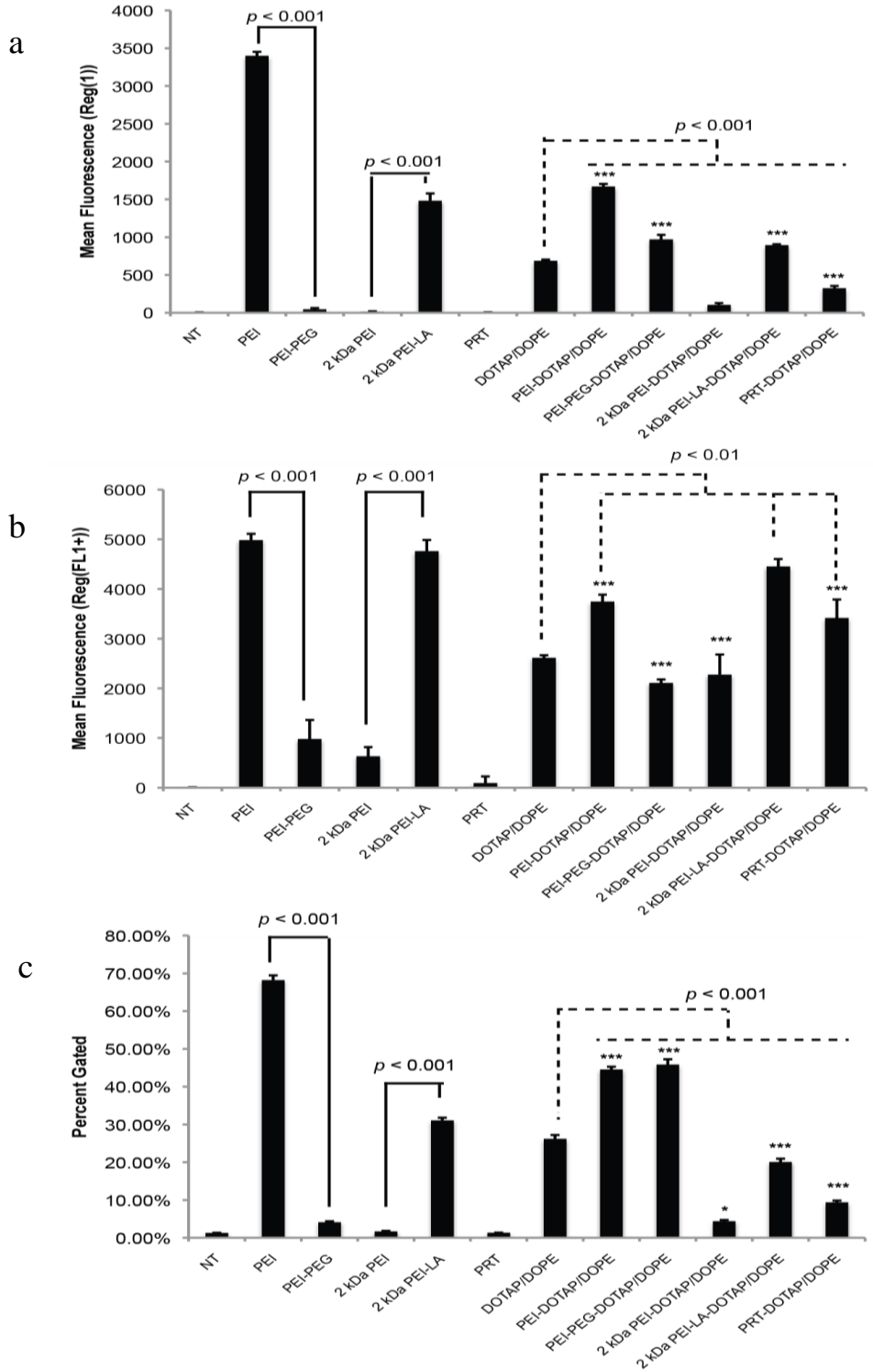


**Figure 6.** HEK293T flow cytometry results of AVPs using PRT, PEI, PEI-PEG, and linoleic acid-modified PEI (PEI-LA) as DNA condensers (n = 3). All use polymer/DNA (w/w) = 3; N/P = 23.2 for unmodified 25 kDa PEI. Dashed line indicates differences between AVP formulations and lipids-only control. Solid lines indicate differences between unmodified and modified polymer. Asterisks indicate significant differences between AVP formulations and polymer-only control. \* =  $p < 0.05$  \*\* =  $p < 0.01$  \*\*\* =  $p < 0.001$

#### 4.6) Efficacy of AVP Formulations on Modification of BMSCs

Transfection of BMSCs with the same formulations as in Figure 6, indicated that the only effective reagent capable of producing definite transfection ( $p < 0.001$ ) was 25 kDa PEI (Fig. 7). Considering the difficulty in transfecting (most) primary cell types, and that 25 kDa PEI was the most effective carrier for HEK293T cells, this is to be expected for BMSCs.

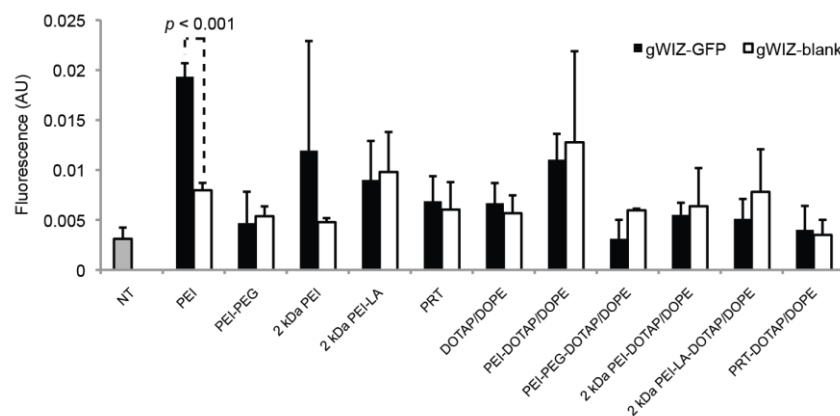


**Figure 7.** BMSC (bone marrow stromal cell) transfection results of AVPs using PRT, PEI, PEI-PEG, and linoleic acid-modified PEI (PEI-LA) as DNA condensers ( $n = 3$ ). All use polymer/DNA (w/w) = 3. Dashed line indicates significant difference between cells transfected with gWIZ-GFP and the negative control plasmid gWIZ-blank. Cell fluorescence was determined via plate reader.

#### **4.7) General Discussion and Conclusions on AVP Transfections**

Of all the AVP formulations tested, only two were deemed successful, that is their effectiveness exceeds that of both their composite polymer and lipid. The most successful AVP formulation was composed of protamine (complexed with DNA at an N/P ratio = 2) combined with DOTAP which gave a mean fluorescence of ~3000 and a percent transfection of 70%. The second most successful formulation was composed of PEI-PEG (complexed with DNA at a w/w = 3) combined with DOTAP/DOPE which gave a mean fluorescence of ~1000 and a percent transfection of ~45%.

It is interesting to note that the two effective AVP formulations included the polycations PEI-PEG and PRT, which are similar in terms of their lower (apparent) positive charge density compared to the other polymers tested. PEGylation decreases the available primary amines and also shields the remaining positive charges. Protamine, while composed of many positively charged amino acids (particularly arginine) it also contains non-charged residues as well. It may be that this decreased charge is advantageous for AVP effectiveness in terms of the complexation process and/or intracellular delivery. In terms of the complexation process, it is conceivable that a decreased zeta potential of the polycation:pDNA complex could assist with the lipid coating/association process by decreasing the charge repulsion between the polypex and the cationic lipids hence increasing the likelihood of properly formed AVPs. In terms of increasing the effectiveness of intracellular delivery, there is evidence to suggest that using a polymer with decreased DNA binding is advantageous in an AVP formulation. This is demonstrated with the increased effectiveness of AVPs composed of PRT compared to PLL, which is likely due to increased dissociation and increased transcription (109, 131).

The question remains then, why do not aliphatic substituted polymers also create effective AVP formulations? Lipid conjugation, like PEGylation, decreases primary amines and should also result in the shielding of the remaining positive charges. In practise, however, it has been

demonstrated that aliphatic substitution increases the zeta potential of polyplexes composed of LMW PEI (164). It was suggested that this is a result of improved stabilization of the polyplex due to hydrophobic interactions increasing the overall zeta potential. Hence, if using a polycation with decreased charge density is advantageous—as it appears with PEI-PEG and PRT—it follows that aliphatic substitution should not actually produce effective AVP formulations, which is consistent with my studies.

Despite this, it is perhaps surprising that more AVP formulations were not found in these studies, given the numerous successful formulations reported in the literature as discussed in the introduction. One reason for this may be decreased encapsulation efficiency with the manufacturing process used in making the AVPs. This may be attributed to the lipid association step being conducted by rapidly pipetting the lipids into the polyplex solutions instead of adding the polyplexes directly to the thin lipid films and then sonicating which might conceivably increase the encapsulation efficiency of polyplexes within liposomes. The method of pipetting rapidly to form AVPs has been conducted previously by multiple groups and the nanoparticles formed proved functional (168). Investigation into the structure of these AVPs using electron microscopy and FRET (fluorescent resonance energy transfer) demonstrated that AVPs made in this manner tend to have double lipid bilayers encapsulating a polyplex core (instead of a single bilayer), at least with AVPs made from DOPE:CHEMS and a pDNA:protamine polyplex, but it may prove true with other AVPs as well (108). This double membranous nature of pipette-mixed AVPs was shown to be advantageous by permitting the fusion of the outer bilayer with the cell membrane and the subsequent release of an intact second bilayer/polyplex into the cytoplasm which may then be directed to the nuclear envelope for a second fusion event. While these AVPs may have functionally superior architecture, previous reports make no statements regarding this method's encapsulation efficiency of polyplexes and this may be a possible disadvantage of pipette-mixing. Such a decreased encapsulation efficiency may be a contributing reason for the low number of ef-

fective AVP formulations reported in this thesis. Relatedly, the discrepancy in AVP effectiveness between the studies reported here and those previously conducted may be a result of published pipette-mixed AVPs being purified by fractionation (minimizing the effect of low encapsulation efficiency) or containing NLS peptides.

Future studies into AVP effectiveness should include investigating a number of particle parameters; assessing encapsulation efficiency of pDNA for each AVP formulation being one. Zeta potential measurements for each polyplex before and after lipid coating would also be appropriate, in order to address the hypothesis that PRT and PEI-PEG appear superior in AVPs compared to other polymers because they exhibit less (apparent) charge. Other useful studies include DLS (dynamic light scattering) measurements, cell uptake and nuclear association studies, as well as DNA binding and dissociation studies. Instead of pursuing these studies, however, a more pertinent avenue of study was pursued regarding the most effective carrier found in the AVP studies.

Indeed, compared to all the AVPs tested, 25 kDa PEI alone was clearly the most effective carrier for both HEK293T cells and BMSCs; however, this does not solve the problem of PEI's toxicity. Instead of combining PEI with lipids in hope of decreasing its effective working concentration, an improved approach may be to alter PEI covalently to decrease its toxicity. This was touched on in the final AVP experiment by the use of PEGylated PEI, however PEGylation was found to decrease the effectiveness of this polymer. Hence, focus was placed on finding the optimal conditions, such as substitution and polymer/pDNA ratio, to permit effective delivery with minimal toxicity. This approach is discussed in the following sections.

#### 4.8) Polymer Characterization

PEGylation of PEI (Figure 8) was confirmed by  $^1\text{H-NMR}$  and all conjugates were found to be within 13-21% of their expected substitution ratios, based on the molar feed ratios in the starting reaction mixture (Figure 9).  $^1\text{H-NMR}$  spectra integration indicated PEG substitutions of the three conjugates to be 2.7, 13.6, and 37.2 PEG chains/PEI backbone, which result in polymers consisting of 17.7%, 52.1%, and 74.8% PEG by weight (Table 3). Conjugation was also confirmed by the colorimetric TNBS assay (Figure 10a), which demonstrated that grafting reactions with a higher mPEG-NHS concentration produced polymers with a relatively decreased slope ( $m$ ) (i.e.,  $\Delta\text{absorbance}/\Delta\text{total polymer concentration}$ ). Based on the TNBS assay, the extent of primary amine modifications for the three conjugates were 52.9%, 79.4%, and 100% (Table 4). The absolute accuracy (especially in the latter case) is expected to be limited by the sensitivity of the TNBS assay. Based on the  $^1\text{H-NMR}$  and TNBS data, percent PEG weight composition and percent primary amine modification corroborated with each other with a significant Pearson correlation (Figure 10b;  $r^2 = 0.9063$ ,  $p = 0.0485$ ). Hence, direct modification of the PEI backbone with PEG was apparent, as opposed to simply the presence of separate unconjugated products. This assortment of polymers with a broad range of confirmed substitutions permitted a comprehensive survey of the effects of PEGylation on PEI polyplexes in regards to their toxicity, effectiveness, and physical properties.

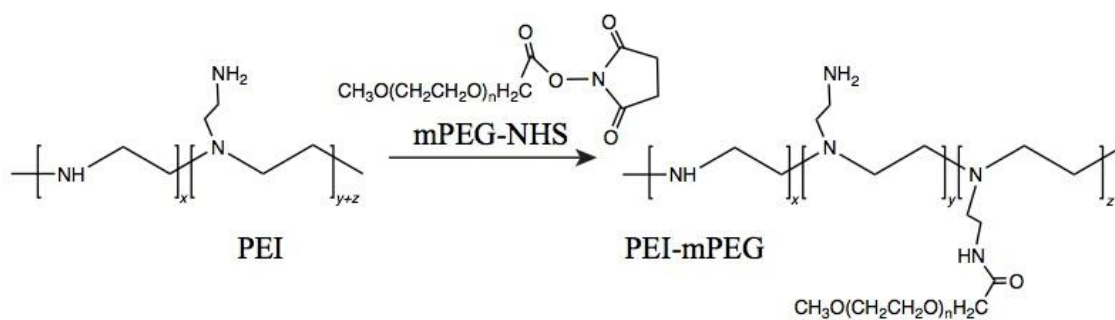


**Figure 8. Reaction scheme for the PEGylation of PEI.** Conjugation of polyethylene glycol (PEG) to PEI was mediated by reaction between the amines of PEI with the NHS (*N*-hydroxysuccinimide) moiety of functionalized methoxy-PEG.

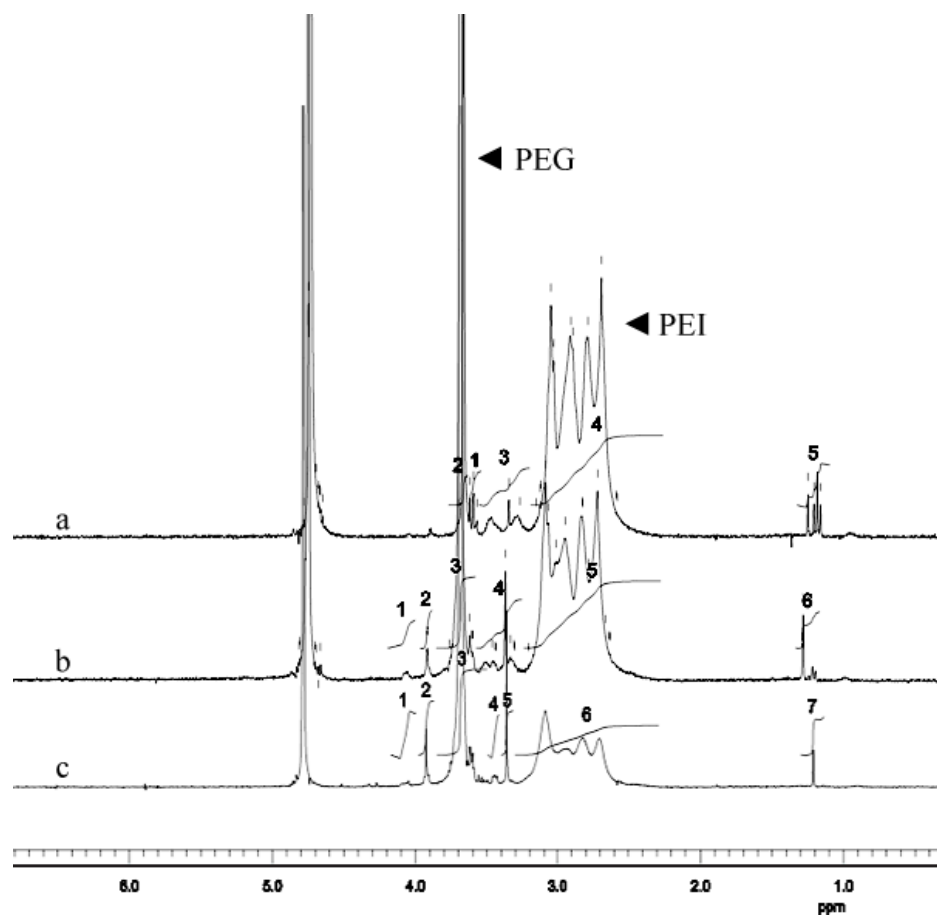


**Figure 9.  $^1\text{H}$ -NMR spectra of polymer products.** Conjugates were synthesized by reacting 25 kDa branched PEI with varying concentrations of 2 kDa mPEG-NHS: 0.5 mM (a), 2.5 mM (b), or 7.5 mM (c). By comparing the peaks of  $\text{CH}_2\text{CH}_2\text{O}$  (~3.6 ppm) to  $\text{CH}_2\text{CH}_2\text{N}$  (~2.5-3.1 ppm), the PEG substitutions of the three conjugates were determined to be 2.68, 13.58, and 37.17 PEG chains/PEI backbone.

**Table 3. <sup>1</sup>H-NMR results.** The degree of substitution of branched PEI (25 kDa) with PEG (2 kDa) was determined using the <sup>1</sup>H-NMR spectra by comparing the peaks of CH<sub>2</sub>CH<sub>2</sub>O (~3.6 ppm) to CH<sub>2</sub>CH<sub>2</sub>N (~2.5-3.1 ppm). The degree of substitution was used to calculate the proportion of PEG weight to PEI weight and amine modification for each polymer. The weight correction factor was also calculated in order to determine the weight of each polymer required to have the same weight of backbone as unmodified PEI.

[PEG]/[PEI] Ratio in Synthesis	PEG Substitution (PEG chains/PEI)	Total Poly- mer MW (kDa)	% PEG Weight (PEG/total polymer)	% Amines Modified (from NMR)	Weight Correction Factor
0 / 0.16 mM	0	25.00	0.00%	0.000%	1
0.5 mM / 0.16 mM	2.68	30.36	17.65%	0.461%	1.2144
2.5 mM / 0.16 mM	13.58	52.16	52.07%	2.336%	2.0864
7.5 mM / 0.16 mM	37.17	99.34	74.83%	6.393%	3.9736

**Table 4. TNBS Assay results.** Modification of primary amines was determined for each polymer using the slopes of the TNBS assay. Percentage of primary amine modification was calculated using the slopes for each polymer and normalizing with respect to unmodified PEI.

PEG Substitution (PEG chains/PEI)	Slope of TNBS Assay ( $\Delta A_{405 \text{ nm}} / (\Delta \mu\text{g/mL Polymer})$ )	% Primary Amines Modi- fied
0	0.0034	0.00%
2.68	0.0016	52.94%
13.58	0.0007	79.41%
37.17	0.000001	99.97%

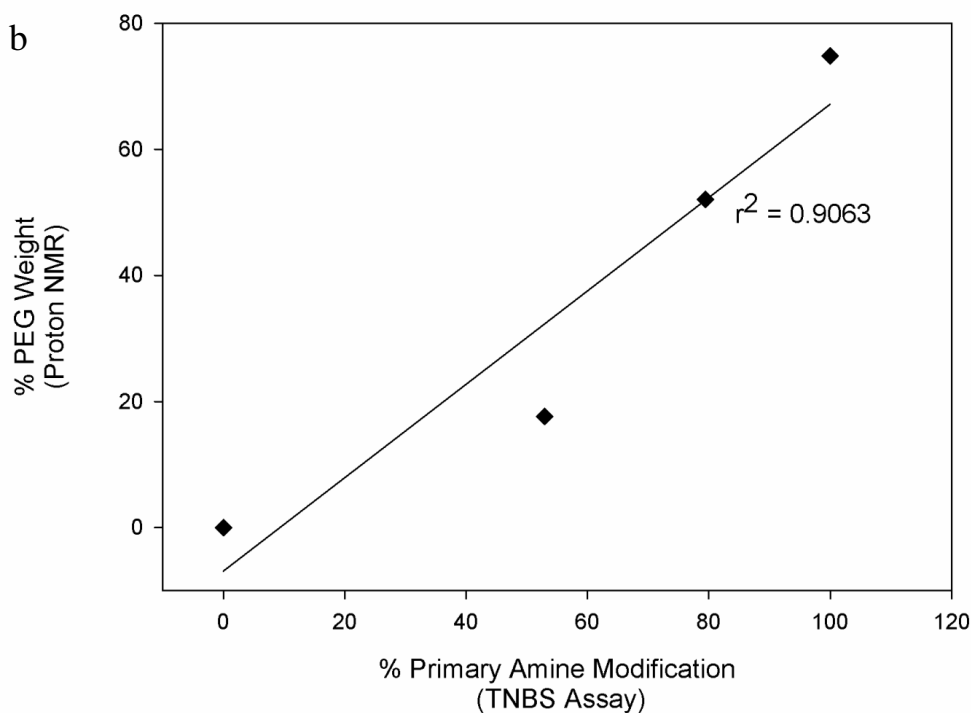
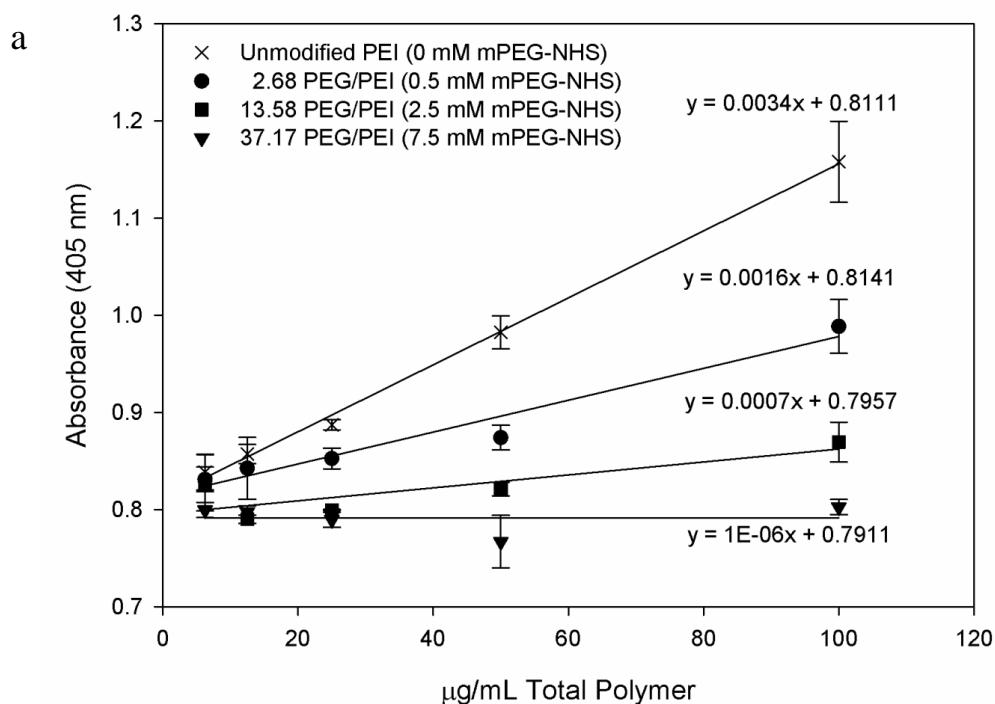


**Figure 10. TNBS assay and correlation to NMR data.** PEI was reacted with various concentrations of mPEG-NHS, and grafting was assessed by the TNBS assay performed in duplicate (a). The slope for each polymer compared to the slope of unmodified PEI was used to determine the % primary amine modification. The % modification (determined by TNBS assay) and the % PEG weight (determined by  $^1\text{H-NMR}$ ) of the conjugates were analyzed by Pearson correlation (b).

#### 4.9) Polymer Toxicity

Assessment of the polymer toxicity using the MTT assay indicated that PEGylation decreased the toxicity of PEI, as seen with a decrease in percent cell viability with increasing polymer concentration (Figure 11a). However, this could be as a result of the decreasing amount of PEI added to the cells as the PEG contribution to the total polymer weight was increased for PEGylated PEIs. When the amount of each polymer added to the cells was corrected so that an equal amount of PEI backbone was added/well, PEGylation appeared to have no effect on toxicity (Figure 11b). Toxicity data was then re-plotted to explore correlations between the %PEG weight and the observed viability. This analysis revealed no significance for any concentration when an equal amount of backbone was applied to the cells (Figure 12b), whereas without this PEG weight correction significant correlations were found (Figure 12a). For polymer concentrations 5, 10 and 15  $\mu\text{g/mL}$  the coefficients of determination ( $r^2$ ) were 0.968, 0.964, and 0.988 respectively ( $p = 0.0162$ ,  $p = 0.0185$ ,  $p = 0.0062$ ). Hence, PEGylation was effective in decreasing toxicity on a *per-polymer* basis, but not on a *per-backbone* basis.

The observation that incorporation of PEG decreases the toxicity of PEI on a *per-polymer* basis is well supported by previous studies (154, 158, 162). This may be expected as these studies conduct their toxicity assays by varying the weight of polymer added to cells and the toxic component, PEI backbone, decreases in proportion to the total polymer weight as PEG substitution and molecular weight increases. All of these studies can not definitively conclude that PEG decreases the toxicity of PEI on a *per-backbone* basis, which is the more pertinent question. Studies which form polyplexes at identical N/P ratios with polymers with varying amounts of PEG composition address this question more accurately; although, still not ideally considering the amine consumption of PEG grafting will increase the amount of polymer needed to produce the same N/P ratio making it slightly inaccurate to equate equal N/P ratios with equal ratios of backbone to DNA. Cytotoxicity assays previously performed in this manner generally indicated that the in-

creased PEG composition decreased toxicity (155, 159, 161). This is contradictory to the findings here that, on a *per-backbone* basis, PEGylation had no effect on toxicity. The major difference between the reported studies and this thesis work is that they assessed the toxicity of their polymer library by forming complexes, whereas my studies used free polymer. Considering that PEI-based polymers are more toxic in free form than formulated as a complex (159), it is possible that the differences in toxicity were not detected as a result of free polymers having similar (and greater) toxicities, whereas with complexed polymers, differences in toxicity due to PEG composition may be more apparent. This is logical considering differences in PEG substitution would likely produce greater hydration differences at the polymer-environment interface in a smaller volume (a polyplex) than in larger volume (a free polymer) where there is more exposed PEI backbone and hence more opportunity for PEI-environment interaction uninhibited by PEG.

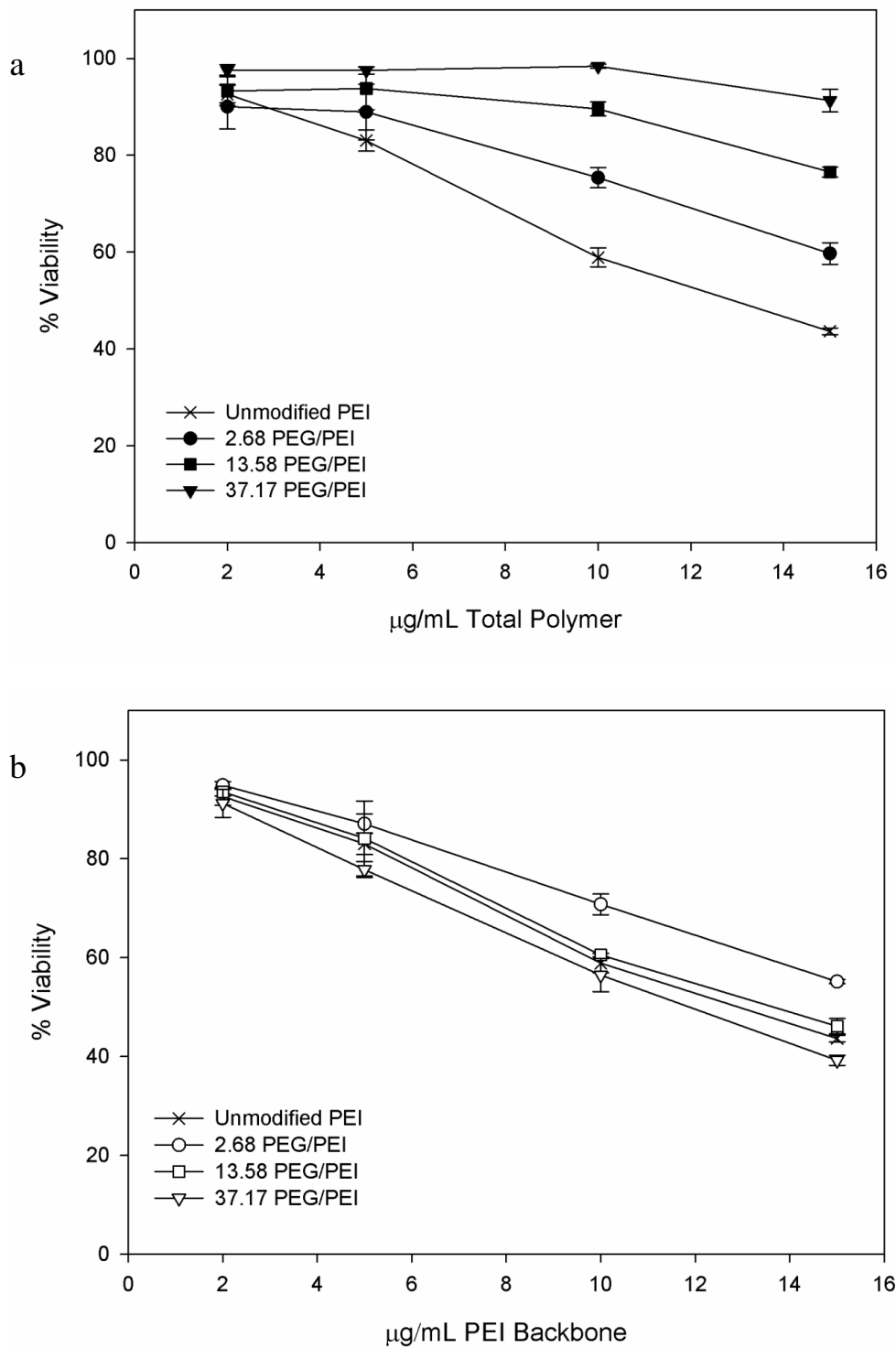


**Figure 11. Assessment of polymer toxicity.** An MTT assay was performed 24 hrs after exposing the polymers to HEK293 cells at varying concentrations. Two independent studies were conducted in which concentrations were based on the total polymer (which includes both PEI and PEG component; a) or the PEI backbone (which is solely based on PEI concentration; b). The toxicity assays were performed in triplicate.

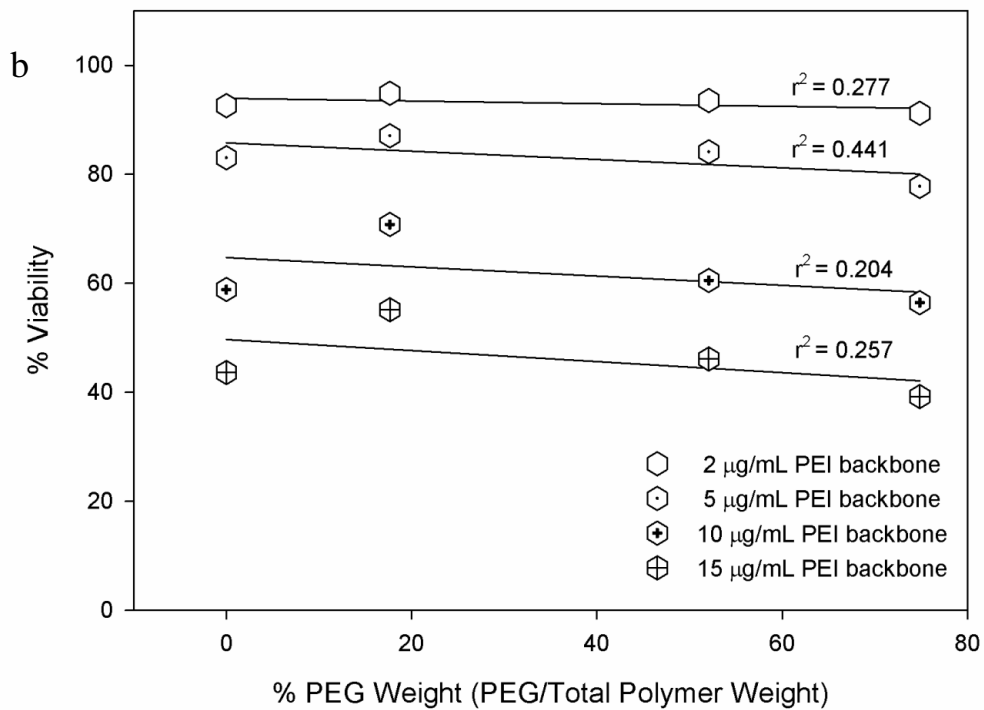
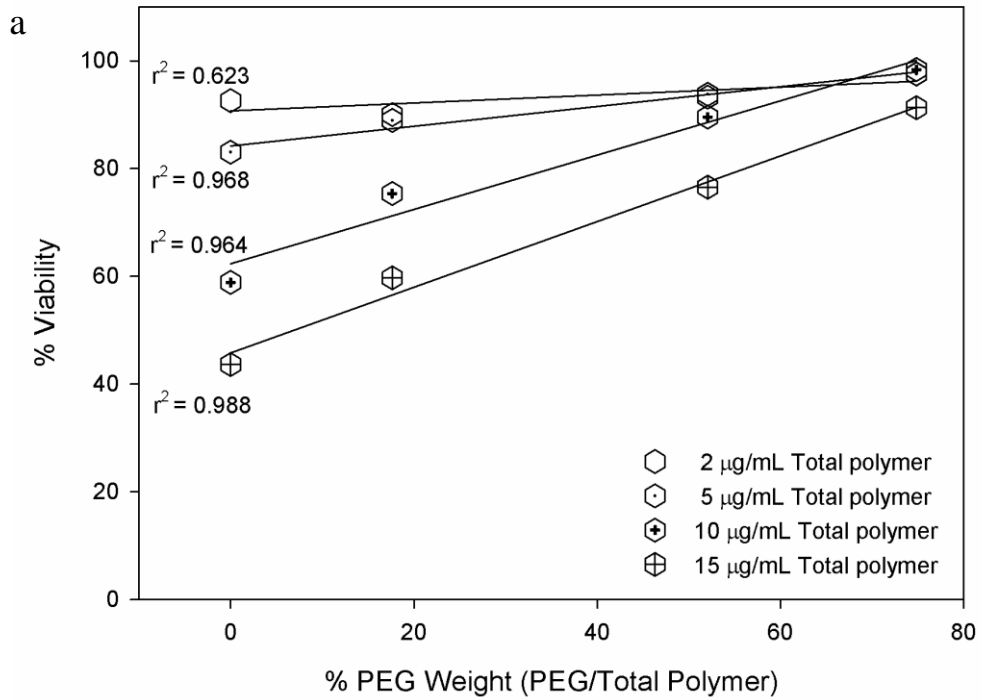


**Figure 12. Correlation between cytotoxicity and PEG composition.** The association between % PEG weight and the results of the MTT assays performed without PEG weight correction (a) and with PEG weight correction (b) was assessed by Pearson correlation.

#### 4.10) Polymer/DNA Binding

The effect of PEGylation on DNA binding is summarized in Figure 13. A similar phenomena was seen for the effect of PEG on polymer/DNA binding. Binding curves with polymer/DNA (w/w) ratios determined using the total polymer weight shifted to the right with increasing PEGylation (Figure 13a), whereas no shifts were seen if the polymers were added such that an equal amount of PEI backbone was present in each solution (Figure 13b). This indicated that PEGylation only affected binding due to its contribution to the weight of the total polymer and not by inhibiting the binding ability of PEI. Upon combining the data from both studies by converting the w/w ratios to N/P values (nitrogen of PEI amines/phosphorous of DNA phosphates), the same pattern was seen: PEGylation only shifted the binding curves rightward if unequal PEI backbone was being added (Figure 14a). N/P ratio calculations (Table 5) were performed assuming  $N/P = 7.74$  at  $w/w = 1$  based on the elemental composition and weight of the repeat units of PEI ( $\text{CH}_2\text{CH}_2\text{NH} = 43 \text{ g/mol}$ ) and DNA (avg. nucleotide =  $330 \text{ g/mol}$ ). This was followed by correction for the amines consumed by PEG grafting using the percent modified amines as calculated from the integrated  $^1\text{H-NMR}$  spectra. A correlation between the  $\text{BC}_{50}$  values (polymer/DNA (w/w) ratios where sigmoidal regressions predict 50% binding) and the percentage of PEG composition was then pursued based on the obtained binding curves. The results (Figure 14b) indicated an increasing  $\text{BC}_{50}$  with increasing %PEG content in each polymer ( $r^2 = 0.922$ ,  $p = 0.0404$ ), indicating a detrimental effect of the presence of PEG in polymer formulation. However, when equal PEI backbone was present, there was no correlation between the  $\text{BC}_{50}$  values and the %PEG content in each polymer. Hence, on a *per-polymer* basis, PEGylation affected DNA binding, but not on a *per-PEI backbone* basis.

These observations suggested that, despite PEGylation, much of the PEI backbone remained accessible for DNA binding and by extension (given the steric inhibition of PEG chains)

a conformational change in the polymer may be occurring to permit binding to DNA. Decreased DNA binding due to increased PEG composition has been noted in several studies (155, 158, 159, 162). These studies monitored DNA binding by adjusting the N/P ratio, and all but one noted a decreased binding affinity specifically with 25 kDa PEI conjugated 2 kDa PEG (the same molecular weight species used in my studies). They are in disagreement, however, with my finding that when equal backbone was present for each polymer, no differences in binding were noted as a function of N/P ratio or weight ratio. These observations reported by other groups were in agreement with the binding curves generated here based on the total polymer weight.

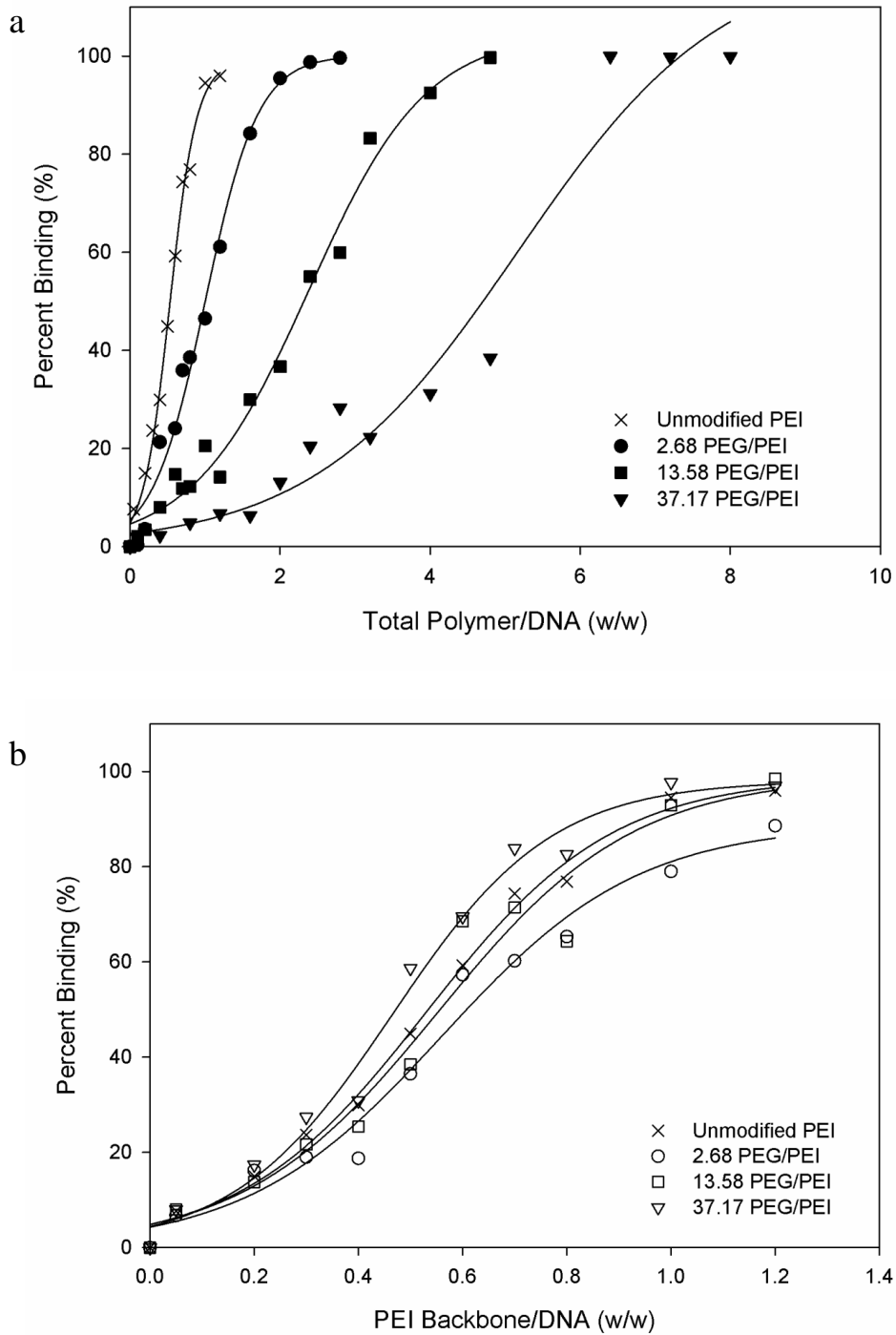


**Figure 13. Assessment of polymer binding to plasmid DNA.** The complexation of gWIZ-GFP with increasing concentrations of polymers was monitored using the SYBR Green I dye. Two independent studies were conducted in which concentrations were based on either total polymer (a) or the PEI backbone (b). Two independent quintuplicate experiments were performed for each experimental set-up.

**Table 5. N/P Ratio Calculations.** The ratio of PEI amine groups to the phosphate groups of DNA (N/P) were calculated for different weight ratios using the substitutions determined by <sup>1</sup>H-NMR. Studies were conducted using ratios 2, 5, and 10 with either equal PEI backbone/DNA (w/w) or equal total polymer (w/w) for every polymer. N/P ratios account for both differences in molecular weight and consumed amines due to PEG grafting. For the study with PEG weight correction (top), N/P values are accompanied by total polymer/DNA (w/w) ratios in parenthesis.

PEI backbone/ DNA (w/w)	N/P for Unmodi- fied PEI	N/P for 2.68 Sub- stituted PEI	N/P for 13.58 Sub- stituted PEI	N/P for 37.17 Sub- stituted PEI
2	15.5 (2)	15.4 (2.4)	15.1 (4.2)	14.5 (7.9)
5	38.7 (5)	38.5 (6.1)	37.8 (10.4)	36.2 (19.9)
10	77.4 (10)	77.0 (12.1)	75.6 (20.9)	72.5 (39.7)
Total Polymer/ DNA (w/w)	N/P for Unmodi- fied PEI	N/P for 2.68 Sub- stituted PEI	N/P for 13.58 Sub- stituted PEI	N/P for 37.17 Sub- stituted PEI
2	15.5	12.7	7.3	3.7
5	38.7	31.7	18.1	9.1
10	77.4	63.4	36.2	18.2

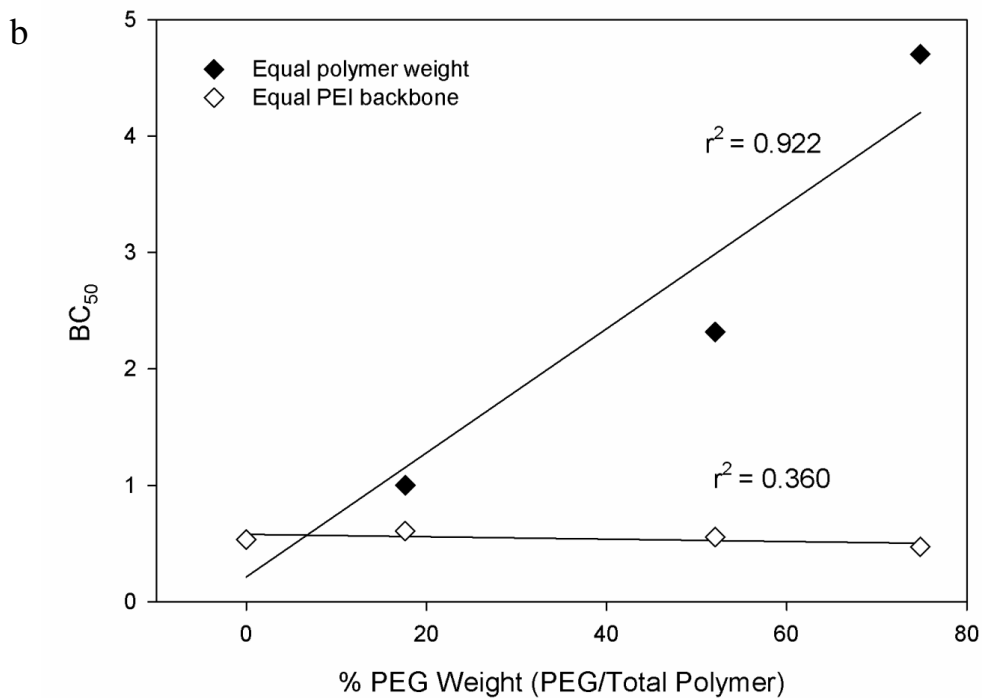
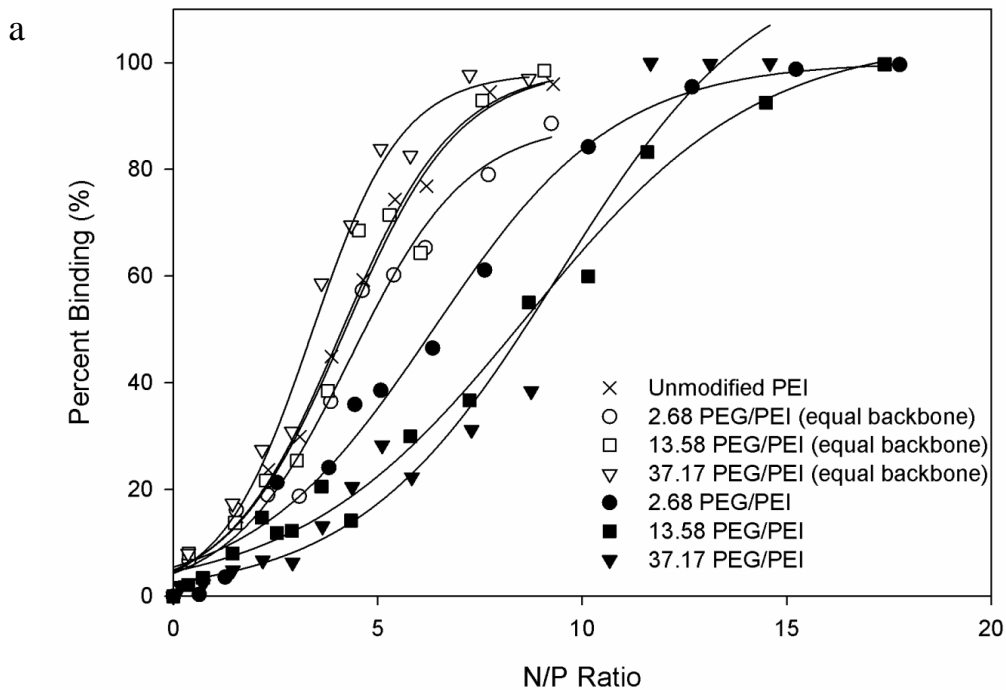


**Figure 14. Polymer binding by N/P ratio and correlation to PEG composition.** Results of the weight corrected and uncorrected binding studies were combined by plotting the curves as a function of N/P ratio. Pearson correlation between the % PEG weight and the BC<sub>50</sub> of each polymer was performed for both studies. BC<sub>50</sub> was determined as the w/w ratio with 50% binding using the sigmoidal regression curves of Figure 13.

#### **4.11) Sizes of PEI-PEG Polyplexes**

DLS measurements indicated most polyplexes were between 200-300 nm, and that several trends were apparent (Figure 15). Particle size generally increased after a 60 min incubation in cell media with 10% serum compared to the initial size at 0 min, and this increase appeared more prominent with increasing polymer/DNA and PEI backbone/DNA ratios. PEGylation appeared to prevent this size increase, especially at the highest PEG substitution. In general, no remarkable differences in size were noted between particles formed with either equal polymer or equal PEI backbone. Particle sizes at both time points also tended to increase with increasing polymer/DNA and PEI backbone/DNA ratios. The only exception was the most substituted polymer; for the study based on PEI backbone/DNA ratios all ratios produced similar sized polyplexes, while for the study based on polymer/DNA ratios the size decreased from a ratio of two to five and then slightly increased from five to ten. The polyplex with the most striking difference in size after 60 min incubation in 10% serum was formed using the moderately substituted polymer (13.6 PEG/PEI) at a PEI backbone/DNA ratio of ten.

The size range noted for most of the polyplexes in this study (~200-300 nm), using media with 10% serum, was generally larger than previous DLS measurements of PEI-PEG polyplexes. In some cases, this lower size range (~100 nm, measured at 0 min incubation) may be attributed to the use of low ionic strength buffers, such as 5 mM HEPES or 10 mM NaCl (154, 161). Larger size ranges (150-250 nm) closer to the range observed here were previously noted using solutions with ionic strengths more similar to the cell media, such as PBS or 150 mM NaCl (158-160). Presumably, the higher ionic strength allowed better shielding of polyplexes, facilitating their interactions and forming more aggregates in solution. The presence of 10% serum may explain the greater size of polyplexes observed in this study. In one study, where the size measurements on

native PEI polyplexes were reported in 1% serum, the observed sizes (210.3-662.5 nm) were in line with the current study at the similar DNA and polymer concentrations (167).

The previous studies were in agreement in this study, in that PEGylation generally decreased polyplex size in the presence of salt and other competing charges, particularly after extended incubation. This is most likely the result of the hydration shell produced by PEG providing steric protection of the polyplex from destabilizing agents. While these studies noted an increase in polymer size with increasing polymer/DNA ratio, both Zhong *et al.*, who used PEG-PEI-PEG triblock copolymers, and Zhang *et al.* who used PEI-PEG, observed a decrease in polyplex size with increasing polymer/DNA ratio (154, 158). The presence of 10% serum in this study, and the use of 5 mM HEPES and PBS in the other studies may be the cause for this difference. We considered the use of serum an absolute necessity to better mimic the culture conditions where the polyplexes will function. A more intensive study using a range of salt and serum concentrations with polyplexes formed with a range of polymer/DNA ratios would need to be conducted to further investigate this.

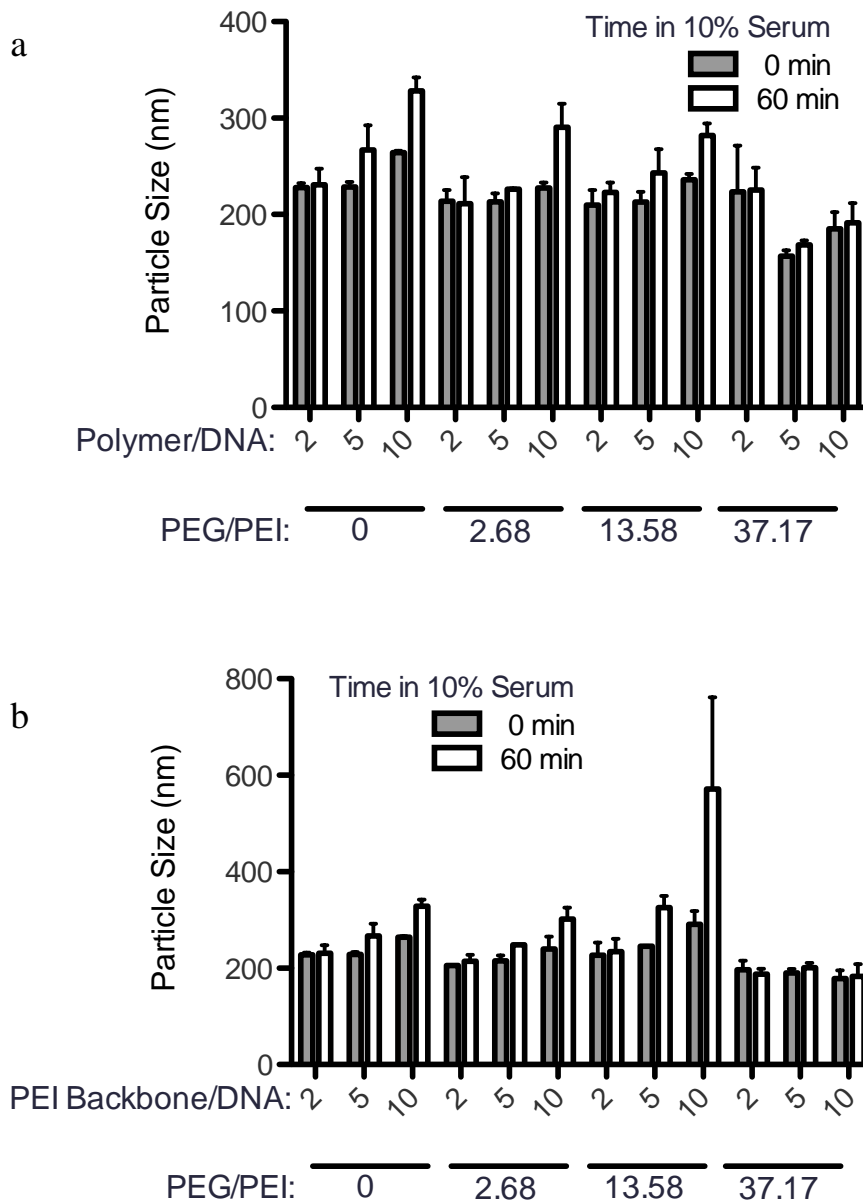


**Figure 15. Polyplex sizes.** After 30 min complexation of each polymer with gWIZ-GFP, polyplexes were added to cell media (low glucose DMEM + 10% FBS (v/v) + 100 U/mL Penicillin + 100 g/L streptomycin) and measured by DLS immediately after addition and after a 60 min incubation at room temperature. Polyplexes were formed at weight ratios (w/w) of 2, 5, and 10 based on total polymer (a) or the PEI backbone (b). Two independent samples were prepared for each polymer-ratio combination and average sizes obtained from these studies were combined.

#### **4.12) Plasmid Uptake Properties of PEI-PEG**

A plasmid uptake study using flow cytometry and Cy3-labeled gWIZ plasmid DNA was conducted to measure the relative cell-association and internalization mediated by each polymer. This study revealed two general trends (Figure 16). Firstly, plasmid uptake was found to increase with increasing polymer/DNA ratio. This was the case whether the complexes were prepared with equal polymer amount or equal PEI backbone amount. The only exception to this was with the moderately and highly PEGylated polyplexes when prepared without PEG weight correction (i.e., equal polymer and unequal backbone); complexes composed of 13.6 PEG/PEI had uptake only at a w/w ratio of 10, while complexes containing 37.2 PEG/PEI had no uptake at any ratio. Lack of uptake detection may be a result of too little PEI backbone due to the lack of weight correction, combined with the fact that approximately only 1 in 5 plasmids will be labelled with Cy3 due to dilution with unlabelled DNA. Secondly, in all cases uptake was higher with complexes containing equal backbone compared to those containing equal polymer. Collectively, both these patterns suggested that increased PEI backbone results in increased uptake. PEGylation, however, appeared to have a more complex effect on DNA uptake which is dependent on polymer/DNA ratio. The surface plot of this study helps illustrate this (Figure 17). At low PEG composition (< 20%) a general trend of increasing cell delivery with increasing N/P ratio was evident, whereas in the higher PEG range, an uptake peak in the range of 40-60% PEG weight at N/P = 40-60 was apparent.

It was previously demonstrated that, using a range of substitutions and molecular weights, PEGylation generally decreased the uptake of plasmid DNA (159). The most plausible reason for this is PEG creating a steric barrier between the surface of the polyplex and the cell surface proteoglycans, inhibiting interaction and decreasing uptake. The data here suggested a more complex relationship where an optimal cellular delivery was evident at select PEG amounts and N/P ra-

tios. The increase in uptake with increasing N/P ratio at low PEG composition is easily explained by the increasing cationic nature of polyplexes which is more conducive to cell interactions. The cause for the peak in the ideal range of N/P ratio and PEG composition is less obvious, seeing that PEG should decrease any ionic interaction between charged amines and the immediate environment of a polyplex. One possibility may be that polyplexes in this range have sufficient amines to initiate binding, despite PEGylation, and this particular composition of PEG chains causes minor destabilization of the polyplex upon binding. Such destabilization would reveal more amines than typically available in a less PEGylated polyplex and resultantly improve binding.

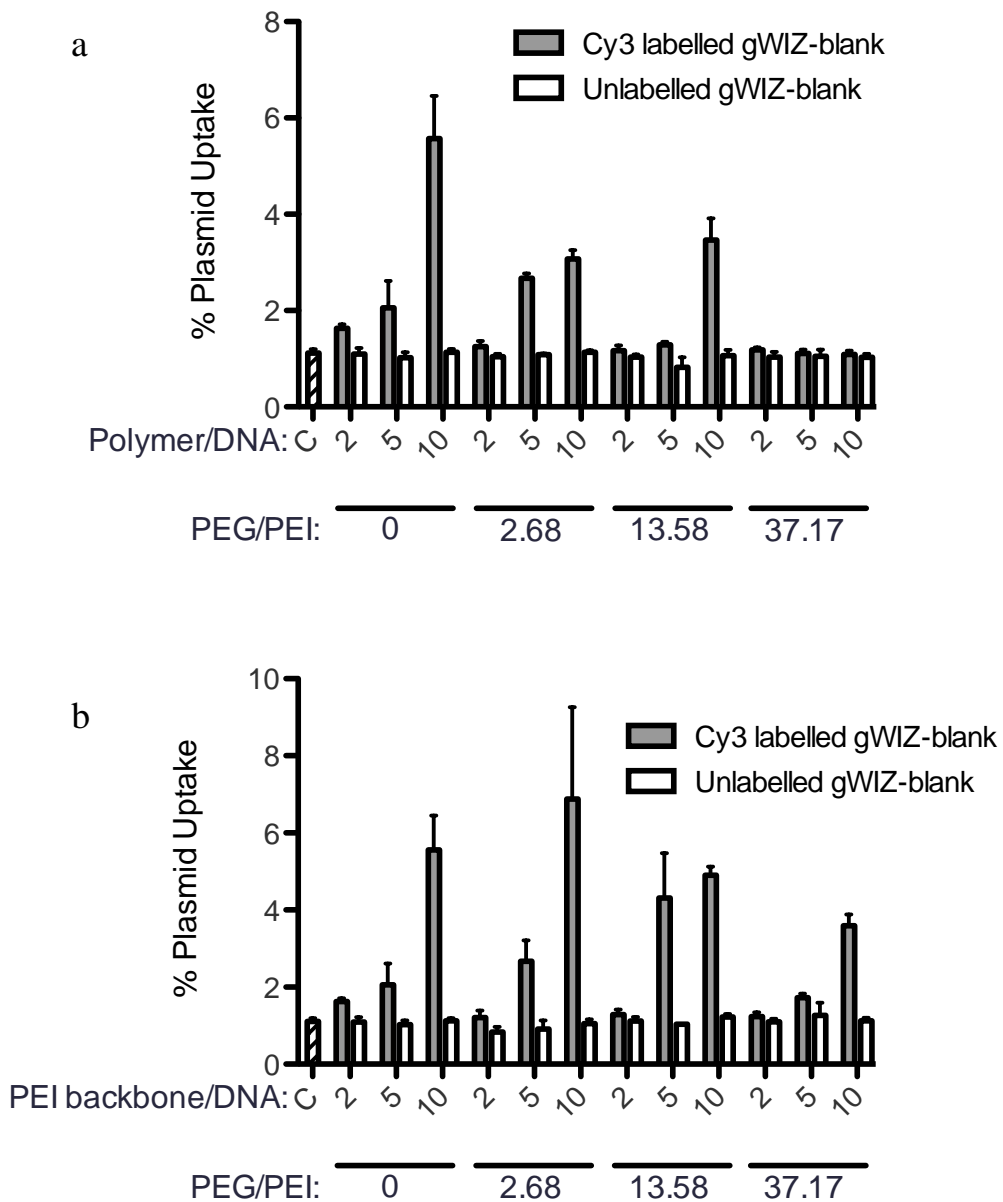


**Figure 16. Assessment of plasmid uptake.** Polyplexes were formed using each polymer and a ~1:5 dilution of fluorescently labelled gWIZ-blank to unlabelled plasmid such that there was an average of five Cy3 labels per plasmid. HEK293 cells were incubated with polyplexes for 5 hrs, followed by 24 hrs of culture in fresh media, after which the percentage of cells with plasmid uptake was assessed by flow cytometry. Polyplexes were formed at weight ratios (w/w) 2, 5, and 10 determined using the molecular weight of the total polymer (a) or the PEI backbone (b). Study was performed in triplicate.

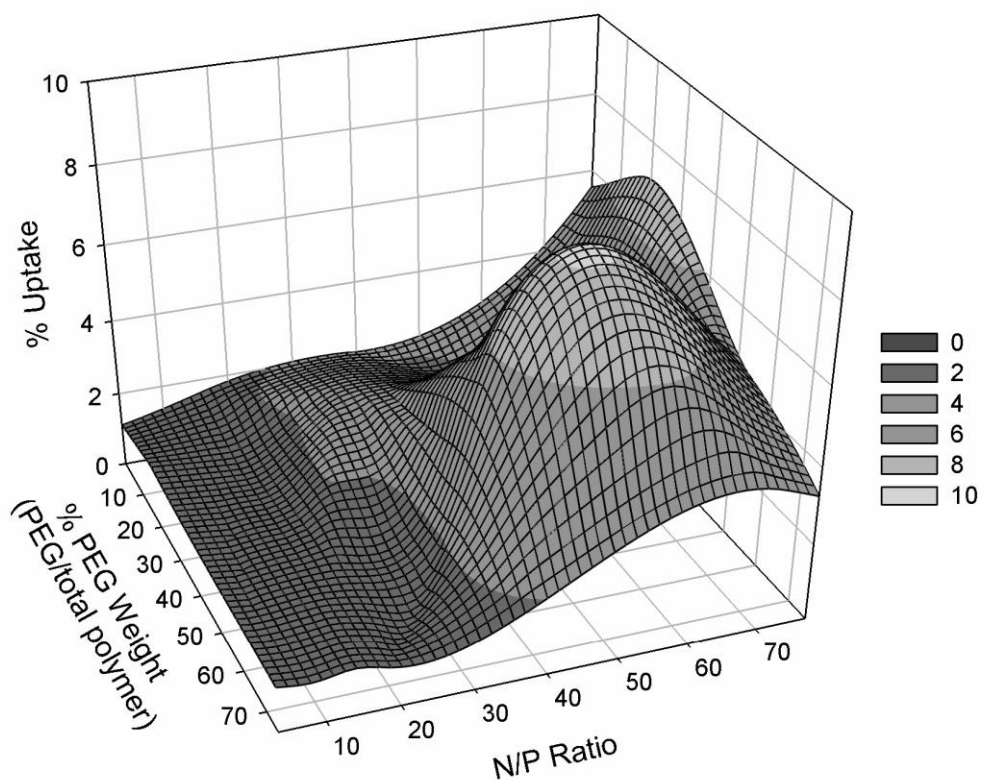


**Figure 17. Surface plot of plasmid uptake.** The percentage of cells with Cy3-labelled plasmid uptake, determined by flow cytometry, represented as a function of N/P ratio and % PEG weight.

#### **4.13) Transfection Properties of PEI-PEG**

Flow cytometry of HEK293T cells transfected with gWIZ-GFP revealed several trends, in regard to mean GFP fluorescence and percentage of cells expressing GFP, which were dependent on a number of variables. These variables included whether equal backbone or equal total polymer weight was used, the degree of PEG substitution of the polymer, and the polymer/DNA weight ratio. If the weight ratio of PEGylated polymer to DNA was determined using the total polymer weight (ie. without correcting for the contribution of PEG to the total weight of the polymer), it was apparent that a low ratio (=2) was relatively ineffective at transgene expression

but effectiveness was greatly improved with increasing weight ratio (Figure 18a and 18c). A higher weight ratio was needed to increase effectiveness for polymers with higher PEG substitution compared to polymers with lower substitution.

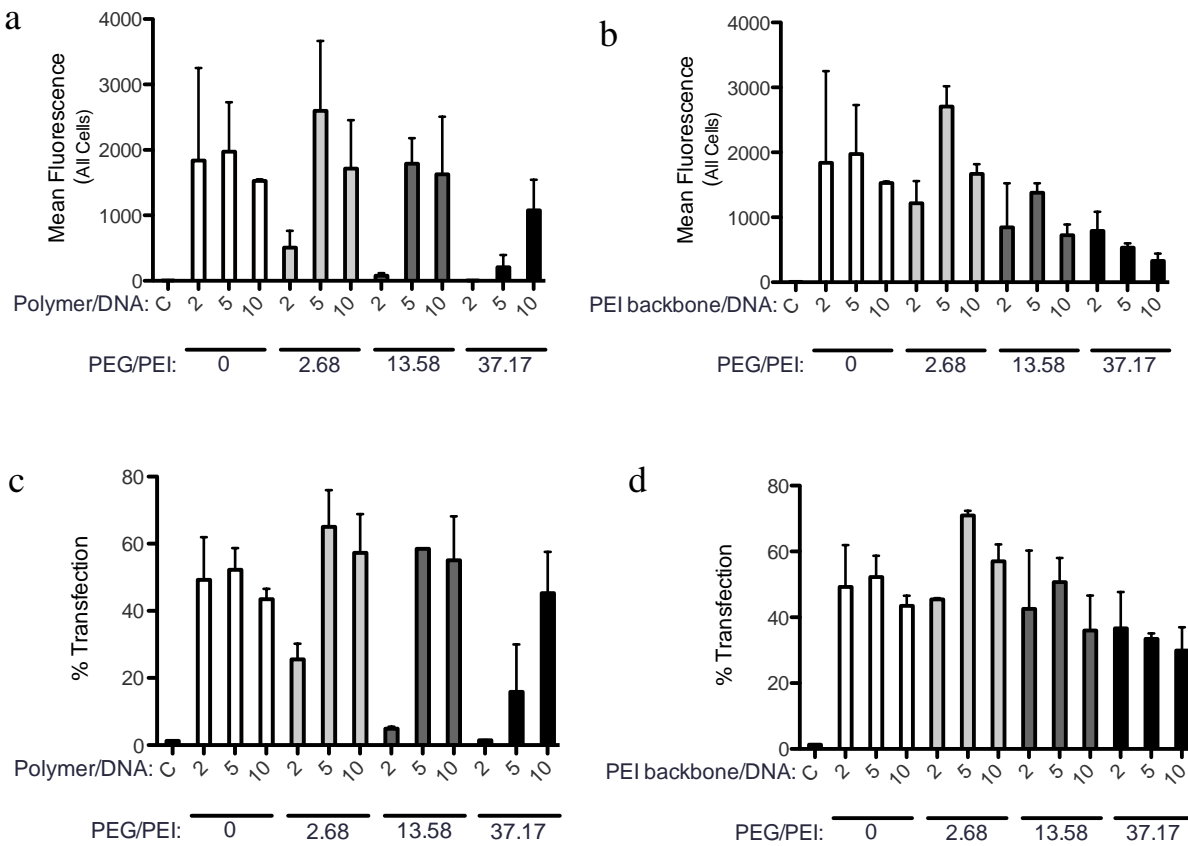


**Figure 18. Transfection efficacy of PEI-PEG.** The mean fluorescence (a, b) and percent transfection (c, d) of HEK293 cells treated with polyplexes formed with gWIZ-GFP. Cells were incubated with polyplexes for 5 hrs, followed by 48 hrs of culture in fresh media. Polyplexes were formed at weight ratios (w/w) 2, 5, and 10 based on the total polymer (a, c) or the PEI backbone (b, d). Data is the mean ( $\pm$  SD) of two independent experiments performed in triplicate ( $n = 2$ ).

The observation of PEGylated PEI having low efficacy at low polymer/DNA ratio, and requiring a higher ratio for comparable transfection compared to unmodified PEI, has been observed previously for N/P ratios  $<10$  with PEI grafted with 2 kDa PEG (160). As in this study, this occurrence has also been previously noted (for N/P  $< \sim 20$ ) to be more severe for polymers

with a higher PEG composition due to greater PEG substitution and/or PEG weight (161). These data suggests that there is insufficient PEI backbone present in PEGylated polymers to produce effective transgene expression at lower weight ratio ( $N/P < \sim 20$ ) when PEG composition (PEG/total polymer (w/w)) exceeds  $\sim 20\%$ , and the PEG chains exceed a certain threshold size (possibly between 0.35 kDa and 0.75 kDa (161)). However, effectiveness can be improved with the addition of more polymer; when one compared the performance of PEG-substituted polymers under optimal conditions to that of native PEI, equivalent transfection efficiencies could be reached by either type of polymers (Figure 18).

When the same transfection study was conducted using PEG weight correction, such that equal PEI backbone was used for all groups, the effects of PEG grafting became more apparent (Figures 18b and 18d). In general, mean GFP fluorescence and percent transfection were relatively lower for polymers with higher PEG substitution. With percent transfection, the general trend of decreasing transfection with increasing PEGylation appeared only past a certain substitution threshold, which is well demonstrated by a decrease in effectiveness for 37.2 PEG/PEI polymer but not 13.6 and 2.7 PEG/PEI polymers. The presence of a substitution threshold has been previously demonstrated with PEI conjugated with both 2 kDa (as in this study) and 5 kDa PEG (158, 162). Zhang *et al.* observed a decrease in transfection at N/P ratios 10, 20, and 30 (compared to unmodified) for 2 kDa PEG-conjugated PEI at 2.9 and 10.5 PEG/PEI, but not 1.89 PEG/PEI. For the 5 kDa PEG-conjugated PEI, the same effect was seen at 1.8 PEG/PEI and 7.2 PEG/PEI but not 0.66 PEG/PEI substitution. Tang *et al.* similarly noted a decrease for 2 kDa PEG-conjugated PEI at 2.5, 5.0, and 14.5 PEG/PEI but not 1.0 or 1.3 PEG/PEI (162). Such a threshold effect has also been noted for grafted PEG chains of lower molecular weight. Grafting with PEG chains of 0.35 kDa, 0.75 kDa, and 1.9 kDa decreased transfection (albeit only at specific N/P ratios) and the substitution threshold resulting in decreased effectiveness appeared lower for polymers grafted with a higher PEG molecular weight (161). Given that the specific

substitution threshold appears dependent on the weight of the conjugated PEG, the grafting threshold for each individual PEGylated polymer must be determined empirically. The grafting threshold of 2 kDa PEG-conjugated PEI, for example, appears to fall in the range of 1.3-2.5 PEGs per 25 kDa PEI, based on the conservative estimate of Tang *et al.* or 2.7-13.6 in this study. Ultimately, knowing this threshold assists in deciding the optimal degree of substitution in combination with knowing the effect of PEG grafting on toxicity and the severity to which exceeding this threshold affects transfection.

Unlike the uncorrected study, however, increasing the ratio of PEGylated polymer to DNA did not generally increase effectiveness when PEG contribution to the total polymer weight was corrected. This observation may have been the result of an increasing proportion of DNA-unbound polymer to DNA-bound polymer as the ratio of PEI backbone/DNA increased and PEG grafting was detrimental to this unbound backbone. PEI backbone not complexed with DNA is likely to compete in binding to cellular components, be it the proteoglycans of cell membranes, the endosomal membrane, the proton-rich endosomal environment, or cytosolic components. Increased PEG grafting of this uncomplexed polymer may interrupt interactions directly or indirectly by presenting steric hindrance between the particle and its binding partner. Alternatively, PEGylation could decrease complex stability as demonstrated by the increased sensitivity of PEGylated PEI to heparin-induced DNA displacement (156, 159); this decrease in effectiveness at high N/P ratio and high PEGylation may be a result of premature unpacking in the cytosol (possibly in endosomes) before nuclear association. The polyplexes within this range of N/P ratio and PEGylation may have a density of hydrophilic PEG chains exceeding an instability threshold not experienced by polyplexes, which either have a lower N/P ratio or lower percent PEG composition.

Perhaps the most notable result of this study was observed with the increase in transfection efficiency from a ratio of 2 to 5 followed by a decrease from a ratio of 5 to 10. This observed

peak was the highest of all the polymer-ratio combinations, including unmodified PEI, and hence suggests PEGylation may be beneficial for PEI effectiveness if the parameters of PEG substitution and weight ratio are amenable. Such an optimal effect of PEGylation has been noted previously (158, 162); Zhang *et al.* observed an increase in transfection compared to unmodified PEI using 2 kDa PEG-conjugated PEI with 1.9 PEG/PEI at a N/P = 30, as well as a smaller increase using 5 kDa PEG-conjugated PEI with 0.7 PEG/PEI at the same N/P ratio. Tang *et al.* observed optimal transfection exceeding that of unmodified PEI using 2 kDa PEG with 1.0 PEG/PEI in the N/P range of 5-20, as well as a similar result using a substitution of 1.3 PEG/PEI. While Petersen *et al.* found all their PEGylated polymers had similar or improved transfection compared to unmodified PEI, the optimal polymer had 35 PEG/PEI of 0.55 kDa PEG used at a N/P = 50, followed by a polymer having 2 PEG/PEI of 5 kDa PEG used in the N/P range 20-50. Hence, it appears that when the grafted PEG chains are in the 2-5 kDa range, a low substitution (0.7-2.7) at N/P = 20-50 is not only favourable in terms of PEGylated polymers, but is also more effective than unmodified PEI. Also, as demonstrated by Peterson *et al.*, conjugating PEG chains of lower weight at a higher substitution may exceed the effectiveness of unmodified PEI, suggesting this phenomenon may be partly the result of the proportion of PEG and PEI within the polymer and not specifically the substitution or PEG length.

The reason for higher efficiency of PEG substituted PEIs may lie in differences in intracellular trafficking. It has been suggested that siRNA delivery is less inhibited by PEI PEGylation than plasmid delivery (156, 159). Malek *et al.* demonstrated that a larger subset of their polymer library produced effective silencing compared to plasmid transfection, many of which were more effective than unmodified PEI, in addition to highlighting that the differences between the best and worst polymers for silencing were smaller as compared to plasmid transfection. Mao *et al.* likewise demonstrated that PEGylated polymers were more effective for silencing compared to unmodified PEI using polymers grafted with a range of PEG molecular weights (2 kDa-

20 kDa). Both groups also indicated that this improved silencing ability of PEGylated PEI was associated with decreased particle stability, leading to increasing siRNA release into the cytosol. By extension, it is rational to suggest this improved cytosolic unpacking may be the same reason for a high degree of PEGylation decreasing plasmid transfection; premature unpacking of polyplexes in the cytosol decreases the likelihood of the plasmid bypassing the nuclear envelope due to its larger size and negative charge. This is supported by the finding that endosomal unpacking of PEI-PEG complexes was negatively correlated to plasmid transfection (169). The question remains then, how does a low degree of PEG substitution increase the transfection efficiency of PEI, compared to completely unmodified PEI? One possibility is that while a polyplex with a high PEG composition will prematurely unpack in the cytosol, a polyplex with a low composition of PEG would remain intact in the cytosol and upon entrance to the nucleus would exhibit improved unpacking by the competing chromatin compared to unmodified PEI. Such a mechanism is supported by the observations that branched PEI remained complexed with pDNA 24 hrs after transfection, and colocalization of the two components was noted in the nucleus which suggests intact polyplexes can undergo nuclear uptake (170, 171). Perhaps a small amount of destability induced by low PEG modification, which is not significant in cytosolic events, may have a significant impact in nuclear events. The increase in transfection efficiency noted with low PEG substitution, whether it is due to modulating the location of unpacking or not, serves as a rationale for PEI PEGylation independent of its effect on polymer toxicity.

Both studies, one with equal total polymer weight and one with equal backbone, make it evident that the effect of PEGylation on the effectiveness of PEI is not a simple relationship and it also depends on the polymer/DNA weight ratio. For this reason, the relationship between effectiveness and the PEG composition of the polymer is featured for each weight ratio (Figures 19 and 20). It is apparent that the percent PEG composition of the polymer produces a very different relationship between the mean fluorescence or percent transfection for each weight ratio. For a

total polymer/DNA ratio of two both the mean fluorescence and percent transfection were increasingly inhibited with increasing PEG composition in a concave up relationship (Figures 19a and 20a). The mean fluorescence became significantly inhibited at 52.1% and 74.8% PEG weight composition ( $p = 0.02$  and  $p = 0.005$ , respectively). Likewise, the percent transfection became significantly inhibited at 52.1% and 74.8% PEG weight composition ( $p = 0.039$  and  $p = 0.034$ , respectively). A strikingly different pattern of mean fluorescence and percent transfection was seen at a total polymer/DNA ratio of five. As the PEG composition increased a concave down relationship was evident with an observed maximum at 17.7% PEG weight followed by a relatively gradual decrease compared to a ratio of two. While a slight decrease was noted at 74.8% PEG, a total polymer/DNA ratio of ten resulted in the mean fluorescence and percent transfection appearing largely unaffected with increasing PEG composition compared to a ratio of two and five. Collectively, the differing relationships for each ratio suggest that on a *per polymer* basis different ratios are more sensitive to PEG composition than others and this sensitivity can result in both increasing or decreasing the effectiveness of PEI.

Relationships were seen on a *per backbone* basis as well by examining the similar study using equal PEI backbone for every polymer at each weight ratio (Figures 19b and 20b). Both the data sets for mean fluorescence and percent transfection plotted against percent PEG weight appeared more compressed compared to the study without weight correction. This is probably due to the relationships being solely a function of PEGylation without the confounding variable of differing PEI backbone. Nonetheless, different relationships were detected. The PEI backbone/DNA ratio of five was the most distinctive for both the mean fluorescence and percent transfection with a concave down pattern with a detected maximum at 17.7% PEG weight. This is similar to what was seen in the study without weight correction, suggesting this phenomena is predominantly a result of the PEG composition for both studies and not a result of differing PEI backbone. The ratios of two and ten demonstrated the most similar relationships for both the

mean fluorescence and percent transfection with a gradual nearly-linear decrease with increasing PEG composition. It is apparent with these differing relationships that on a *per backbone* basis altering PEG composition can either increase or decrease transfection efficiency; the other contributing variable is, of course, the PEI backbone/DNA weight ratio.

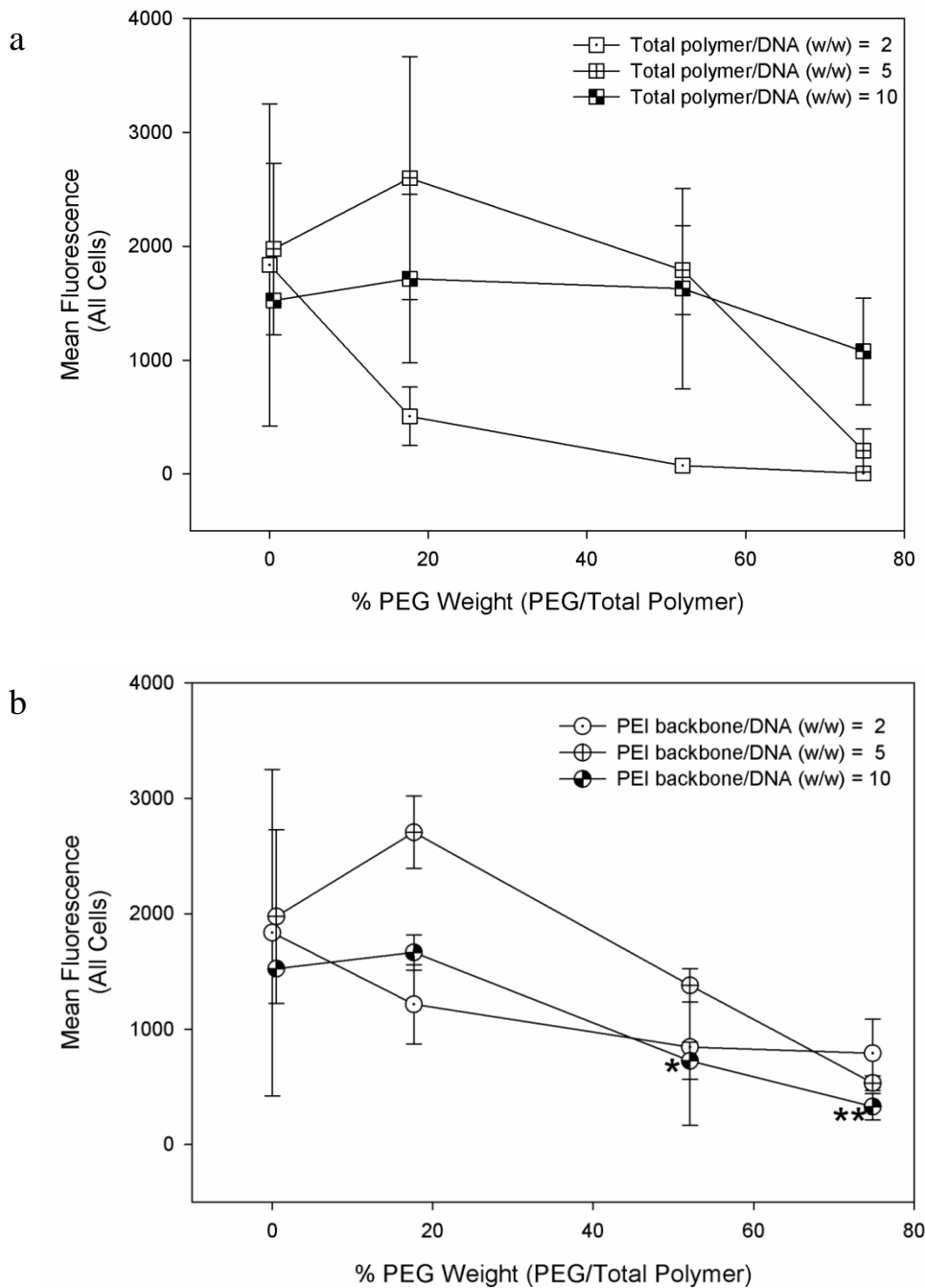


**Figure 19. Mean fluorescence as a function of PEG composition.** The mean fluorescence of HEK293 cells treated with polyplexes formed with gWIZ-GFP, presented as a relationship with percent PEG weight. Polyplexes were formed at weight ratios (w/w) 2, 5, and 10 determined using the molecular weight of the total polymer (a) or the PEI backbone (b). Asterisks indicate a significant difference between the specified data point and the fluorescence of unmodified PEI at the same weight ratio. \*  $p \leq 0.05$ , \*\*  $p \leq 0.01$

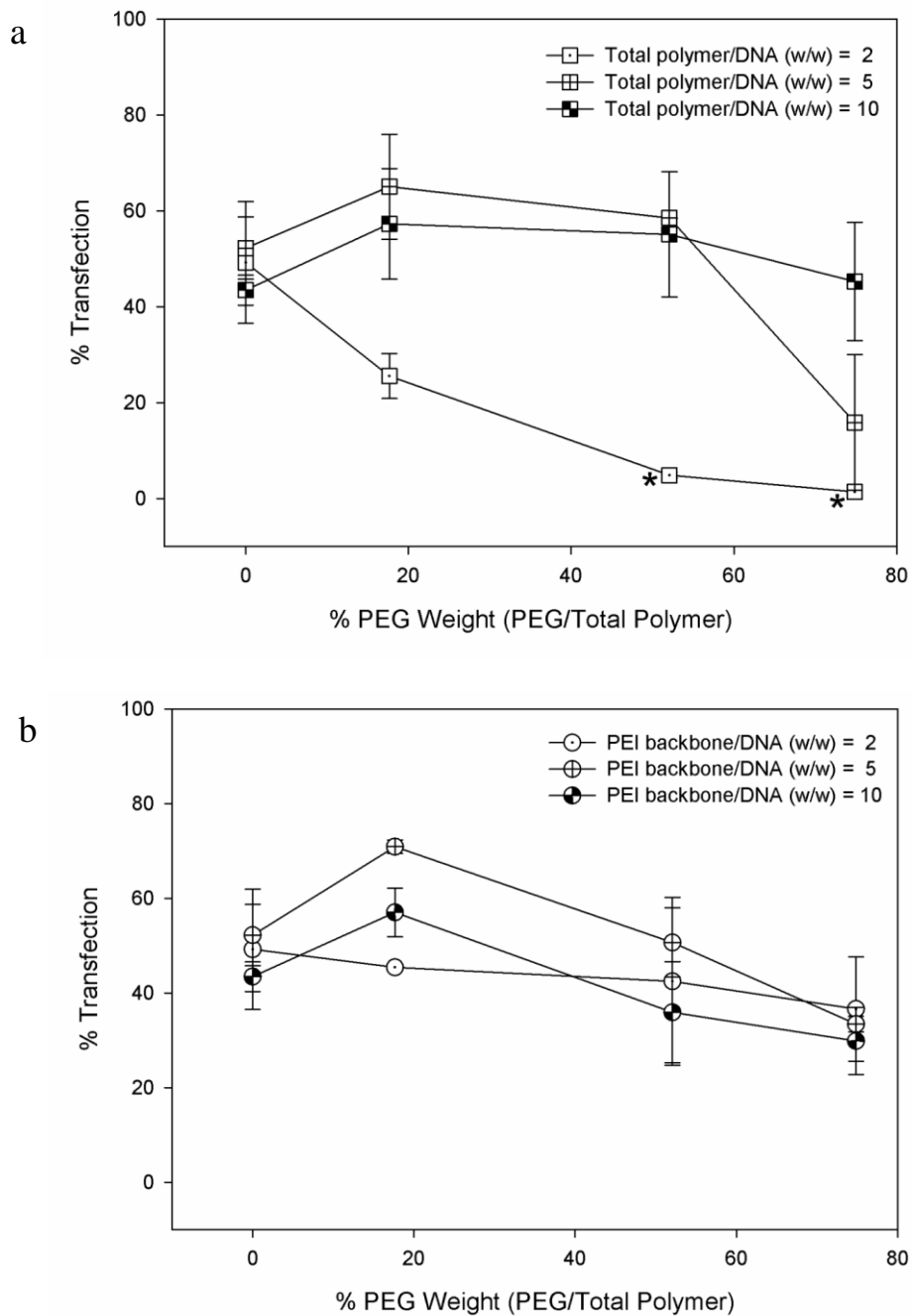


**Figure 20. Percent transfection as a function of PEG composition.** The percent transfection of HEK293 cells treated with polyplexes formed with gWIZ-GFP, presented as a relationship with percent PEG weight. Polyplexes were formed at weight ratios (w/w) 2, 5, and 10 determined using the molecular weight of the total polymer (a) or the PEI backbone (b). Asterisks indicate a significant difference between the specified data point and the percent transfection of unmodified PEI at the same weight ratio. \*  $p \leq 0.05$

In order to highlight the effect of weight ratio on transfection, data from the equal polymer and equal PEI backbone studies were combined by converting the polymer/DNA and PEI backbone/DNA weight ratios to N/P ratios (Figure 21). Following the data with increasing N/P ratio, the data of every polymer were tightly compressed at low N/P ratio, followed by divergence with increasing N/P ratio for each PEGylated polymer. The results in the low N/P range, where transfection efficiency starkly increased with N/P ratio, appears to illustrate the N/P ratio cutoff for effective transgene expression. The degree of PEGylation appeared to have little influence on effectiveness in this range, as seen with seemingly indiscriminate order of data points of each PEGylated polymer. The N/P ratio appeared to be the predominant acting variable seeing that the data in this range are linear and superimposed, especially for percent transfection. This is not the case at higher N/P ratios as seen with the different *effectiveness ceilings* for each polymer. For  $\sim N/P > 20$ , polymers with moderate and high PEG substitution (13.6 and 37.2 PEG/PEI) had decreased effectiveness compared to unmodified PEI, while minor PEG substitution (2.7 PEG/PEI) resulted in similar or increased effectiveness. This transition of ‘superimposed linearity’ to differing ‘*effectiveness ceilings*’ for each polymer may serve as a specific mechanistic illustration of polyplex formation and functioning. In the low N/P range, the necessity for an adequate number of positive charges to form condensed particles is seen. In the higher N/P range, where there is enough PEI backbone present to produce adequately functioning polyplexes, the influence of PEG grafting on cellular processing events is observed.

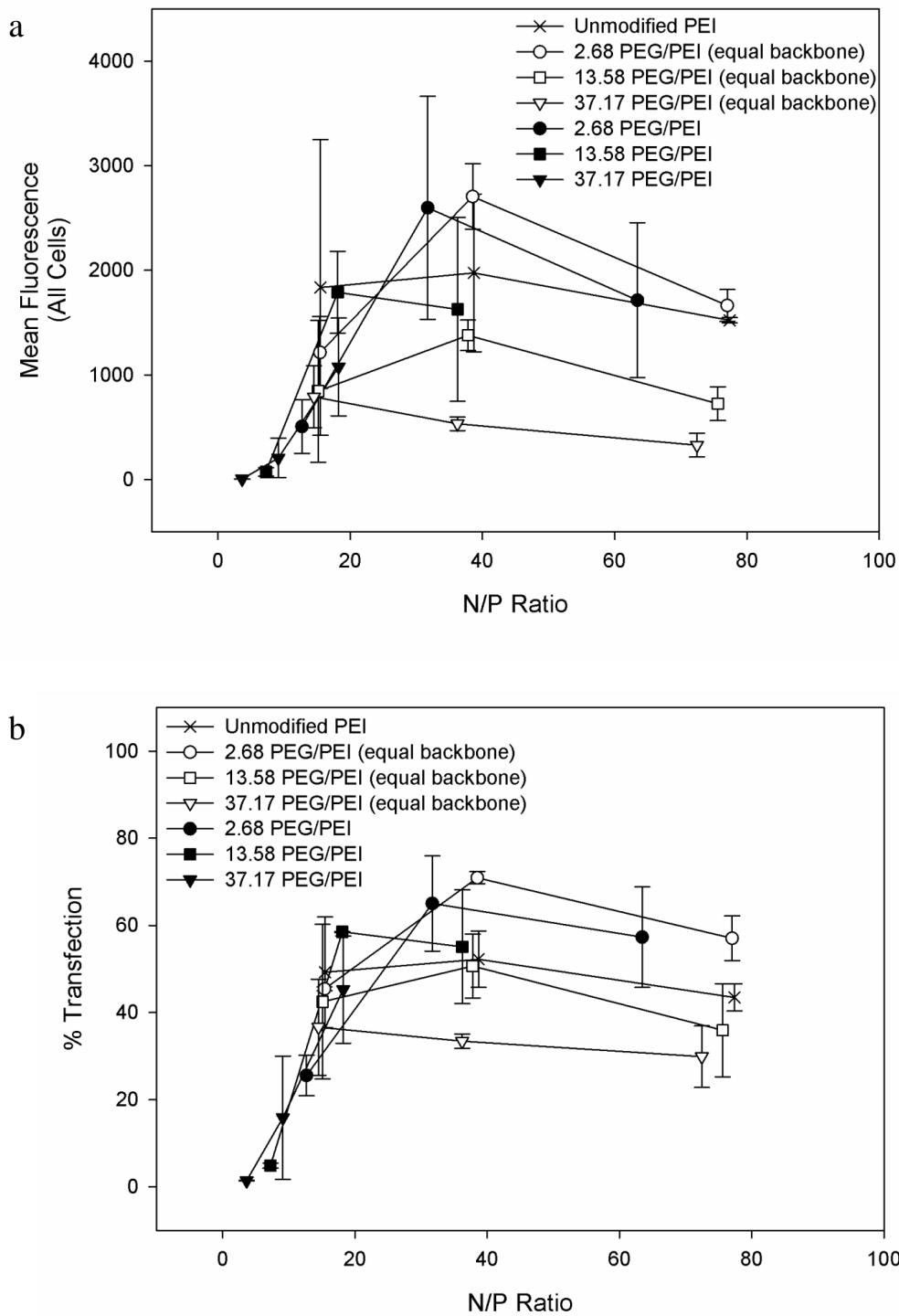


**Figure 21. Transfection efficacy as a function of N/P ratio.** The mean fluorescence (a) and percent transfection (b) of HEK293 cells treated with polyplexes formed with gWIZ-GFP, presented as a relationship with N/P ratio.

While specifically analyzing the role of PEG composition and N/P ratio independently is invaluable, ultimately the two variables work in concert and for deeper insight they must be considered together; for this purpose 3D surfaces exploring the effect of both variables on mean fluorescence and percent transfection are displayed (Figure 22). It is evident that there is an optimal combination of the two variables as seen with the multiple peaks and ridges of both surfaces, as well as ineffective combinations highlighted by the valleys and troughs of the surfaces. Both surfaces clearly illustrate that the relationship of effectiveness with PEG substitution is complex and is inextricably related to N/P ratio as well.

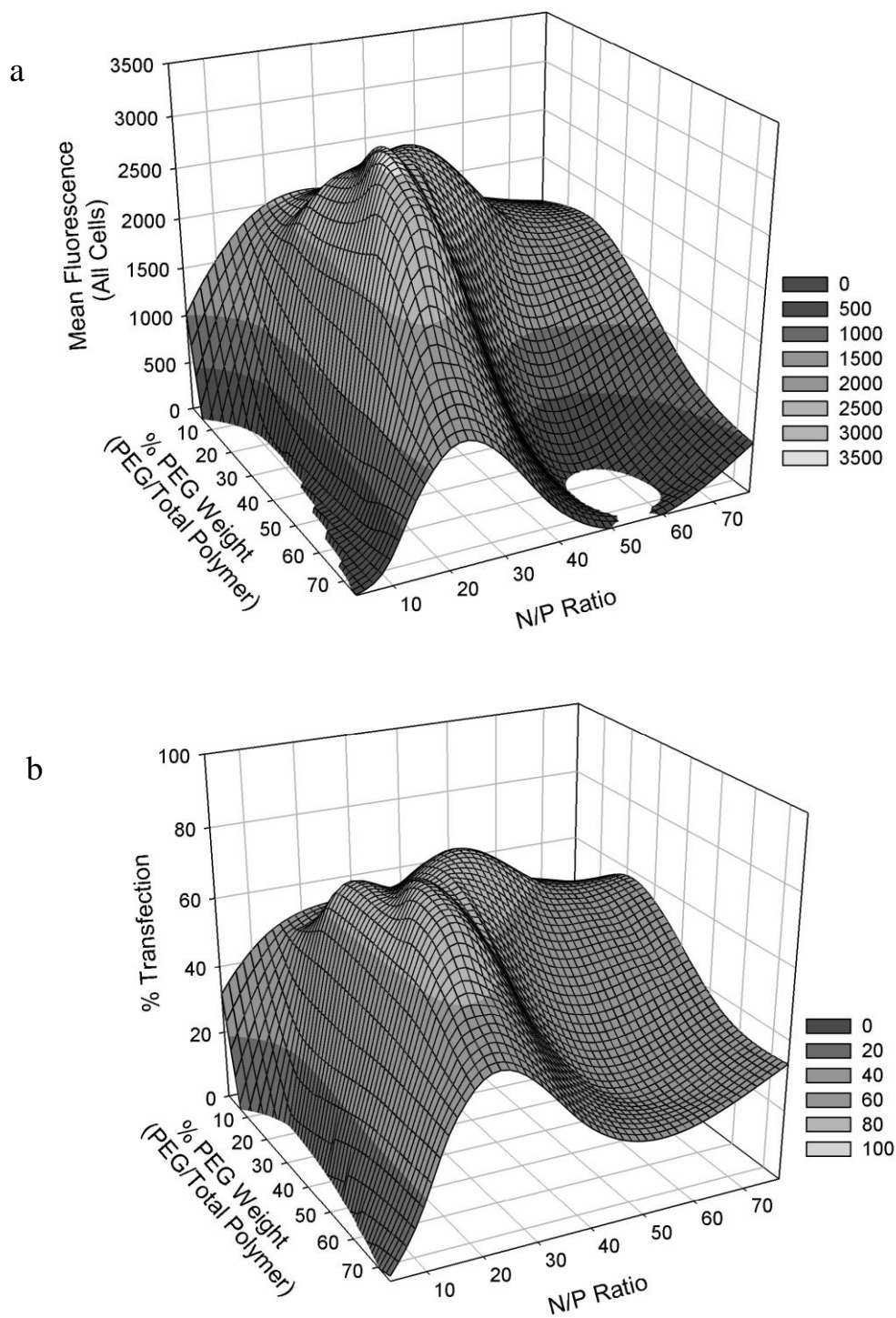


**Figure 22. Surface plots of mean fluorescence (top) and percent transfection (bottom).** The mean fluorescence and percent transfected cells as a result of treatment with gWIZ-GFP polyplexes, as determined by flow cytometry. The transfection efficiency was plotted as a dependent function of N/P ratio and % PEG weight.

#### **4.14) General Discussion and Conclusions on PEI-PEG Transfections**

Previously, the effects of both %PEG weight and N/P ratio on transfection efficiency have been singly described. As illustrated by the 3D surfaces plotted in this thesis, these two variables combine to produce a complex relationship that is insufficiently explained by the simple combination of the two variables alone and their general effects on transfection. Ultimately, we expect the the resulting surfaces to be the result of the physicochemical and intracellular trafficking differences among the polyplexes examined. The experiments performed as part of this study, which were not directly related to transfection, may be suggestive of factors that have a significant role in determining the characteristics of the resulting surfaces.

In regards to DNA binding ability, differences resulting from PEGylation were observed on a *per polymer* basis, but no differences were detected on a *per backbone* basis. When the uncorrected binding curves were viewed as a function of N/P ratio, the binding curves were relatively more compressed with 50% binding points all within ~5 N/P values of each other. Given the small differences in binding as a function of N/P ratio, it is unlikely that differences in binding ability have any effect on transfection. This is supported by transfection data in a number of ways. Firstly, binding is complete above a  $N/P = 20$ , so that the differences in DNA binding affecting transfection should predominantly take place under a  $N/P = 20$ . However, as seen in figures 21a and 21b, the predominant relationship below a  $N/P = 20$  was a linear increase in transfection with increasing N/P ratio and not one concerned with differences in PEG composition. Secondly, in the region of  $N/P = 0-20$  on both surfaces, seen in figure 22, an incline is noted with increasing N/P ratio which appears to increase with the same slope at all percent PEG weight values. The shape of the surface in this region not only suggests that the most critical variable is an adequate N/P ratio to form effective complexes, but that PEGylation had no effect in this low N/P range and binding differences likely have no effect on transfection.

Regarding the polyplex size, all polyplexes were in the range of 200-300 nm (with the exception of one polymer formulation increasing to ~600 nm after incubation in 10% serum). Considering this small size range, it is unlikely that different uptake mechanisms were employed for internalization, due to the polyplexes falling under the threshold of 500 nm for fluid phase endocytosis. For polyplexes with sizes < 500 nm, uptake appears reliant on both clathrin-mediated and caveolin-mediated endocytosis (with the preferred mechanism dependent on cell type), while polyplexes > 500 nm utilize fluid phase endocytosis (139, 140, 172). As the vast majority of polyplexes would be internalized in a similar manner, and hence have no trafficking advantages relative to each other, differences in transfection can not be attributed to polyplex size. Note that this analysis assumes no specific changes in uptake mechanisms due to the presence of PEG, and that particle size dictates the internalization mechanism.

Uptake, as well, appears to have a minimal effect on transfection. While uptake is obviously needed for transfection, the increased uptake of some polyplexes compared to others did not seem particularly advantageous. This is evident with the uptake peak of figure 17 (40-60% PEG; N/P = 40-60) being present in the same region with low transfection (> 45% PEG; N/P > 45%) seen in figures 22a and 22b, and not in the region with high transfection (<55% PEG; N/P = 20-35%). This lack of overlap is suggestive that uptake and transfection are not directly related.

While no singular aspect of these polyplex properties can specifically and solely account for the relationship between N/P ratio and percent PEG weight on transfection efficiency, it does not necessarily preclude them from having some role in a broader sense. For the polymers tested in these studies, all their properties appeared to be in the same effective range for transfection, and hence did not elicit detectable differences in effectiveness. This would have not been the case if larger differences were found for these properties. Ultimately, the surfaces of mean fluorescence and percent transfected cells are likely the combined product of many aspects of polyplex properties, particularly those contributing to differences in intracellular trafficking. This is exem-

plified by the rationales given for two observations discussed earlier; namely, the decrease in effectiveness observed at high PEG substitution and high N/P ratio seen as the striking valley on both surfaces, as well as the increase in effectiveness observed at low PEG substitution and moderate N/P ratio seen as the most prominent peak on both surfaces. The decrease was previously attributed to either inhibitory effect of free polymers to interact with their environment, or decreased stability resulting in premature unpacking in the cytosol (possibly in endosomes) before nuclear localization. While the increase in transfection was suggested to be the result of ideal stability, both resisting unpacking in the cytosol (unlike more PEGylated polymers) and unpacking in the nucleus more readily compared to unmodified PEI. These possible differences in trafficking may be explained by differences in polyplex properties in which the valley and peak on transfection surfaces arise from the corresponding polyplexes having different properties (hydrophilicity, surface charge, particle density, etc.). Ultimately, these surfaces provide valuable insights not only useful for the optimization of this transfection system but for highlighting the importance of intracellular events and the ability of polyplexes to transfect cells if their properties are properly controlled by PEGylation and N/P ratio.

The complex relationship between PEG substitution and N/P ratio made evident by my studies is suggestive of why there exists disagreements in the published literature regarding the effect of PEGylation on PEI effectiveness. The fact that some studies report a beneficial effect whereas others report an inhibitory effect may be the result of various studies only observing a limited portion of the effectiveness surface, such that some studies may be in a trough while others limit their observations to a peak. Given the various effects of PEG length on transfection noted in previous studies, the shape of such surfaces likely depends not only on the N/P ratio and PEG substitution but on the molecular weight of the grafted PEI as well. While this makes making direct comparisons between studies difficult, it also suggests that the screening of any PEI-PEG library requires an in-depth study for each PEG weight conjugated using a wide range of

substitutions and N/P ratios. While many previous studies have noted the importance of substitution and N/P ratio, the relevance of the two variables acting in concert has only been considered to necessitate description via a *transfection surface* recently (169). Ulasov *et al.* reported the *transfection surfaces* (PEG chains/PEI vs. N/P vs. % transfection) of numerous cell types, all having similar peaks, but with the elevation and location dependent on cell type. The study reported in this thesis investigated a broader range of substitutions and N/P ratios in comparison using 0-37.2 PEG/PEI with a maximum N/P = ~70, whereas Ulasov *et al.* used 0-8 PEG/PEI with a maximum N/P = ~40. That said, for the limited range they tested, the surfaces they observed are remarkably similar to the surfaces reported in this thesis within the same corresponding region. Most notably, Ulasov *et al.* noted a peak at PEG/PEI = 1.2 in the N/P range of 30-40, while this work observed a similar peak at the low substitution of PEG/PEI = 2.7 in the N/P range of 31.7-38.5. This provides support for the accuracy of both our observations and suggests HEK293 cells transfect in a similar manner to the cell types Ulasov *et al.* tested. By extension, the similarity noted in the corresponding regions of the two studies, suggests that the more expansive surface reported in this thesis may be applicable to all the cell types tested by Ulasov *et al.* and not solely HEK293 cells.

It is important to recognize both the limits and transferable predictions of these surfaces. For example, while the transfection surface of PEGylated PEI generated in this work appear supported by the surfaces of Ulasov *et al.*, it nonetheless only describes the optimal conditions for *in vitro* applications. While these observations are useful for experimental purposes, *ex vivo* gene therapy approaches, and possibly localized *in vivo* gene therapies, these data may not accurately predict the efficacy of injected polyplexes for locally- or systemically-delivered gene therapies. It has been demonstrated with mice injections that blood levels remained higher for polyplexes with many short PEG chains compared to fewer longer PEG chains (173). This is presumably due to differences in opsonization, and this study highlights the importance of optimization in the most

appropriate and similar conditions that the polyplexes will be applied in. Depending on the environment, different barriers to effective transgene expression are present and need to be bypassed.

In terms of the transferability of the observations reported in this thesis, besides being applicable to other cell types, knowing the optimal PEG substitution and N/P ratios of PEGylated PEI may be useful in designing novel nanocarriers. The ideal relative composition of PEI and PEG could serve as a guide for the PEGylation of alternative polycations to PEI, as well as providing a starting ratio for grafting polyamines to PEG, or synthesizing linear block copolymers. The same PEGylated PEI transfection system could be combined with the assisting biomimetic peptides discussed previously. The incorporation of endosomal escape peptides and nuclear localization sequences (NLS) into PEI-PEG polyplexes formed using the optimal PEG substitution and N/P ratio outlined in my studies may produce an additive effect on transfection efficiency. Finally, the complex relationship noted between N/P ratio and PEG substitution in determining transgene expression may be indicative that such multivariable relationships exist for other conjugated ligands as well, such as NLS peptides and other such trafficking signals. This would suggest that detailed studies, similar to those described in this thesis regarding PEG grafting, should be conducted for each ligand in order to develop the best possible nanocarrier for gene delivery.

## 5) REFERENCES

1. Verma I, Weitzman M. Gene therapy: twenty-first century medicine. *Annu. Rev. Biochem.* 2005;74:711–738.
2. Kay M, Glorioso J, Naldini L. Viral vectors for gene therapy: the art of turning infectious agents into vehicles of therapeutics. *Nature medicine.* 2001;7(1):33–40.
3. Sinn P, Sauter S, McCray P. Gene therapy progress and prospects: development of improved lentiviral and retroviral vectors—design, biosafety, and production. *Gene Therapy.* 2005;12(14):1089–1098.
4. Segura MM, Alba R, Bosch A, Chillon M. Advances in Helper-Dependent Adenoviral Vector Research. 2008;8(4):222–235.
5. Howarth J, Lee Y, Uney J. Using viral vectors as gene transfer tools (Cell Biology and Toxicology Special Issue: ETCS-UK 1 day meeting on genetic manipulation of cells). *Cell biology and toxicology.* 2010;26(1):1–20.
6. Alba R, Bosch A, Chillon M. Gutless adenovirus: last-generation adenovirus for gene therapy. *Gene Therapy.* 2005;12:S18–S27.
7. Pizzato M, Marlow S, Blair E, Takeuchi Y. Initial binding of murine leukemia virus particles to cells does not require specific Env-receptor interaction. *Journal of Virology.* 1999;73(10):8599.
8. Haynes C, Erlwein O, Schnierle BS. Modified Envelope Glycoproteins to Retarget Retroviral Vectors. 2003;3(5):405–410.
9. Harrison S. Mechanism of membrane fusion by viral envelope proteins. *Advances in virus research.* 2005;64:231–261.
10. Cronin J, Zhang X, Reiser J. Altering the tropism of lentiviral vectors through pseudotyping. *Current gene therapy.* 2005;5(4):387–398.
11. Burns J, Friedmann T, Driever W, Burrascano M, Yee J. Vesicular stomatitis virus G glycoprotein pseudotyped retroviral vectors: concentration to very high titer and efficient gene transfer into mammalian and nonmammalian cells. *Proceedings of the National Academy of Sciences of the United States of America.* 1993;90(17):8033–8037.
12. Deyle D, Li Y, Olson E, Russell D. Nonintegrating Foamy Virus Vectors. *Journal of Virology.* 2010;84(18):9341.
13. De Rijck J, Vandekerckhove L, Christ F, Debyser Z. Lentiviral nuclear import: a complex interplay between virus and host. *Bioessays.* 2007;29(5):441–451.
14. Roe T, Reynolds T, Yu G, Brown P. Integration of murine leukemia virus DNA depends on mitosis. *EMBO J.* 1993;12(5):2099.
15. Lewis P, Emerman M. Passage through mitosis is required for oncoretroviruses but not for the human immunodeficiency virus. *Journal of Virology.* 1994;68(1):510–516.
16. Miller D, Adam M, Miller A. Gene transfer by retrovirus vectors occurs only in cells that are actively replicating at the time of infection. *Molecular and cellular biology.* 1990;10(8):4239–4242.

17. Bergelson J, Cunningham J, Droguett G, Kurt-Jones E, Krithivas A, Hong J, et al. Isolation of a common receptor for Cocksackie B viruses and adenoviruses 2 and 5. *Science*. 1997;275(5304):1320.
18. Wickham T, Mathias P, Cheresch D, GR N. Integrins  $\alpha\beta 3$  and  $\alpha\beta 5$  promote adenovirus internalization but not virus attachment. *Cell*. 1993;73(2):309–319.
19. Meier O, Greber U. Adenovirus endocytosis. *J. Gene Med*. 2004;6(S1):S152–S163.
20. Waehler R, Russell S, Curiel D. Engineering targeted viral vectors for gene therapy. *Nature Reviews Genetics*. 2007;8(8):573–587.
21. Kanerva A, Wang M, Bauerschmitz G, Lam J, Desmond R, Bhoola S, et al. Gene transfer to ovarian cancer versus normal tissues with fiber-modified adenoviruses. *Molecular Therapy*. 2002;5(6):695–704.
22. Mercier G, Campbell J. A chimeric adenovirus vector encoding reovirus attachment protein  $\sigma 1$  targets cells expressing junctional adhesion molecule 1. *Proceedings of the National Academy of Sciences*. 2004;101(16):6188–6193.
23. Hedley S, Maur der A, Hohn S, Escher D, Barberis A. An adenovirus vector with a chimeric fiber incorporating stabilized single chain antibody achieves targeted gene delivery. *Gene Therapy*. 2005;13:88–94.
24. Blumenthal R, Seth P, Willingham M, Pastan I. pH-dependent lysis of liposomes by adenovirus. *Biochemistry*. 1986;25:2231–2237.
25. Wang K, Guan T, Cheresch D. Regulation of adenovirus membrane penetration by the cytoplasmic tail of integrin beta 5. *Journal of Virology*. 2000;74(6):2731–2739.
26. Kelkar S, Pfister K, Crystal R, Leopold P. Cytoplasmic dynein mediates adenovirus binding to microtubules. *Journal of Virology*. 2004;78(18):10122.
27. Saphire A, Guan T, Schirmer E, Nemerow G, Gerace L. Nuclear import of adenovirus DNA in vitro involves the nuclear protein import pathway and hsc70. *Journal of Biological Chemistry*. 2000;275(6):4298.
28. Trotman LC, Mosberger N, Fornerod M, Stidwill RP, Greber UF. Import of adenovirus DNA involves the nuclear pore complex receptor CAN/Nup214 and histone H1. *Nature Cell Biology*. 2001 Dec.;3(12):1092–1100.
29. Wodrich H, Cassany A, D'Angelo MA, Guan T, Nemerow G, Gerace L. Adenovirus core protein pVII is translocated into the nucleus by multiple import receptor pathways. *Journal of Virology*. 2006 Oct.;80(19):9608–9618.
30. Davison AJ, Benko M, Harrach B. Genetic content and evolution of adenoviruses. *J. Gen. Virol*. 2003 Nov.;84(Pt 11):2895–2908.
31. McConnell MJ, Imperiale MJ. *Biology of Adenovirus and Its Use as a Vector for Gene Therapy*. Human Gene Therapy. 2004;15:1022–1033.
32. Kennedy MA, Parks RJ. Adenovirus virion stability and the viral genome: size matters. *Mol. Ther*. 2009 Oct.;17(10):1664–1666.

33. Harui A, Suzuki S, Kochanek S, Mitani K. Frequency and stability of chromosomal integration of adenovirus vectors. *Journal of Virology*. 1999;73(7):6141.
34. Bangari D, Mittal S. Current strategies and future directions for eluding adenoviral vector immunity. *Current gene therapy*. 2006;6(2):215.
35. Löser P, Hillgenberg M, Arnold W, Both G, Hofmann C. Ovine adenovirus vectors mediate efficient gene transfer to skeletal muscle. *Gene Therapy*. 2000;7(17):1491–1498.
36. Chirmule N, Propert K, Magosin S, Qian Y, Qian R, Wilson J. Immune responses to adenovirus and adeno-associated virus in humans. *Gene Therapy*. 1999;6(9):1574.
37. Summerford C, Samulski R. Membrane-associated heparan sulfate proteoglycan is a receptor for adeno-associated virus type 2 virions. *Journal of Virology*. 1998;72(2):1438–1445.
38. Summerford C, Bartlett J, Samulski R.  $\alpha V\beta 5$  integrin: a co-receptor for adeno-associated virus type 2 infection. *Nature medicine*. 1999;5(1):78–82.
39. Qing K, Mah C, Hansen J, Zhou S, Dwarki V, A Srivastava. Human fibroblast growth factor receptor 1 is a co-receptor for infection by adeno-associated virus 2. *Nature medicine*. 1999;5(1):71-77.
40. Kaludov N, Brown K, Walters R, Zabner J. Adeno-associated virus serotype 4 (AAV4) and AAV5 both require sialic acid binding for hemagglutination and efficient transduction but differ in sialic acid linkage specificity. *Journal of Virology*. 2001;:6884–6893.
41. Di Pasquale G, Davidson B, Stein C, Martins I. Identification of PDGFR as a receptor for AAV-5 transduction. *Nature medicine*. 2003;9(10):1306–1312.
42. Bartlett J, Wilcher R, Samulski R. Infectious entry pathway of adeno-associated virus and adeno-associated virus vectors. *Journal of Virology*. 2000;74(6):2777.
43. Wu Z, Asokan A, Samulski R. Adeno-associated virus serotypes: vector toolkit for human gene therapy. *Molecular Therapy*. 2006;14(3):316–327.
44. Harbison CE, Chiorini JA, Parrish CR. The parvovirus capsid odyssey: from the cell surface to the nucleus. *Trends Microbiol*. 2008 May;16(5):208–214.
45. Weis K. Regulating access to the genome: nucleocytoplasmic transport throughout the cell cycle. *Cell*. 2003 Feb. 21;112(4):441–451.
46. McCarty D, Young S Jr, Samulski R. Integration of adeno-associated virus (AAV) and recombinant AAV vectors. *Genetics*. 2004;38.
47. Dyall J, Szabo P, Berns K. Adeno-associated virus (AAV) site-specific integration: Formation of AAV–AAVS1 junctions in an in vitro system. *Proceedings of the National Academy of Sciences*. 1999;96(22):12849.
48. Giraud C, Winocour E, Berns K. Site-specific integration by adeno-associated virus is directed by a cellular DNA sequence. *Proceedings of the National Academy of Sciences of the United States of America*. 1994;91(21):10039.
49. Grieger J, Samulski R. Packaging capacity of adeno-associated virus serotypes: impact of larger genomes on infectivity and postentry steps. *Journal of Virology*. 2005;79(15):9933.

50. Pechan P, Herrlinger U, Aghi M, Jacobs A, Breakefield X. Combined HSV-1 recombinant and amplicon piggyback vectors: Replication-competent and defective forms, and therapeutic efficacy for experimental gliomas. *J. Gene Med.* 1999;1(3):176–185.
51. Laquerre S, Argnani R, Anderson D, Zucchini S, Manservigi R, Glorioso J. Heparan sulfate proteoglycan binding by herpes simplex virus type 1 glycoproteins B and C, which differ in their contributions to virus attachment, penetration, and cell-to-cell spread. *Journal of Virology.* 1998;72(7):6119.
52. Fink D, DeLuca N, Yamada M, Wolfe D, Glorioso J. Design and application of HSV vectors for neuroprotection. *Gene Therapy.* 2000;7(2):115–119.
53. Laquerre S, Anderson D, Stolz D. Recombinant herpes simplex virus type 1 engineered for targeted binding to erythropoietin receptor-bearing cells. *Journal of Virology.* 1998;72(12):9683–9697.
54. Anderson D, Laquerre S, Goins W, Cohen J, Glorioso J. Pseudotyping of glycoprotein D-deficient herpes simplex virus type 1 with vesicular stomatitis virus glycoprotein G enables mutant virus attachment and entry. *Journal of Virology.* 2000;74(5):2481.
55. Grandi P, Wang S, Schuback D, Krasnykh V, Spear M, Curiel D, et al. HSV-1 virions engineered for specific binding to cell surface receptors. *Molecular Therapy.* 2004;9(3):419–427.
56. Grandi P, Fernandez J, Szentirmai O, Carter R. Targeting HSV-1 virions for specific binding to epidermal growth factor receptor-vIII-bearing tumor cells. *Cancer gene therapy.* 2010;9(3):419–427.
57. Jackson SA, DeLuca NA. Relationship of herpes simplex virus genome configuration to productive and persistent infections. *Proceedings of the National Academy of Sciences.* 2003;100(13):7871-7876.
58. Smith R, Geller A, Escudero K, Wilcox C. Long-term expression in sensory neurons in tissue culture from herpes simplex virus type 1 (HSV-1) promoters in an HSV-1-derived vector. *Journal of Virology.* 1995;69(8):4593.
59. Stavropoulos T, Strathdee C. An enhanced packaging system for helper-dependent herpes simplex virus vectors. *Journal of Virology.* 1998;72(9):7137.
60. Kong Y, Yang T, Geller A. An efficient in vivo recombination cloning procedure for modifying and combining HSV-1 cosmid. *Journal of virological methods.* 1999;80(2):129–136.
61. Edelstein M, Abedi M, Wixon J. Gene therapy clinical trials worldwide to 2007—an update. *J. Gene Med.* 2007;9(10):833–842.
62. Rosenberg S, Aebersold P, Cornetta K. Gene Transfer into Humans — Immunotherapy of Patients with Advanced Melanoma, Using Tumor-Infiltrating Lymphocytes Modified by Retroviral Gene Transduction. *New England Journal of Medicine.* 1990;323:570–578.
63. Blaese RM, Culver KW, Miller AD, Carter CS, Fleisher T, Clerici M, et al. T Lymphocyte-Directed Gene Therapy for ADA- SCID: Initial Trial Results After 4 Years. *Science.* 1995 Oct. 20;270(5235):475–480.
64. Raper SE, Chirmule N, Lee FS, Wivel NA, Bagg A, Gao G-P, et al. Fatal systemic inflammatory response syndrome in a ornithine transcarbamylase deficient patient following adenoviral gene

- transfer. *Mol. Genet. Metab.* 2003 Aug.;80(1-2):148–158.
65. Edelstein ML, Abedi MR, Wixon J, Edelstein RM. Gene therapy clinical trials worldwide 1989–2004—an overview. *J. Gene Med.* 2004 May 26;6(6):597–602.
  66. Cavazzana-Calvo M, Hacein-Bey S, Basile G. Gene Therapy of Human Severe Combined Immunodeficiency (SCID)-X1 Disease. *Science.* 2000;288:669–672.
  67. Hacein-Bey-Abina S, Kalle Von C, Schmidt M, McCormack MP, Wulffraat N, Leboulch P, et al. LMO2-associated clonal T cell proliferation in two patients after gene therapy for SCID-X1. *Science.* 2003 Oct. 17;302(5644):415–419.
  68. Boztug K, Schmidt M, Schwarzer A, Banerjee PP, Díez IA, Dewey RA, et al. Stem-cell gene therapy for the Wiskott-Aldrich syndrome. *N. Engl. J. Med.* 2010 Nov. 11;363(20):1918–1927.
  69. Doherty G, McMahon H. Mechanisms of Endocytosis. *Annu. Rev. Biochem.* 2009;78:857–902.
  70. Mayor S, Pagano R. Pathways of clathrin-independent endocytosis. *Nature Reviews Molecular Cell Biology.* 2007 Aug. 1;8(8):603–612.
  71. Wagner E. Application of membrane-active peptides for nonviral gene delivery. *Advanced Drug Delivery Reviews.* 1999;38(3):279–289.
  72. Wagner E, Plank C, Zatloukal K, Cotten M, Birnstiel M. Influenza virus hemagglutinin HA-2 N-terminal fusogenic peptides augment gene transfer by transferrin-polylysine-DNA complexes: toward a synthetic virus-like gene-transfer vehicle. *Proceedings of the National Academy of Sciences of the United States of America.* 1992;89(17):7934.
  73. Subramanian A, Ma H, Dahl K, Zhu J, Diamond S. Adenovirus or HA- 2 fusogenic peptide- assisted lipofection increases cytoplasmic levels of plasmid in nondividing endothelium with little enhancement of transgene expression. *J. Gene Med.* 2002;4(1):75–83.
  74. Pichon C, Goncalves C, Midoux P. Histidine-rich peptides and polymers for nucleic acids delivery. *Advanced Drug Delivery Reviews.* 2001;53(1):75–94.
  75. Zauner W, Blaas D, Kuechler E, Wagner E. Rhinovirus-mediated endosomal release of transfection complexes. *Journal of Virology.* 1995;69(2):1085–1092.
  76. Gottschalk S, Sparrow JT, Hauer J, Mims MP, Leland FE, Woo SL, et al. A novel DNA-peptide complex for efficient gene transfer and expression in mammalian cells. *Gene Therapy.* 1996 May;3(5):448–457.
  77. Rittner K, Benavente A, Bompard-Sorlet A, Heitz F. New basic membrane-destabilizing peptides for plasmid-based gene delivery in vitro and in vivo. *Molecular Therapy.* 2002;5(2):104–114.
  78. Futaki S, Masui Y, Nakase I, Sugiura Y, Nakamura T, Kogure K, Harashima H. Unique features of a pH-sensitive fusogenic peptide that improves the transfection efficiency of cationic liposomes. *The Journal of Gene Medicine.* 2005;7:1450–1458.
  79. Wyman T, Nicol F, Zelphati O, Scaria P, Plank C. Design, Synthesis, and Characterization of a Cationic Peptide That Binds to Nucleic Acids and Permeabilizes Bilayers†. *Biochemistry.* 1997;36(10):3008–3017.
  80. Xiong X-B, Uludağ H, Lavasanifar A. Virus-mimetic polymeric micelles for targeted siRNA de-

- livery. *Biomaterials*. 2010 Aug.;31(22):5886–5893.
81. Rudolph C, Plank C, Lausier J, Schillinger U, Müller R, Rosenecker J. Oligomers of the arginine-rich motif of the HIV-1 TAT protein are capable of transferring plasmid DNA into cells. *Journal of Biological Chemistry*. 2003;278(13):11411.
  82. Torchilin VP, Rammohan R, Weissig V, Levchenko T. TAT peptide on the surface of liposomes affords their efficient intracellular delivery even at low temperature and in the presence of metabolic inhibitors. *Proceedings of the National Academy of Sciences*. 2001;98(15):8786–8791.
  83. Futaki S, Nakase I, Suzuki T, Youjun Z, Sugiura Y. Translocation of Branched-Chain Arginine Peptides through Cell Membranes: Flexibility in the Spatial Disposition of Positive Charges in Membrane-Permeable Peptides†. *Biochemistry*. 2002;41(25):7925–7930.
  84. Futaki S, Suzuki T, Ohashi W, Yagami T, Tanaka S, Ueda K, et al. Arginine-rich peptides. *Journal of Biological Chemistry*. 2001;276(8):5836.
  85. Nakamura Y, Kogure K, Futaki S, Harashima H. Octaarginine-modified multifunctional envelope-type nano device for siRNA. *Journal of Controlled Release*. 2007;119(3):360–367.
  86. Futaki S. Oligoarginine vectors for intracellular delivery: Design and cellular-uptake mechanisms. *Peptide Science*. 2006;84(3):241–249.
  87. Futaki S, Nakase I, Tadokoro A, Takeuchi T, Jones A. Arginine-rich peptides and their internalization mechanisms. *Biochemical Society Transactions*. 2007;35:784–787.
  88. Rentsendorj A, Agadjanian H, Chen X, Cirivello M, MacVeigh M, Kedes L, et al. The Ad5 fiber mediates nonviral gene transfer in the absence of the whole virus, utilizing a novel cell entry pathway. *Gene Therapy*. 2004;12(3):225–237.
  89. Rentsendorj A, Xie J, MacVeigh M, Agadjanian H, Bass S, Kim D, et al. Typical and atypical trafficking pathways of Ad5 penton base recombinant protein: implications for gene transfer. *Gene Therapy*. 2006;13(10):821–836.
  90. Fontes M, Teh T, Kobe B. Structural basis of recognition of monopartite and bipartite nuclear localization sequences by mammalian importin- $\alpha$  1. *Journal of Molecular Biology*. 2000;297(5):1183–1194.
  91. Aronsohn A, Hughes J. Nuclear localization signal peptides enhance cationic liposome-mediated gene therapy. *Journal of Drug Targeting*. 1998;5(3):163–169.
  92. Brandén LJ, Mohamed AJ, Smith CIE. A peptide nucleic acid–nuclear localization signal fusion that mediates nuclear transport of DNA. *Nature Biotechnology*. 1999;17:784–787.
  93. Ludtke J, Zhang G, Sebestyén M, Wolff J. A nuclear localization signal can enhance both the nuclear transport and expression of 1 kb DNA. *Journal of Cell Science*. 1999;112:2033.
  94. Sebestyén M, Ludtke J, Bassik M, Zhang G, Budker V, Lukhtanov E, et al. DNA vector chemistry: the covalent attachment of signal peptides to plasmid DNA. *Nature Biotechnology*. 1998;16(1):80–85.
  95. Talsma S, Babensee J, Murthy N, Williams I. Development and in vitro validation of a targeted delivery vehicle for DNA vaccines. *Journal of Controlled Release*. 2006;112(2):271–279.

96. Chan C, Senden T, Jans D. Supramolecular structure and nuclear targeting efficiency determine the enhancement of transfection by modified polylysines. *Gene Therapy*. 2000;7(19):1690.
97. Kurihara D, Akita H, Kudo A, Masuda T, Futaki S, Harashima H. Effect of Polyethyleneglycol Spacer on the Binding Properties of Nuclear Localization Signal-Modified Liposomes to Isolated Nucleus. *Biol. Pharm. Bull.* 2009;32(7):1303–1306.
98. Murray K, Etheridge C, Shah S, Matthews D, Russell W, Gurling H, et al. Enhanced cationic liposome-mediated transfection using the DNA-binding peptide  $\mu$  (mu) from the adenovirus core. *Gene Therapy*. 2001;8(6):453–460.
99. Tagawa T, Manvell M, Brown N, Keller M, Perouzel E, Murray K, et al. Characterisation of LMD virus-like nanoparticles self-assembled from cationic liposomes, adenovirus core peptide  $\mu$  (mu) and plasmid DNA. *Gene Therapy*. 2002;9(9):564–576.
100. Keller M, Harbottle R, Perouzel E, Colin M, Shah I, Rahim A, et al. Nuclear localisation sequence templated nonviral gene delivery vectors: investigation of intracellular trafficking events of LMD and LD vector systems. *Chembiochem*. 2003;4(4):286–298.
101. You J, Kamihira M, Iijima S. Enhancement of transfection efficiency by protamine in DDAB lipid vesicle-mediated gene transfer. *Journal of Biochemistry*. 1999;125(6):1160.
102. Noguchi A, Hirashima N, Nakanishi M. Cationic cholesterol promotes gene transfection using the nuclear localization signal in protamine. *Pharm Res*. 2002;19(7):933–938.
103. MA A. Increased receptor-mediated gene delivery to the liver by protamine-enhanced-asialofetuin-lipoplexes. *Gene Therapy*. 2003;10(1):5–14.
104. Ueno N, Bartholomeusz C, Xia W, Anklesaria P, Bruckheimer E, Mebel E, et al. Systemic gene therapy in human xenograft tumor models by liposomal delivery of the E1A gene. *Cancer research*. 2002;62(22):6712.
105. Yuan H, Zhang W, Du Y, Hu F. Ternary nanoparticles of anionic lipid nanoparticles/protamine/DNA for gene delivery. *International Journal of Pharmaceutics*. 2010;392:224–231.
106. Chen J, Yu Z, Chen H, Gao J, Liang W. Transfection efficiency and intracellular fate of polycation liposomes combined with protamine. *Biomaterials*. 2010;32:1412–1418.
107. Faneca H, Simoes S, Pedroso de Lima M. Association of albumin or protamine to lipoplexes: enhancement of transfection and resistance to serum. *J. Gene Med*. 2004;6(6):681–692.
108. Nakamura T, Moriguchi R, Kogure K, Minoura A, Masuda T, Akita H, et al. Delivery of condensed DNA by liposomal non-viral gene delivery system into nucleus of dendritic cells. *Biol. Pharm. Bull.* 2006;29(6):1290–1293.
109. Moriguchi R, Kogure K, Akita H, Futaki S, Miyagishi M, Taira K, et al. A multifunctional envelope-type nano device for novel gene delivery of siRNA plasmids. *International Journal of Pharmaceutics*. 2005;301(1-2):277–285.
110. Khalil I, Kogure K, Futaki S, Harashima H. High density of octaarginine stimulates macropinocytosis leading to efficient intracellular trafficking for gene expression. *Journal of Biological Chemistry*. 2006;281(6):3544.

111. Khalil I, Kogure K, Futaki S, Hama S, Akita H, Ueno M, et al. Octaarginine-modified multifunctional envelope-type nanoparticles for gene delivery. *Gene Therapy*. 2007;14(8):682.
112. Nakamura Y, Kogure K, Yamada Y, Futaki S, Harashima H. Significant and prolonged antisense effect of a multifunctional envelope-type nano device encapsulating antisense oligodeoxynucleotide. *Journal of Pharmacy and Pharmacology*. 2006;58(4):431–437.
113. Egle R, Milek M, Mlinaric-Rascan I, Fahr A, Kristl J. A novel gene delivery system for stable transfection of thiopurine-S-methyltransferase gene in versatile cell types. *European Journal of Pharmaceutics and Biopharmaceutics*. 2008;69(1):23–30.
114. Tönges L, Lingor P, Egle R, Dietz G, Fahr A, Bähr M. Stearylated octaarginine and artificial virus-like particles for transfection of siRNA into primary rat neurons. *Rna*. 2006;12(7):1431.
115. Nahde T, Müller K, Fahr A, Müller R, Brüsselbach S. Combined transductional and transcriptional targeting of melanoma cells by artificial virus-like particles. *J. Gene Med*. 2001;3(4):353–361.
116. Mueller K, Nahde T, Fahr A, Müller R, Brüsselbach S. Highly efficient transduction of endothelial cells by targeted artificial virus-like particles. *Cancer gene therapy*. 2001;8(2):107.
117. Wattiaux R, Jadot M, Warnier-Pirotte M-T, Wattiaux-De Coninck S. Cationic lipids destabilize lysosomal membrane in vitro. *FEBS letters*. 1997 Nov. 10;417(2):199–202.
118. Crook K, Stevenson BJ, Dubouchet M, Porteous DJ. Inclusion of cholesterol in DOTAP transfection complexes increases the delivery of DNA to cells in vitro in the presence of serum. *Gene Therapy*. 1998 Jan.;5(1):137–143.
119. Caracciolo G, Caminiti R, Digman MA, Gratton E, Sanchez S. Efficient escape from endosomes determines the superior efficiency of multicomponent lipoplexes. *J Phys Chem B*. 2009 Apr. 16;113(15):4995–4997.
120. Hafez IM, Maurer N, Cullis PR. On the mechanism whereby cationic lipids promote intracellular delivery of polynucleic acids. *Gene Therapy*. 2001 Aug.;8(15):1188–1196.
121. Hoekstra D, Rejman J, Wasungu L, Shi F, Zuhorn I. Gene delivery by cationic lipids: in and out of an endosome. *Biochemical Society Transactions*. 2007 Feb.;35(Pt 1):68–71.
122. Hafez I, Cullis P. Roles of lipid polymorphism in intracellular delivery. *Advanced Drug Delivery Reviews*. 2001;47:139–148.
123. Collins D, Litzinger DC, Huang L. Structural and functional comparisons of pH-sensitive liposomes composed of phosphatidylethanolamine and three different diacylsuccinylglycerols. *Biochimica et Biophysica Acta (BBA) - Biomembranes*. 1990 Jun.;1025(2):234–242.
124. Kogure K, Moriguchi R, Sasaki K, Ueno M, Futaki S, Harashima H. Development of a non-viral multifunctional envelope-type nano device by a novel lipid film hydration method. *Journal of Controlled Release*. 2004;98(2):317–323.
125. Fattal E, Couvreur P, Dubernet C. “Smart” delivery of antisense oligonucleotides by anionic pH-sensitive liposomes. *Advanced Drug Delivery Reviews*. 2004 Apr. 23;56(7):931–946.
126. Cho S, Lee H, Kim J. pH-dependent release property of dioleoylphosphatidyl ethanolamine liposomes. *Korean Journal of Chemical Engineering*. 2008;25(2):390–393.

127. Balhorn R. The protamine family of sperm nuclear proteins. *Genome biology*. 2007;8(9):227.
128. Ando T, Ishii S, Yamasaki M, Iwai K, Hashimoto C, Sawada F. Studies on Protamines. *Journal of Biochemistry*. 1957;44(5):275.
129. Chargaff E. Studies on the chemistry of blood coagulation. *Journal of Biological Chemistry*. 1937;122:153–167.
130. Brewer L, Corzett M, Balhorn R. Protamine-induced condensation and decondensation of the same DNA molecule. *Science*. 1999;286:120.
131. Masuda T, Akita H, Harashima H. Evaluation of nuclear transfer and transcription of plasmid DNA condensed with protamine by microinjection: the use of a nuclear transfer score. *FEBS letters*. 2005;579(10):2143–2148.
132. Sorgi FL, Bhattacharya S, Huang L. Protamine sulfate enhances lipid-mediated gene transfer. *Gene Therapy*. 1997 Dec. 18;4(9):961–968.
133. Kogure K, Akita H, Yamada Y, Harashima H. Multifunctional envelope-type nano device (MEND) as a non-viral gene delivery system. *Advanced Drug Delivery Reviews*. 2008;60(4-5):559–571.
134. Khalil I, Futaki S, Niwa M, Baba Y, Kaji N, Kamiya H, et al. Mechanism of improved gene transfer by the N-terminal stearylation of octaarginine: enhanced cellular association by hydrophobic core formation. *Gene Therapy*. 2004;11(7):636–644.
135. Farrell L, Pepin J, Kucharski C, Lin X, Xu Z, Uludag H. A comparison of the effectiveness of cationic polymers poly-l-lysine (PLL) and polyethylenimine (PEI) for non-viral delivery of plasmid DNA to bone marrow stromal cells (BMSC). *European Journal of Pharmaceutics and Biopharmaceutics*. 2007;65(3):388–397.
136. Inoue Y, Kurihara R, Tsuchida A, Hasegawa M, Nagashima T, Mori T, et al. Efficient delivery of siRNA using dendritic poly (l-lysine) for loss-of-function analysis. *Journal of Controlled Release*. 2008;126:59–66.
137. Boussif O, Lezoualc'h F, Zanta M, Mergny M, Scherman D, Demeneix B, et al. A versatile vector for gene and oligonucleotide transfer into cells in culture and in vivo: polyethylenimine. *Proceedings of the National Academy of Sciences*. 1995. p. 7297–7301.
138. Rejman J, Oberle V, Zuhorn I, Hoekstra D. Size-dependent internalization of particles via the pathways of clathrin- and caveolae-mediated endocytosis. *Biochemical Journal*. 2004;377(Pt 1):159.
139. Rejman J, Bragonzi A, Conese M. Role of clathrin- and caveolae-mediated endocytosis in gene transfer mediated by lipo- and polyplexes. *Molecular Therapy*. 2005 Sep.;12(3):468–474.
140. Vongersdorff K, Sanders N, Vandenbroucke R, Desmedt S, Wagner E, Ogris M. The Internalization Route Resulting in Successful Gene Expression Depends on both Cell Line and Polyethylenimine Polyplex Type. *Molecular Therapy*. 2006 Nov.;14(5):745–753.
141. Ogris M, Steinlein P, Carotta S, Brunner S, Wagner E. DNA/polyethylenimine transfection particles: influence of ligands, polymer size, and PEGylation on internalization and gene expression. *The AAPS journal*. 2001;3(3):43–53.

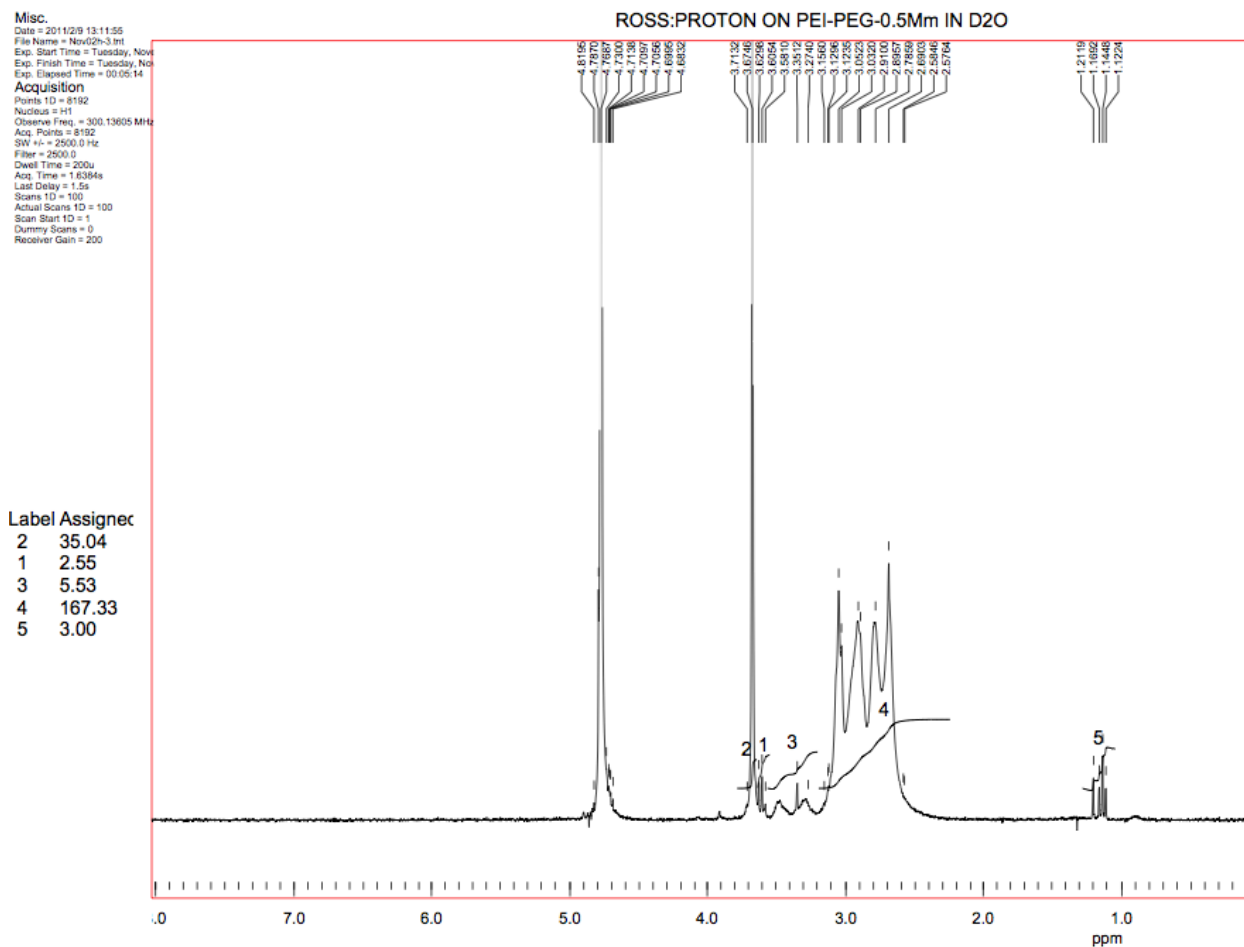
142. Behr J. The proton sponge: a trick to enter cells the viruses did not exploit. *CHIMIA International Journal for Chemistry*. 1997;51:34–36.
143. Sonawane ND. Chloride Accumulation and Swelling in Endosomes Enhances DNA Transfer by Polyamine-DNA Polyplexes. *Journal of Biological Chemistry*. 2003 Sep. 18;278(45):44826–44831.
144. Godbey WT, Wu KK, Mikos AG. Size matters: molecular weight affects the efficiency of poly(ethylenimine) as a gene delivery vehicle. *Journal of Biomedical Materials Research*. 1999 Jun. 5;45(3):268–275.
145. Wightman L, Kircheis R, Rössler V, Carotta S, Ruzicka R, Kursa M, et al. Different behavior of branched and linear polyethylenimine for gene delivery in vitro and in vivo. *J. Gene Med*. 2001;3:362–372.
146. Moghimi S, Symonds P, Murray J, Hunter A, Debska G. A two-stage poly (ethylenimine)-mediated cytotoxicity: implications for gene transfer/therapy. *Molecular Therapy*. 2005;11(6):990.
147. Kafil V, Omidi Y. Cytotoxic Impacts of Linear and Branched Polyethylenimine Nanostructures in A431 Cells. *BioImpacts*. 2011;1(1):23–30.
148. Kunath K, Harpe von A, Fischer D, Petersen H, Bickel U, Voigt K, et al. Low-molecular-weight polyethylenimine as a non-viral vector for DNA delivery: comparison of physicochemical properties, transfection efficiency and in vivo distribution with high-molecular-weight polyethylenimine. *Journal of Controlled Release*. 2003;89:113–125.
149. Jiang H, Arote R, Jere D, Kim Y, Cho M, Cho C. Degradable polyethylenimines as gene carriers. *Mats. Sci. Tech*. 2008 Sep. 1;24(9):1118–1126.
150. Bahadur K C R, Uludağ H. A Comparative Evaluation of Disulfide-Linked and Hydrophobically-Modified PEI for Plasmid Delivery. *Journal of Biomaterials Science*. 2011 Jan. 1;22(7):873–892.
151. Koo H, Jin G-W, Kang H, Lee Y, Nam K, Zhe Bai C, et al. Biodegradable branched poly(ethylenimine sulfide) for gene delivery. *Biomaterials*. 2010 Feb.;31(5):988–997.
152. Lungwitz U, Breunig M, Blunk T, Göpferich A. Polyethylenimine-based non-viral gene delivery systems. *Eur J Pharm Biopharm*. 2005 Jul.;60(2):247–266.
153. Ahn C, Chae S, Bae Y, Kim S. Biodegradable poly(ethylenimine) for plasmid DNA delivery. *Journal of Controlled Release*. 2002;80:273–282.
154. Zhong Z, Feijen J, Lok MC, Hennink WE, Christensen LV, Yockman JW, et al. Low Molecular Weight Linear Polyethylenimine- b-poly(ethylene glycol)- b-polyethylenimine Triblock Copolymers: Synthesis, Characterization, and in Vitro Gene Transfer Properties. *Biomacromolecules*. 2005 Nov.;6(6):3440–3448.
155. Petersen H, Fechner P, Martin A, Kunath K, Stolnik S, Roberts C, et al. Polyethylenimine-graft-poly (ethylene glycol) copolymers: influence of copolymer block structure on DNA complexation and biological activities as gene delivery system. *Bioconjugate Chem*. 2002;13(4):845–854.
156. Mao S, Neu M, Germershaus O, Merkel O, Sitterberg J, Bakowsky U, et al. Influence of Polyethylene Glycol Chain Length on the Physicochemical and Biological Properties of Poly(ethylene imine)-graft-Poly(ethylene glycol) Block Copolymer/SiRNA Polyplexes. 2006;17:1209–1218.

157. Remaut K, Lucas B, Raemdonck K, Braeckmans K, J Demeester A, Smedt SCD. Protection of Oligonucleotides against Enzymatic Degradation by Pegylated and Nonpegylated Branched Polyethyleneimine. *Biomacromolecules*. 2007;8:1333–1340.
158. Zhang X, Pan S-R, Hu H-M, Wu G-F, Feng M, Zhang W, et al. Poly(ethylene glycol)-block-polyethylenimine copolymers as carriers for gene delivery: Effects of PEG molecular weight and PEGylation degree. *J. Biomed. Mater. Res*. 2008;84A(3):795–804.
159. Malek A, Czubayko F, Aigner A. PEG grafting of polyethylenimine (PEI) exerts different effects on DNA transfection and siRNA-induced gene targeting efficacy. *Journal of Drug Targeting*. 2008;16(2):124–139.
160. Germershaus O, Merdan T, Bakowsky U, Martin Behe, Kissel T. Trastuzumab–Polyethylenimine–Polyethylene Glycol Conjugates for Targeting Her2-Expressing Tumors. *Bioconjugate Chem*. 2006;17:1190–1199.
161. Sung S, Min S, Cho K, Lee S, Min Y, Yeom Y, et al. Effect of polyethylene glycol on gene delivery of polyethylenimine. *Biol. Pharm. Bull*. 2003;26(4):492–500.
162. Tang G, Zeng J, Gao S, Ma Y, Shi L, Li Y, et al. Polyethylene glycol modified polyethylenimine for improved CNS gene transfer: effects of PEGylation extent. *Biomaterials*. 2003;24(13):2351–2362.
163. Neamnark A, Suwantong O, Bahadur K, Hsu C, Supaphol P, Uludag H. Aliphatic lipid substitution on 2 kDa polyethylenimine improves plasmid delivery and transgene expression. *Mol. Pharmaceutics*. 2009;6(6):1798–1815.
164. Bahadur K, Landry B, Aliabadi H, Lavasanifar A, Uludag H. Lipid-Substitution on Low Molecular Weight (0.6-2.0 kDa) Polyethylenimine Leads to Higher Zeta-Potential with Plasmid DNA and Enhances Transgene Expression. *Acta Biomaterialia*. 2011;7(5):2209–2217.
165. Jiang H, Secretan C, Gao T, Bagnall K, Korbitt G, Lakey J, et al. The Development of Osteoblasts from Stem Cells to Supplement Fusion of the Spine During Surgery for AIS. *Research into Spinal Deformities*. 2008; 5:467
166. Hafez I, Cullis P. Cholesteryl hemisuccinate exhibits pH sensitive polymorphic phase behavior. *BBA-Biomembranes*. 2000;1463(1):107–114.
167. Hsu C, Hendzel M, Uludag H. Improved transfection efficiency of an aliphatic lipid substituted 2 kDa polyethylenimine is attributed to enhanced nuclear association and uptake in rat bone marrow stromal cell. *J. Gene Med*. 13:46–59.
168. Lee R, Huang L. Folate-targeted, anionic liposome-entrapped polylysine-condensed DNA for tumor cell-specific gene transfer. *Journal of Biological Chemistry*. 1996;271(14):8481.
169. Ulasov A, Khramtsov Y, Trusov G, Rosenkranz A, Sverdlov E, Sobolev A. Properties of PEI-based Polyplex Nanoparticles That Correlate With Their Transfection Efficacy. *Molecular Therapy*. 2011;19(1):103–112.
170. Itaka K, Harada A, Yamasaki Y, Nakamura K, Kawaguchi H, Kataoka K. In situ single cell observation by fluorescence resonance energy transfer reveals fast intra-cytoplasmic delivery and easy release of plasmid DNA complexed with linear polyethylenimine. *J. Gene Med*. 2004 Jan. 6;6(1):76–84.

171. Godbey W, Wu K, Mikos A. Tracking the intracellular path of poly(ethylenimine)/DNA complexes for gene delivery. *Proceedings of the National Academy of Sciences*. 1999;96:5177–5181.
172. Hufnagel H, Hakim P, Lima A, Hollfelder F. Fluid Phase Endocytosis Contributes to Transfection of DNA by PEI-25. *Mol. Ther.* 2009 Jun. 16;17(8):1411–1417.
173. Kunath K, Harpe von A, Petersen H, Fischer D, Voigt K, Kissel T, et al. The structure of PEG-modified poly (ethylene imines) influences biodistribution and pharmacokinetics of their complexes with NF- $\kappa$ B decoy in mice. *Pharm Res.* 2002;19(6):810–817.

## 6) APPENDIX A

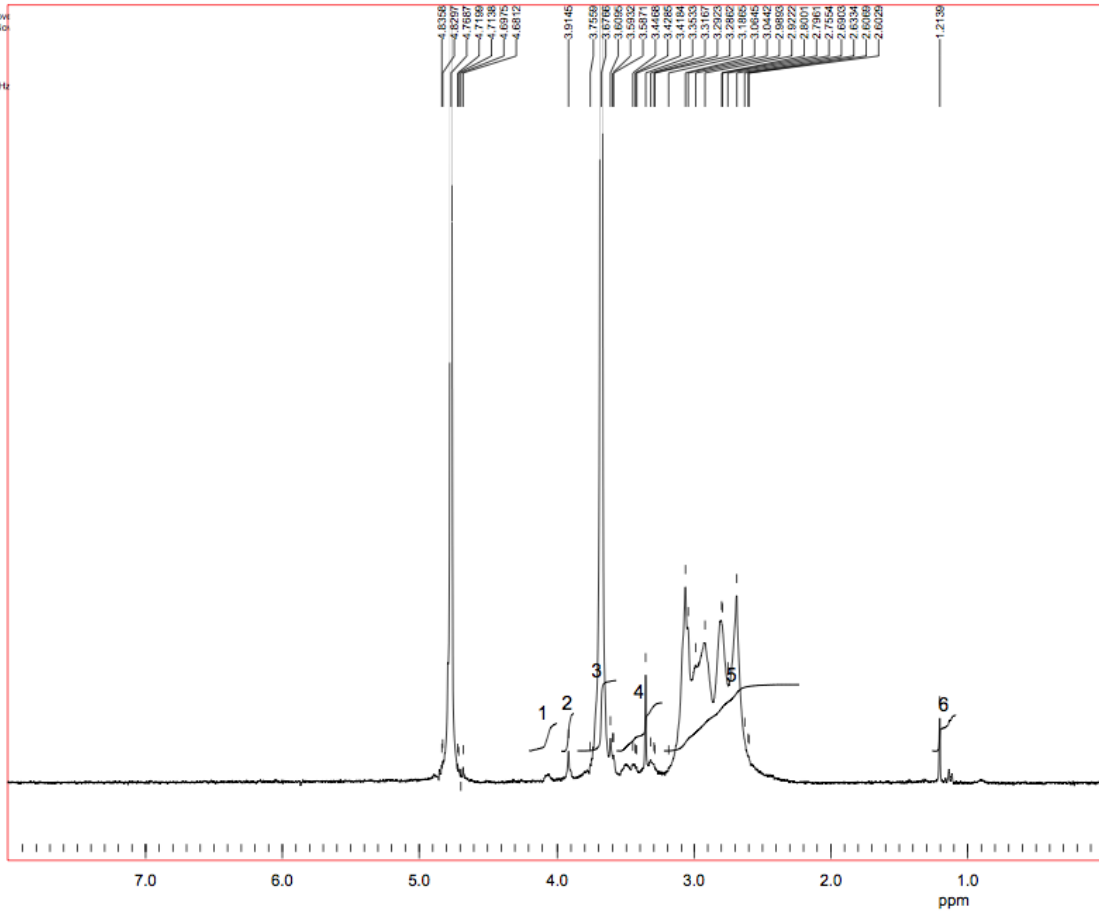
The following pages are unmodified proton-NMR spectra of PEI reacted with 0.5 mM, 2.5 mM, and 7.5 mM methoxy-polyethylene glycol.



Misc.  
 Date = 2011/2/9 13:13:13  
 File Name = Nov02h-4.h1  
 Exp. Start Time = Tuesday, Nov  
 Exp. Finish Time = Tuesday, Nov  
 Exp. Elapsed Time = 00:05:14

Acquisition  
 F1 (1H) = 4192  
 Nucleus = 1H  
 Observe Freq. = 300.13605 MHz  
 Acq. Points = 8192  
 SW +/- = 2500.0 Hz  
 Filter = 2500.0  
 Dwell Time = 200u  
 Acq. Time = 1.6394s  
 Last Delay = 1.5s  
 Scans 1D = 100  
 Actual Scans 1D = 100  
 Scan Start 1D = 1  
 Dummy Scans = 0  
 Receiver Gain = 200

ROSS:PROTON ON PEI-PEG-2.5Mm IN D2O



Label Assignec

1	1.17
2	1.57
3	186.64
4	7.98
5	175.81
6	3.00

Misc.  
Date = 2011/2/2 10:07:11  
File Name = F6502h-1.tst  
Exp. Start Time = Wednesday, 2  
Exp. Finish Time = Wednesday, 2  
Exp. Elapsed Time = 00:06:14  
Acquisition  
Points 1D = 4192  
Nucleus = H1  
Observe Freq. = 300.13605 MHz  
Acq. Points = 8192  
SW +/- = 2500.0 Hz  
Filter = 2500.0  
Dwell Time = 200u  
Acq. Time = 1.6384s  
Last Delay = 1.5s  
Scans 1D = 100  
Actual Scans 1D = 100  
Scan Start 1D = 1  
Dummy Scans = 0  
Receiver Gain = 100

ROSS FITZSIMMONS:PROTON ON PEI-PEG 7.5mM IN D2O

Label Assignec

- 1 0.36
- 2 1.84
- 3 186.86
- 4 0.68
- 5 3.00
- 6 64.30
- 7 0.65

